



IAEA HUMAN HEALTH SERIES

No. 15

Dual Energy X Ray Absorptiometry for Bone Mineral Density and Body Composition Assessment



IAEA

International Atomic Energy Agency

IAEA HUMAN HEALTH SERIES PUBLICATIONS

The mandate of the IAEA human health programme originates from Article II of its Statute, which states that the “Agency shall seek to accelerate and enlarge the contribution of atomic energy to peace, health and prosperity throughout the world”. The main objective of the human health programme is to enhance the capabilities of IAEA Member States in addressing issues related to the prevention, diagnosis and treatment of health problems through the development and application of nuclear techniques, within a framework of quality assurance.

Publications in the IAEA Human Health Series provide information in the areas of: radiation medicine, including diagnostic radiology, diagnostic and therapeutic nuclear medicine, and radiation therapy; dosimetry and medical radiation physics; and stable isotope techniques and other nuclear applications in nutrition. The publications have a broad readership and are aimed at medical practitioners, researchers and other professionals. International experts assist the IAEA Secretariat in drafting and reviewing these publications. Some of the publications in this series may also be endorsed or co-sponsored by international organizations and professional societies active in the relevant fields.

There are two categories of publications in this series:

IAEA HUMAN HEALTH SERIES

Publications in this category present analyses or provide information of an advisory nature, for example guidelines, codes and standards of practice, and quality assurance manuals. Monographs and high level educational material, such as graduate texts, are also published in this series.

IAEA HUMAN HEALTH REPORTS

Human Health Reports complement information published in the IAEA Human Health Series in areas of radiation medicine, dosimetry and medical radiation physics, and nutrition. These publications include reports of technical meetings, the results of IAEA coordinated research projects, interim reports on IAEA projects, and educational material compiled for IAEA training courses dealing with human health related subjects. In some cases, these reports may provide supporting material relating to publications issued in the IAEA Human Health Series.

All of these publications can be downloaded cost free from the IAEA web site:

<http://www.iaea.org/Publications/index.html>

Further information is available from:

Marketing and Sales Unit
International Atomic Energy Agency
Vienna International Centre
PO Box 100
1400 Vienna, Austria

Readers are invited to provide their impressions on these publications. Information may be provided via the IAEA web site, by mail at the address given above, or by email to:

Official.Mail@iaea.org.

DUAL ENERGY X RAY
ABSORPTIOMETRY
FOR BONE MINERAL DENSITY
AND BODY COMPOSITION
ASSESSMENT

The following States are Members of the International Atomic Energy Agency:

AFGHANISTAN	GHANA	NORWAY
ALBANIA	GREECE	OMAN
ALGERIA	GUATEMALA	PAKISTAN
ANGOLA	HAITI	PALAU
ARGENTINA	HOLY SEE	PANAMA
ARMENIA	HONDURAS	PARAGUAY
AUSTRALIA	HUNGARY	PERU
AUSTRIA	ICELAND	PHILIPPINES
AZERBAIJAN	INDIA	POLAND
BAHRAIN	INDONESIA	PORTUGAL
BANGLADESH	IRAN, ISLAMIC REPUBLIC OF	QATAR
BELARUS	IRAQ	REPUBLIC OF MOLDOVA
BELGIUM	IRELAND	ROMANIA
BELIZE	ISRAEL	RUSSIAN FEDERATION
BENIN	ITALY	SAUDI ARABIA
BOLIVIA	JAMAICA	SENEGAL
BOSNIA AND HERZEGOVINA	JAPAN	SERBIA
BOTSWANA	JORDAN	SEYCHELLES
BRAZIL	KAZAKHSTAN	SIERRA LEONE
BULGARIA	KENYA	SINGAPORE
BURKINA FASO	KOREA, REPUBLIC OF	SLOVAKIA
BURUNDI	KUWAIT	SLOVENIA
CAMBODIA	KYRGYZSTAN	SOUTH AFRICA
CAMEROON	LATVIA	SPAIN
CANADA	LEBANON	SRI LANKA
CENTRAL AFRICAN REPUBLIC	LESOTHO	SUDAN
CHAD	LIBERIA	SWEDEN
CHILE	LIBYAN ARAB JAMAHIRIYA	SWITZERLAND
CHINA	LIECHTENSTEIN	SYRIAN ARAB REPUBLIC
COLOMBIA	LITHUANIA	TAJIKISTAN
CONGO	LUXEMBOURG	THAILAND
COSTA RICA	MADAGASCAR	THE FORMER YUGOSLAV REPUBLIC OF MACEDONIA
CÔTE D'IVOIRE	MALAWI	TUNISIA
CROATIA	MALAYSIA	TURKEY
CUBA	MALI	UGANDA
CYPRUS	MALTA	UKRAINE
CZECH REPUBLIC	MARSHALL ISLANDS	UNITED ARAB EMIRATES
DEMOCRATIC REPUBLIC OF THE CONGO	MAURITANIA	UNITED KINGDOM OF GREAT BRITAIN AND NORTHERN IRELAND
DENMARK	MAURITIUS	UNITED REPUBLIC OF TANZANIA
DOMINICAN REPUBLIC	MEXICO	UNITED STATES OF AMERICA
ECUADOR	MONACO	URUGUAY
EGYPT	MONGOLIA	UZBEKISTAN
EL SALVADOR	MONTENEGRO	VENEZUELA
ERITREA	MOROCCO	VIETNAM
ESTONIA	MOZAMBIQUE	YEMEN
ETHIOPIA	MYANMAR	ZAMBIA
FINLAND	NAMIBIA	ZIMBABWE
FRANCE	NEPAL	
GABON	NETHERLANDS	
GEORGIA	NEW ZEALAND	
GERMANY	NICARAGUA	
	NIGER	
	NIGERIA	

The Agency's Statute was approved on 23 October 1956 by the Conference on the Statute of the IAEA held at United Nations Headquarters, New York; it entered into force on 29 July 1957. The Headquarters of the Agency are situated in Vienna. Its principal objective is "to accelerate and enlarge the contribution of atomic energy to peace, health and prosperity throughout the world".

IAEA HUMAN HEALTH SERIES No. 15

DUAL ENERGY X RAY
ABSORPTIOMETRY
FOR BONE MINERAL DENSITY
AND BODY COMPOSITION
ASSESSMENT

INTERNATIONAL ATOMIC ENERGY AGENCY
VIENNA, 2010

COPYRIGHT NOTICE

All IAEA scientific and technical publications are protected by the terms of the Universal Copyright Convention as adopted in 1952 (Berne) and as revised in 1972 (Paris). The copyright has since been extended by the World Intellectual Property Organization (Geneva) to include electronic and virtual intellectual property. Permission to use whole or parts of texts contained in IAEA publications in printed or electronic form must be obtained and is usually subject to royalty agreements. Proposals for non-commercial reproductions and translations are welcomed and considered on a case-by-case basis. Enquiries should be addressed to the IAEA Publishing Section at:

Marketing and Sales Unit, Publishing Section
International Atomic Energy Agency
Vienna International Centre
PO Box 100
1400 Vienna, Austria
fax: +43 1 2600 29302
tel.: +43 1 2600 22417
email: sales.publications@iaea.org
<http://www.iaea.org/books>

© IAEA, 2010

Printed by the IAEA in Austria
December 2010
STI/PUB/1479

Emended version, March 2013.

Details of revisions are available at: www-pub.iaea.org/books/

IAEA Library Cataloguing in Publication Data

Dual energy X ray absorptiometry for bone mineral density and body composition assessment. — Vienna : International Atomic Energy Agency, 2010.

p. ; 24 cm. — (IAEA human health series, ISSN 2075-3772 ; no. 15)
STI/PUB/1479

ISBN 978-92-0-110610-0

Includes bibliographical references.

1. X-ray spectroscopy. — 2. Bone densitometry. — 3. Body composition.
— 4. Radiation — Safety measures. I. International Atomic Energy Agency.
II. Series.

IAEAL

10-00657

FOREWORD

The IAEA assists Member States in their efforts to develop effective evidence based interventions to combat malnutrition in all its forms using nuclear techniques. The unique characteristics of nuclear techniques in nutrition, in particular stable isotope techniques and dual energy X ray absorptiometry (DXA), make these methods highly suitable for development and evaluation of interventions to address the double burden of malnutrition, i.e. ‘undernutrition’ and ‘overnutrition’, globally.

This publication provides information on the theoretical background and practical application of state of the art methodology for bone mineral density (BMD) measurements and body composition assessment by DXA. The IAEA has contributed to the development and transfer of technical expertise in the use of DXA in Member States through support to national and regional nutrition projects via the technical cooperation programme and coordinated research projects addressing priority areas in nutrition. This book will be an important part of the IAEA’s efforts to transfer technology and to contribute to capacity building in this field.

The publication was developed by an international group of experts and is intended for nutritionists, radiation technologists, researchers and health professionals using DXA for BMD measurements and body composition assessment. In particular, the major contributor to this book, J. Shepherd (United States of America) is gratefully acknowledged for generously sharing his technical expertise and extensive experience in this field.

The IAEA officer responsible for this publication was L. Davidsson of the Division of Human Health.

EDITORIAL NOTE

This publication does not address questions of responsibility, legal or otherwise, for acts or omissions on the part of any person.

Although great care has been taken to maintain the accuracy of information contained in this publication, neither the IAEA nor its Member States assume any responsibility for consequences which may arise from its use.

The use of particular designations of countries or territories does not imply any judgement by the publisher, the IAEA, as to the legal status of such countries or territories, of their authorities and institutions or of the delimitation of their boundaries.

The mention of names of specific companies or products (whether or not indicated as registered) does not imply any intention to infringe proprietary rights, nor should it be construed as an endorsement or recommendation on the part of the IAEA.

CONTENTS

1.	INTRODUCTION	1
1.1.	Background	1
1.2.	Objective	1
1.3.	Scope	1
1.4.	Structure	1
2.	INTRODUCTION TO DUAL ENERGY X RAY ABSORPTIOMETRY	2
2.1.	What is DXA?	2
2.2.	DXA bone density	3
2.3.	Three compartment model of body composition	3
2.4.	Measurements from DXA scans	4
2.5.	DXA measurement sites	5
3.	BACKGROUND INFORMATION INCLUDING SAFETY AND ETHICAL CONSIDERATIONS	6
3.1.	Historical methods for bone densitometry	6
3.2.	Why use DXA instead of other body composition methods? ..	7
3.3.	Limitations of DXA measurements	7
3.4.	Responsibilities under radiation protection regulations for the use of DXA	9
3.4.1.	Safety considerations	9
3.5.	Dose	9
3.5.1.	Typical patient doses from DXA	10
3.6.	Ethical considerations	11
3.6.1.	Patient radiation protection	11
3.6.2.	Radiation protection for children	12
3.6.3.	Radiation protection for pregnant women	13
3.6.4.	Personnel radiation protection	14
3.6.5.	Public radiation protection	15
4.	DXA TECHNIQUE FOR BONE AND SOFT TISSUE COMPOSITION	16
4.1.	Physics of absorptiometry	16

4.2.	Biological composition standards	18
4.3.	Principles of DXA	20
4.4.	Theory of DXA body composition	23
4.5.	DXA systems	26
4.6.	Generating dual energy images: Voltage switching versus K-edge filtering	30
5.	DXA SCAN ACQUISITION	31
5.1.	DXA regions of interest	31
5.1.1.	Spine	31
5.1.2.	Proximal femur	32
5.1.3.	Forearm	34
5.1.4.	Total body	34
5.1.5.	Vertebral fracture assessment	36
5.2.	Clinical protocol for DXA acquisition	38
5.2.1.	Before scanning the patient	38
5.2.2.	Scanning the patient	39
6.	DXA SCAN ANALYSIS	42
6.1.	Automatic analysis	42
6.2.	Special regions and derived results	45
6.2.1.	Skeletal muscle	45
6.2.2.	Adipose tissue	46
6.2.3.	Intra-abdominal adipose tissue and DXA	46
6.2.4.	Subcutaneous adipose tissue	50
6.2.5.	Standardized bone mineral density	51
6.2.6.	Bone mineral apparent density	52
6.3.	Obese patients	52
6.4.	Children	55
6.5.	Quality Control	57
6.5.1.	Scanning the spine phantom	57
6.5.2.	Air scan procedure (table top radiographic uniformity)	58
6.5.3.	Whole body quality control for DXA	60
6.5.4.	Special paediatric phantoms	62
6.5.5.	Research studies	62
6.5.6.	Training of personnel	62
6.5.7.	Precision and repeatability	65

6.5.8.	Accuracy and cross-calibration of DXA systems	67
6.5.9.	Monitoring the stability of a DXA system	70
6.6.	Artefacts	71
6.6.1.	Soft tissue composition and baseline measurement	71
6.6.2.	Patient obesity, weight change and bone size	71
6.6.3.	Contrast agents from other procedures	73
6.6.4.	Pacemakers	75
6.6.5.	Calcium tablets	75
6.6.6.	Patient movement	76
6.6.7.	Metal in the scan field: Total hip and knee arthroplasty	76
7.	REPORTING RESULTS	79
7.1.	Demographic information needed	79
7.2.	Reference data and associated values	80
7.2.1.	Use of reference data for generating T and Z scores	81
7.2.2.	Fracture risk models	83
7.2.3.	Use of Z scores in children	86
7.2.4.	Reference ranges for PCTFM	86
7.2.5.	How to collect local reference data	87
APPENDIX I:	DXA DENSITOMETER QC REPORT	91
APPENDIX II:	DXA PATIENT QUESTIONNAIRE	92
APPENDIX III:	NORMATIVE DXA DATA FOR PAEDIATRIC SUBJECTS	96
REFERENCES	105
CONTRIBUTORS TO DRAFTING AND REVIEW	115

1. INTRODUCTION

1.1. BACKGROUND

Dual energy X ray absorptiometry (DXA) is an X ray imaging technique primarily used to derive the mass of one material in the presence of another through knowledge of their unique X ray attenuation at different energies. DXA is an extremely accurate and precise method for quantifying bone mineral density (BMD) and mass body composition assessment, which is, thus, suitable for the development and evaluation of interventions to address the double burden of malnutrition, i.e. ‘undernutrition’ and ‘overnutrition’, globally.

1.2. OBJECTIVE

This publication provides information on the theoretical background and practical application of state of the art methodology for BMD measurements and body composition assessment by DXA. It is intended for nutritionists, radiation technologists, researchers and health professionals using DXA for such analysis.

1.3. SCOPE

This manual focuses on DXA scan acquisition and analysis. Scan acquisition includes the various regions of interest (ROIs), e.g. spine, proximal femur, forearm and whole body, that can be scanned as well as the clinical protocol for DXA scan acquisition. Analytical procedures used for interpreting scans for different tissues of the body as well as special considerations for obese patients and children are detailed. Quality control and artefacts are also discussed.

1.4. STRUCTURE

Section 2 presents an overview of DXA. Section 3 provides background information, including safety and ethical considerations. Section 4 describes the DXA technique for bone and soft tissue composition. Section 5 addresses DXA scan acquisition while Section 6 covers DXA scan analysis. The topic of Section 7 is preparing a DXA report. Finally, three appendices provide relevant auxiliary information, namely an example of a DXA densitometer quality control

(QC) report, a DXA patient questionnaire, and normative DXA data for paediatric subjects.

2. INTRODUCTION TO DUAL ENERGY X RAY ABSORPTIOMETRY

2.1. WHAT IS DXA?

DXA is an X ray imaging technique primarily used to derive the mass of one material in the presence of another through knowledge of their unique X ray attenuation at different energies. Two images are made from the attenuation of low and high average X ray energy. DXA is a special imaging modality that is not typically available with general use X ray systems because of the need for special beam filtering and near perfect spatial registration of the two attenuations. Dedicated commercial DXA systems first became available in the late 1980s [1].

DXA is an extension of an earlier imaging technique called dual energy photon absorptiometry (DPA). The DXA technique differs from DPA only in that DPA uses the attenuation of monochromatic emissions from a radioisotope (i.e. ^{153}Gd), while DXA uses polychromatic X ray spectra for each image, centred at different energies. DXA's primary commercial application has been to measure BMD to assess fracture risk and to diagnose osteoporosis; the X ray energies used are optimized for bone density assessment. For osteoporosis diagnosis, the lumbar spine, proximal hip and, sometimes, the distal forearm are scanned. The ROIs used and the diagnostic criteria are well defined. The whole body can also be scanned to measure whole body bone mass and soft tissue body composition [2, 3]. In image areas that contain only soft tissue, lipid and lean tissue can be assessed [4], from which per cent lipid mass can be calculated, while areas that contain bone use an estimated per cent lipid from the surrounding tissue [5]. Reference populations have been scanned and defined by sex, ethnicity and age. Diagnosis of disease is typically undertaken by comparing individuals to their peer group or to a young healthy population. Currently, there are estimated to be over 50 000 whole body DXA systems in use worldwide.

2.2. DXA BONE DENSITY

DXA is one of the most accurate and precise methods for quantifying BMD and mass in vivo. Bone mineral mass, primarily consisting of hydroxyapatite, is the mineral component of bone that is left after a bone is defleshed, lipids extracted and ashed. The nature of the DXA system is that it creates a planar (two dimensional) image that is the combination of low and high energy attenuations. Although density is typically thought of as a mass per unit volume, DXA can only quantify the bone density as a mass per unit area, since it uses planar images and cannot measure the bone depth. In contrast, the measurement of bone density using a computed tomography (CT) system, called quantitative computed tomography (QCT), can measure the true volume and volumetric bone density. Bone size varies as a function of age. Thus, DXA bone density values increase from birth to adulthood, primarily because the bones become larger. Bone size is also influenced by ethnic differences and sex. One has to be careful to compare DXA bone density values to a similar population or results can be easily misinterpreted. Asians typically have lower DXA bone density values compared to sex and age matched Caucasians, partly due to bone size differences [6].

2.3. THREE COMPARTMENT MODEL OF BODY COMPOSITION

DXA defines the composition of the body as three materials having specific X ray attenuation properties: bone mineral, lipid (triglycerides, phospholipid membranes, etc.) and lipid free soft tissue. The term fat is commonly used to refer to adipose tissue. However, adipose tissue contains lipid free mass, such as water and proteins as well. Fat is best described chemically as the lipids in our body that are soluble in organic solvents and not in water, the largest category of body fat being triglycerides found in adipocytes. The non-lipid soft tissue mass (STM) is the sum of body water, protein, glycerol and soft tissue mineral mass. For each pixel in a DXA image, these three mass components are quantified. However, the distribution of the lipid, bone mineral and non-lipid soft tissue within the volume projected onto the image pixel is not known. The model forces all tissue types into these three components. For example, the distinction between subcutaneous adipose tissue (SAT) and visceral adipose tissue (VAT) is lost for trunk measurements when both are projected in the same pixels. The same is true for skin, visceral non-adipose tissue and muscle when all are projected in the same pixels. This limitation is true for most composition models that cannot represent the body as a true three dimensional volume.

2.4. MEASUREMENTS FROM DXA SCANS

There are relatively few values reported from DXA body composition systems. They are listed here. The bone measures are available from all DXA scan modes while the body composition measures are only available from the whole body scan mode.

Bone mineral content (BMC). BMC is the mineral mass component of bone in the form of hydroxyapatite, $\text{Ca}_{10}(\text{PO}_4)_6(\text{OH})_2$. BMC is typically measured in grams. Note that BMC does not include the mass of any of the organic components of bone (marrow, collagen, etc.). Thus, accuracy can only be assessed against ashed bone samples.

Bone area (BA). BA is the projected area of the bone onto the image plane, typically in cm^2 . The accuracy of the BA is questionable, especially in whole body scans where bold assumptions need to be made, particularly in the upper torso.

Areal bone mineral density (aBMD). aBMD is the mineral mass of bone per unit image area in g/cm^2 . Here, a distinction is made between areal density and true volume density. Volume density, the mineral mass per unit bone volume, cannot be directly measured by DXA but can be measured by QCT. aBMD is defined as:

$$\text{aBMD} = \text{BMC}/\text{BA} \text{ (g/cm}^2\text{)} \quad (1)$$

The following measures are only from whole body scans.

Fat mass (FM). DXA FM is the common term used in the DXA field for lipid mass, and is the sum of all lipid mass. Strictly speaking, fat is chemically defined as triglycerides. However, in this book, DXA FM will be defined as all lipid mass, including phospholipids, organ, marrow and subcutaneous adipose. FM is measured in either g or kg.

Lean soft tissue mass (LSTM). Bone free, fat free STM is the sum of all soft tissue lean, essentially water, protein, soft tissue mineral and glycogen. It is measured in units of g or kg.

Fat free mass (FFM). FFM is the sum of all the non-body lipid, such that:

$$\text{FFM} = \text{LSTM} + \text{BMC} \text{ (g)} \quad (2)$$

Soft tissue mass: STM is the sum of lean soft tissue and FMs:

$$\text{STM} = \text{FM} + \text{LSTM} \text{ (g)} \quad (3)$$

Total body mass (TBM). TBM is the equivalent measure to scale weight, typically represented in g or kg. In terms of the above:

$$\text{TBM} = \text{FM} + \text{FFM} = \text{FM} + \text{BMC} + \text{LSTM} \text{ (g)} \quad (4)$$

TBM accuracy can be assessed against a calibrated scale. Studies that have investigated the agreement between scale mass and DXA total mass have found excellent agreement.

Per cent fat mass (PCTFM). PCTFM is a region's FM divided by its total mass times 100:

$$\text{PCTFM} = \text{FM}/\text{TBM} \times 100 \quad (5)$$

2.5. DXA MEASUREMENT SITES

When evaluating bone density using DXA to diagnose osteoporosis, there are several common measurement sites, including the lumbar spine, the proximal hip and the forearm. The standard protocol is to scan two sites, typically the spine and hip. If one of these sites is not available, then the forearm is used. The current standards for using DXA for diagnosing osteoporosis can be found in the position statements of the International Society for Clinical Densitometry (ISCD) [7]. The whole body scan is primarily used for bone mass measurements in children and for body composition measurements in adults. Other technologies can measure bone density for osteoporosis assessment. The most common alternatives to DXA are QCT and quantitative ultrasound (QUS). QCT uses special scan protocols on standard CT systems to quantify volumetric bone density. QUS is the use of ultrasound attenuation and the speed of sound to quantify fracture risk and estimate bone density.

The measure of body composition is done using whole body DXA scans. It is possible to get a PCTFM measure from hip and spine scans with some DXA systems. However, the utility of PCTFM from these ROIs is not clear.

3. BACKGROUND INFORMATION INCLUDING SAFETY AND ETHICAL CONSIDERATIONS

3.1. HISTORICAL METHODS FOR BONE DENSITOMETRY

Many methods have been proposed or are being used to measure bone density and quality, and most involve an X ray procedure. Bone can be physically examined and its properties measured by excision of the bone from the patient. Iliac crest core biopsy was and, in some circumstances, still is a popular bone quality assessment. Although this procedure is fairly simple, it is invasive. X ray plain films of the hip and spine have also been used to assess osteoporosis. The Singh index, a visual assessment of radiopacity of the trabecular tissue in the trochanter, and the calcar width were two measurements used to evaluate osteoporosis from plain films of the hip [8, 9]. However, a change of approximately 30% in the trabecular density had to occur before the change could be detected, and X rays needed to be of high spatial resolution, and thus of high dose. The metacarpal index (MCI) is also a technique that can be applied to film X rays [10]. MCI is defined as the ratio of the thickness of the metacarpal cortical shell to the overall diameter. Changes in cortical bone thickness could be quantified with precision, but cortical bone does not turn over and change as quickly as trabecular bone.

When films could be digitized, techniques such as radiographic absorptiometry (RA) were introduced [11, 12]. Unlike MCI and the Singh index, RA is true absorptiometry; in this case, the quantification of bone density in the phalanges by comparing their X ray absorption to that of different thicknesses of aluminium. The phalanges contain a significant amount of trabecular bone with little overlapping STM. Measuring trabecular-rich tissue allows for the more sensitive monitoring of bone loss due to its low precision error and absolute calibration to standards. However, the fingers are neither load bearing nor a high mortality fracture site.

The desire to measure fracture sites with a high mortality and sensitivity to change with disease was not being met with the above methods. In the 1970s, DPA and QCT were two of the first absorptiometry methods used for the hip and spine. DPA consisted of a dedicated scanner containing the isotope ^{153}Gd as the radiation imaging source to scan either the hip, spine or whole body [13–15]. DPA data had limited accuracy due to the poor image quality and high noise from the limited gamma ray flux from practical ^{153}Gd sources. On the other hand, QCT provided true volumetric densitometry of the spine by measuring the area of the bone in a tomogram of a known thickness [16, 17]. However, most CT systems

are heavily used for patients in need of emergency medicine and critical care, and it is costly to provide it as a screening measure.

DXA was introduced commercially as the direct successor to DPA in 1987 [18]. The main advantages of an X ray system over a DPA radionuclide system are shortened examination time due to an increased photon flux of the X ray tube and improved trueness and precision resulting from higher resolution [19]. Since the inception of DXA, virtually all other methods have fallen out of favour because DXA is an optimal combination of cost, effectiveness and availability [20].

3.2. WHY USE DXA INSTEAD OF OTHER BODY COMPOSITION METHODS?

There are many techniques to measure body composition, so why use DXA? The criterion measure of total body water (TBW) assessment uses the dilution of stable isotopes in body water to derive the total. This is a relatively inexpensive technique that quantifies TBW mass [21]. However, TBW takes 3–8 h to complete, while DXA takes less than 5 min. Bioimpedance analysis relates electrical resistance and reactance to intracellular and extracellular water. Since most extracellular water is in lean tissue and fat is, for the most part, extracellular and water free, the per cent body fat can be modelled when the height, weight, age and sex are known. Other whole body methods include hydrodensitometry, neutron activation and anthropometry. However, these techniques are difficult to use for regional measures. Only imaging methods, such as DXA, CT and MRI, can estimate regional bone, fat and soft tissue lean distributions. DXA is low dose in comparison to whole body CT scanning and inexpensive compared to MRI. In addition, DXA PCTFM measures are very precise where test/retest repeatability is commonly found to be 0.5%. Lastly, DXA is easily tied to physical standards that are verifiable in the field, such as steric acid and water, such that cross-calibration and pooling of data across clinical centres is possible.

3.3. LIMITATIONS OF DXA MEASUREMENTS

Bone volume projected into pixel is not known. DXA systems measure bone density in units of grams per unit area since DXA does not have the ability to measure tissue thickness. Thus, DXA systems cannot tell the difference between thick low density bone and thin high density bone.

Fan beam magnification. Fan beam imaging inherently magnifies the BA with a magnification factor that is proportional to the height of the scanner table.

Thus, bone size can vary solely due to body diameter. In general, there is an associated demagnification of bone mass, such that aBMD remains relatively stable. BMC magnification is particularly an issue in growing skeletons and there is ongoing discussion regarding the appropriateness of the use of projectional techniques in children and growing young adults [22–25].

Two compartments and only two. DXA can only solve for two materials simultaneously. This is a fundamental theorem of X ray absorptiometry, since the attenuation characteristics of any one material can be represented by combining two other materials together in the appropriate way [26]. Thus, soft tissue composition can only be solved in areas exclusive of bone, and bone mass can only be determined with an assumption of the soft tissue composition overlaying the bone. Since bone is typically contained in 40% or more of the body image pixels, the soft tissue composition has to be estimated from surrounding tissue. In some cases, accurate estimates cannot be made, such as the head, hands, feet and upper torso because there is not adequate soft tissue outside the bone projection, and manufacturers turn to proprietary methods to reference the soft tissue.

Lack of standardization. Generally, BMD values across manufacturers cannot be directly compared and are not interchangeable for several reasons. First, there are known differences in relative accuracy in aBMD, BMC and BA between systems. For example, the differences in aBMD between the two largest manufacturers, Hologic (Hologic, Inc., Bedford, MA, United States of America) and GE Lunar (GE Healthcare, Madison, WI, United States of America) systems are approximately 8% in BMD and 20% in BMC. There is also a lack of standardization on the placement of ROIs. Two examples are the femoral neck ROI and the forearm ROIs between the Hologic and GE systems. There have been some attempts to take out the systematic differences between systems for aBMD of the spine, total hip and femoral neck by using standardized BMD (sBMD) units [27]. The standardization that does exist is covered in Section 6.2.5. However, no attempt has been made to standardize BMC, and aBMD values have not been derived for other ROIs, including the lateral spine, fingers, heel or whole body.

Degenerative changes. Degenerative changes [28–31], aortic calcifications [32, 33] and fractured vertebrae are difficult to visualize and can cause significant bias to the BMD results. Disc degeneration, aortic calcifications and fractures typically increase aBMD values. Disc degeneration and fractures reduce the BA, increasing aBMD, while aortic calcifications project additional mineral in the spine area. These biases are systematic and typically found in older populations beyond the age of 65 years. Thus, the utility of spine scans decreases in older adults, although lateral spine projections remove aortic calcification from the projected BA and, thus, may reflect bone mass more accurately in the elderly.

3.4. RESPONSIBILITIES UNDER RADIATION PROTECTION REGULATIONS FOR THE USE OF DXA

Most countries require that the legal person responsible for the DXA facility unit apply to the radiation protection regulatory body for authorization — either registration or a licence. In some countries, formal notification may be sufficient. In each situation, the applicant will need to submit to the regulatory body the relevant information necessary to demonstrate the protection and safety of the practice. Typically, this includes information on the medical practitioners and technologists involved; their education and training in radiation protection; details on the DXA equipment and the room where it is to be located; and the facility's radiation protection programme for personnel, patients and public protection.

3.4.1. Safety considerations

General requirements for protection and safety are given in the International Basic Safety Standards for Protection against Ionizing Radiation and for the Safety of Radiation Sources (BSS) [34], with more specific guidance in IAEA publications on radiological protection for medical exposure to ionizing radiation [35], and applying radiation safety standards in diagnostic radiology and interventional procedures using X rays [36]. Once satisfied, the regulatory body issues authorization, typically with conditions or limitations that need to be complied with.

3.5. DOSE

DXA systems generate ionizing radiation. Thus, subjects being scanned and equipment operators, consequently, receive a (small) radiation dose as a result of any procedure. The absorbed dose to tissue is quantified as the amount of energy absorbed in a kilogram of tissue. The unit of measure is the Gray (Gy), where 1 Gy is equivalent to 1 J/kg. Another useful quantity of dose is 'effective dose', measured in sievert (Sv). Effective dose takes account not only of the amount of energy absorbed, but also the type of radiation and the susceptibility of the tissue to radiation damage. The effective dose is calculated as the sum of the absorbed doses to radiosensitive organs multiplied by their associated weighting factors, w_T and w_R . The tissue weighting factors and radiation weighting factors are defined in Ref. [37]. In other words, the effective dose, E , is the tissue weighted sum of the equivalent doses in all specific tissues and organs of the body, given by the expression:

$$E = \sum_T w_T \sum_R w_R D_{T,R}$$

where $D_{T,R}$ is the absorbed dose, w_R is the radiation weighting factor equal to one for diagnostic X rays, and w_T is the tissue weighting factor for different tissues (Table 1).

Effective dose is used in assessing occupational and public exposure to radiation. It is also useful in characterizing the dose typically received by a patient from a given X ray procedure.

3.5.1. Typical patient doses from DXA

Patient effective doses in DXA depend on the type of unit (pencil beam, fan beam, cone beam), the protocol or mode used for the scan (scan area, tube current, scan speed) and the body region being scanned.

DXA scans of the forearm are very low, typically less than 1 μ Sv irrespective of the type of scanner and protocol or mode. Lumbar spine, hip or whole body scans each result in an effective dose of about 1 μ Sv for a pencil beam unit and up to about 10 μ Sv for a fan beam unit [38–43]. Some earlier fan beam DXA units initially delivered effective doses as high as 80 μ Sv [40, 43]. There is not much data for doses from cone beam units, but doses appear to be similar to those for fan beam units.

Many DXA units offer different acquisition modes — typically, the tube current and/or scanning speed is changed. The patient dose may change by a factor of 1.5 to 3 [38], or more, between using the lowest and highest dose mode for the same examination. As noted later (Section 6.3), it may be necessary to use the higher dose modes for obese patients.

TABLE 1. TISSUE WEIGHTING FACTORS BASED ON REF. [37]

Tissue	w_T	$\sum w_T$
Bone marrow (red), colon, lung, stomach, breast, remainder tissues ^a	0.12	0.72
Gonads	0.08	0.08
Bladder, oesophagus, liver, thyroid	0.04	0.16
Bone surface, brain, salivary glands, skin	0.01	0.04
Total		1.00

^a Remainder tissues: adrenals, extrathoracic region, gall bladder, heart, kidneys, lymphatic nodes, muscle, oral mucosa, pancreas, prostate, small intestine, spleen, thymus, uterus/cervix.

Paediatric patient effective doses, using an appropriate paediatric protocol, are similar to those for an adult [38, 39, 41]. However, adult protocols applied to children can lead to doses approaching 20 μSv [38].

To put these DXA patient doses into perspective, it is helpful to consider exposure from other sources. Human beings are constantly exposed to ionizing radiation from natural sources, including cosmic rays and naturally occurring radioactive material in foods, soil, water and air. This is collectively referred to as natural background radiation. The average annual natural background radiation dose to humans worldwide is about 2400 μSv , but this can vary from 1000 to 10 000 μSv , with some populations receiving 20 000 $\mu\text{Sv/a}$ [44]. Thus, in comparison, effective patient doses from DXA are small and are similar to those received on average from one or two days of exposure to natural background radiation. Adult effective doses, represented in μSv , for various radiological procedures and conditions, including DXA procedures, are shown in Fig. 1.

3.6. ETHICAL CONSIDERATIONS

3.6.1. Patient radiation protection

The BSS [34] require that all medical exposures are appropriately justified. The diagnostic benefit from DXA must outweigh the radiation detriment that might ensue. The ICRP [45] recommends that both generic justification and individual justification are applied. For generic justification, the national professional bodies, in conjunction with national health authorities and the radiation protection regulatory body, will have decided which DXA procedures generally improve the diagnosis or treatment, or provide necessary information about the exposed individuals. Individual justification considers whether the application of the particular DXA procedure to a particular individual is justified or not.

DXA procedures may also be used as part of a biomedical research project, such as in the role of a metric where the measurement of bone density or body composition is part of assessing the efficacy of the treatment under investigation. In this situation, the benefit from the use of radiation is expected to be accrued by society, such as through improved health care options. The use of DXA procedures in this role must normally also be justified by an ethics committee.

If a given DXA procedure is justified, then the BSS [34] require that its performance is optimized. For DXA, this means ensuring that the patient dose is the minimum necessary to determine bone density or body composition to an appropriate level of certainty. To this end, appropriate choices of parameters, such

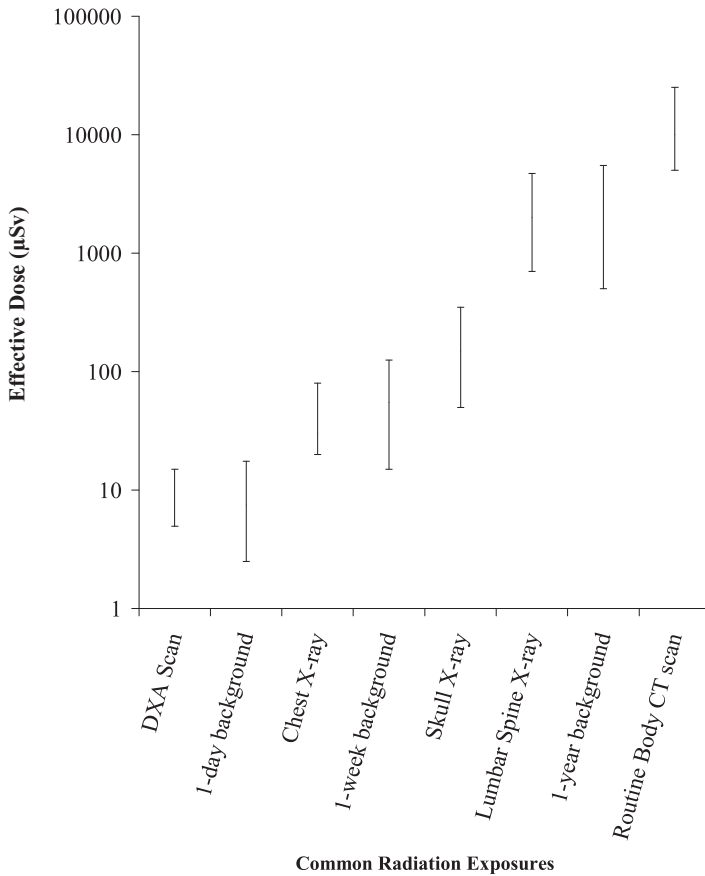


FIG. 1. Adult effective doses for various procedures and exposures.

as tube current, scan speed, scan area and body region (either directly or indirectly through selection of scan protocol and/or mode), are made for the particular individual undergoing the procedure. In addition to the QC tests for scanner measurement performance described elsewhere (Section 6.5), periodic QC tests should be made on X ray performance [34], including radiation output consistency, patient dose, X ray field size and beam divergence, and the exposure mechanism [46].

3.6.2. Radiation protection for children

The same radiation protection principles of justification and optimization apply to the use of DXA for children. Alternative non-ionizing methods for determining bone density (e.g. QUS) should be carefully considered in the case of

children, if appropriate. Due to the increased radiosensitivity of children, particular efforts need to be taken in the optimization of the DXA procedure. Many DXA units offer paediatric protocols, often with a reduced tube current and reduced scan lengths, and such features should be utilized when performing DXA scans of children. A qualified expert should advise on the appropriate means for the optimization of paediatric examinations on each DXA unit in a facility. Simply adjusting default adult scan lengths for child patients can reduce doses significantly [38]. Typical doses for paediatric DXA procedures are discussed above in Section 3.5.1.

It is important that the operator of the DXA unit takes time and care to gain the confidence of the child to increase cooperation and help minimize movement during the scan acquisition that may result in movement artefacts. Such artefacts lead to the need for repeat measurements and, hence, increased dose. Parents may be asked to act as a comforter for a child to help improve cooperation during the DXA scan. Parents acting in this role must receive information on radiation protection and a lead apron should be made available for wearing.

More specific information on scanning children is given in Section 6.4.

3.6.3. Radiation protection for pregnant women

In justifying a DXA procedure in the case of a pregnant woman, consideration should also be given to the urgency of the DXA procedure. If it can be postponed, this is recommended. However, if it is needed, then it should be performed, and the optimization of radiation protection should include means for reducing exposure to the foetus.

It is normal practice for waiting rooms, cubicles and other appropriate places in diagnostic X ray facilities to have signs requesting a female patient to notify the doctor, technologist or other personnel if she is or might be pregnant. A DXA facility should be no exception with respect to the use of such signs. Some DXA facilities may have a patient questionnaire in which the female patient is asked whether there is a chance that she is pregnant (see Appendix II). Procedures for determining the pregnancy status of a female of reproductive age are normally in place only for X ray procedures that may give a significant dose to the foetus and, therefore, are not warranted for DXA examinations.

Even with these precautions, the accidental scanning of a pregnant patient does sometimes happen. Here is an example: A patient took a pregnancy test on the same day as her appointment for a DXA examination as part of a study. The pregnancy test was negative and the patient received a whole body DXA that day. Two weeks later, the patient found out that she was indeed pregnant and informed her study doctor to ask if there was any concern.

Doses to the foetus from DXA procedures on pregnant women are very low, even for protocols that include the foetus in the primary beam. Reported doses are of the order of a few μSv or less [47, 48]. Potential radiation effects at these dose levels are so unlikely that their probability of occurrence cannot be calculated.

The exclusion of pregnant women may be a condition in an approved biomedical research project, and such screening of participants normally occurs before needing to present for any DXA procedures that may be part of the project. It should be noted that researchers should be aware of local regulations regarding giving pregnancy tests, since in some jurisdictions adolescents under the age of 16 are automatically granted legal emancipation from parents if they become pregnant.

3.6.4. Personnel radiation protection

Operators that perform the DXA procedure may also receive a radiation dose due to scattered radiation from the patient. This scattered dose is much less than the dose in the primary beam. While the occupational dose limit prescribed in the BSS is 20 000 $\mu\text{Sv/a}$ averaged over five consecutive years with a limit of 50 000 μSv in any single year [34], the application of the principle of optimization of protection means that occupational doses must be as low as reasonably achievable.

With DXA, occupational doses are determined primarily by the workload of the DXA unit (number of patients per day), the distance the technologist or other personnel are from the patient during the scan, and the type of scanner and the protocols/mode being used. The instantaneous dose rates of scatter are lowest for pencil beam units, higher for fan beam units and highest for cone beam units, where instantaneous dose rates have been reported of around 200 $\mu\text{Sv/h}$ at a distance of 1 m from the patient [49]. Fan beam and cone beam DXA units also facilitate higher patient throughput and, hence, potentially higher integrated levels of scatter. With a workload of 20 patients/d, the annual dose for a person always positioned at a distance of 1 m from the patient is between 100 and 1500 μSv , depending on the scanner model [46, 50, 51].

In practical terms, the operator's desk should be positioned at least 1 m away from a pencil beam system, and at least 2 m away from a fan beam system [50]. Some older, less common fan beam models require a distance of 3.5 m [43]. In the case of fan beam and cone beam configurations or if the distances above cannot be accommodated, the use of protective screens or shields may be considered. Specific recommendations for occupational radiation protection should be made by a suitably qualified expert on the basis of an on-site assessment at the time of installation and commissioning. With these precautions,

it is most likely that the operator dose will be in the lower range of acceptable occupational exposures.

Requirements for personal monitoring depends on national regulations. In some countries, it is required that all occupationally exposed workers, who normally work in a controlled area, should wear a dose monitoring device (film, thermoluminescent dosimeter or other) for the purposes of monitoring their individual exposure. In cases where personal monitoring is not required, it may be more suitable to monitor the workplace, with suitable dosimeters placed at selected points of interest within the DXA facility, such as the operator's work position.

Female operators of DXA units should inform their employer if they become pregnant. The BSS [34] require the employer to adapt the working conditions in respect of occupational exposure, so as to ensure that the foetus is afforded the same broad level of protection as required for members of the public. In the case of working in a DXA facility, there is normally no need for any change, provided sound radiation protection practice was already being followed. A qualified expert should provide specific advice.

3.6.5. Public radiation protection

Any exposure to a person in an adjacent room depends on the workload (number of patients), the type of DXA scanner, the distance from the table axis to the walls and the wall composition. In a properly designed DXA facility with adequate room size, the radiation levels in adjoining rooms is normally at a level acceptable for members of the public. Typically, no additional shielding is required in the walls. However, care does need to be taken with cone beam and some fan beam DXA units [46]. In some cases, additional radiation shielding may be required if the distance from the table axis to the adjacent wall is less than 1 m. If the walls of the scanner room are of solid construction (i.e. solid concrete or brick, not cavity blocks or partition walls) or the desk in the office in the next room is more than 2 m away from the DXA system, then it is likely that the dose will be within acceptable levels. Estimates of dose to the public, based on measurements, should be made by a qualified expert at the time of installation and commissioning.

4. DXA TECHNIQUE FOR BONE AND SOFT TISSUE COMPOSITION

4.1. PHYSICS OF ABSORPTIOMETRY

X rays in the energy range used for DXA interact with tissue using three processes: photoelectric absorption, Compton (inelastic) scattering and coherent (elastic) scattering [52, 53]. Coherent scattering occurs when X rays pass close to an atom and cause ‘bound’ electrons to vibrate (resonate) at a frequency corresponding to that of the X ray photon. The electron re-radiates this energy in all directions and at exactly the same frequency as the incoming photons without absorption. Although a certain amount of elastic scattering occurs at all X ray energies, it never accounts for more than 10% of the total interaction processes in diagnostic radiology. Compton scattering occurs when the incoming photon loses some of its energy to the electron and then continues in a new direction (i.e. it is scattered) but with increased wavelength and, hence, with decreased energy. Compton scatter creates two major problems in X ray imaging. First, it reduces the contrasts in the image unless it is removed by collimation before the detector. Second, it presents a radiation risk to the personnel using the equipment. Attenuation by the photoelectric effect occurs when a photon interacts with the atom by ejecting an electron from its orbit or shell around a nucleus. The input photon is totally absorbed in the process; however, a lower energy fluorescent photon is usually emitted. Whenever the input photon energy is just slightly greater than the energy required to remove an electron from a particular shell around the nucleus, there is a sharp increase in the probability of a photoelectric interaction. This phenomenon is known as an absorption edge. There are two reasons for the sudden increase in absorption. First, the number of electrons available for interaction and ejection from the atom increases. Second, a resonance phenomenon occurs whenever the photon energy just exceeds the binding energy of a given shell.

The above absorption processes contribute to the total attenuation of an X ray flux passing through a subject as represented by the following equation:

$$I = I_0 e^{-\mu t} \quad (6)$$

where I_0 is the unattenuated X ray intensity before it passes through a material with a thickness, t (cm) and a total linear attenuation coefficient, μ (cm^{-1}). There are several important considerations regarding linear attenuation for X rays:

- μ decreases with increasing energy in the diagnostic energy range, i.e. the radiation becomes more penetrating;
- μ increases with increasing tissue density, i.e. the radiation is less penetrating because there are more atoms per unit volume in the material with which to collide;
- μ increases with atomic number, most strongly at very low energies;
- Absorption edges cause a sharp increase of μ for energies just above the edge energy.

Another convenient way of expressing attenuation is as a ‘mass’ attenuation coefficient by representing the thickness as mass per unit area by multiplying thickness by density. Then, Eq. (7) can be written as:

$$I = I_0 e^{-\mu t} = I_0 e^{-\mu \left(\frac{\rho}{\rho}\right) t} = I_0 e^{-\left(\frac{\mu}{\rho}\right) t \rho} = I_0 e^{-\left(\frac{\mu}{\rho}\right) \sigma} \quad (7)$$

where (μ/ρ) = mass attenuation coefficient in units of cm^2/g and σ = areal mass density = ρt . Eq. (8) is valid for calculating the attenuation for any medium (solid, liquid or gas). To determine the total attenuation from all three attenuation interactions, one simply sums the mass attenuation coefficients from each effect:

$$\left(\frac{\mu}{\rho}\right)_{\text{Total}} = \left(\frac{\mu}{\rho}\right)_{\text{Photoelectric}} + \left(\frac{\mu}{\rho}\right)_{\text{Compton}} + \left(\frac{\mu}{\rho}\right)_{\text{Coherent}} \quad (8)$$

Most attenuation tables in physics handbooks list each attenuation effect separately with the total. Table 2 provides the total mass attenuation coefficients for common materials relevant for DXA studies. Further attenuation coefficients are available from reference books such as the CRC Handbook on Chemistry and Physics [54] and Internet web sites such as the NIST materials database (see <http://physics.nist.gov/PhysRefData/Xcom/Text/XCOM.html>).

When a substance is not a homogeneous material, the mass fractions are sum weighted by their mass attenuation coefficients to form a composite mass attenuation coefficient. Examples of composite attenuations are when X rays are attenuated by different tissues such as bone, marrow, fat, muscle, etc. If the beam passes through N different materials, Eq. (8) is written as [53]:

$$I = I_0 e^{-\sum_{i=1}^N \left(\frac{\mu}{\rho}\right)_i \sigma_i} \quad (9)$$

TABLE 2. MASS ATTENUATION COEFFICIENTS FOR TISSUES ENCOUNTERED IN BODY COMPOSITION (DENSITIES ARE GIVEN AT 25°C AT 1 ATM FOR AIR AND WATER) [54]

Total mass attenuation coefficients					
Material	Air	Water	Muscle tissue	Cortical bone tissue	Adipose tissue
Mass density ρ (g/cm ³)	0.0012	1.0	1.040	1.650	0.916
Photon energy (keV)	Mass attenuation coefficient, (μ/ρ) (cm ² /g)				
10	4.91	5.066	5.154	19.79	3.081
15	1.522	1.568	1.604	6.193	1.009
20	0.7334	0.7613	0.7777	2.753	0.5332
30	0.3398	0.3612	0.3651	0.9534	0.2959
40	0.2429	0.2629	0.2635	0.5089	0.2353
50	0.2053	0.2245	0.224	0.3471	0.2102
60	0.1861	0.2046	0.2036	0.2727	0.1961
80	0.1658	0.1833	0.1819	0.2082	0.1794
100	0.154	0.1706	0.1692	0.1803	0.1684
150	0.1356	0.1505	0.1492	0.1493	0.1497
200	0.1234	0.137	0.1358	0.1334	0.1366

4.2. BIOLOGICAL COMPOSITION STANDARDS

The biological standards of the body that are most relevant to DXA body composition measures are outlined below. In the molecular model, the body is represented as five compartments: water, protein, mineral, glycogen and lipid [55].

Table 3 summarizes the density and stoichiometry most widely used to model each component. These are presented to be of assistance in both understanding the modelling of DXA body composition and to allow for phantoms to be derived that best mimic the stoichiometry of human body composition using Eq. (9).

TABLE 3. BODY COMPOSITION OF A REFERENCE MAN [61]
(adapted from Wang [55], with exceptions noted)

Component	Fraction in reference man ^a	Stoichiometry	Molecular weight	Density (g/cm ³)
Water		H ₂ O		1.000
• Extracellular	26%			
• Intracellular	34%			
Protein	15%	C ₁₀₀ H ₁₅₉ N ₂₆ O ₃₂ S _{0.7}	2257.4	1.34
Mineral	5.3%	([Ca ₃ (PO ₄) ₂] ₃ Ca(OH) ₂)		2.982 [57]
Lipid				
• Phospholipids	2.1%	NA	NA	NA
• Triglycerides	17%	C ₅₁ H ₉₈ O ₆	806	0.900
Residual	0.6%	NA		1.404 [62]
• Glycogen ^a		C ₆ H ₁₀ O ₅		1.52

^a A reference man is defined as “being between 20–30 years of age, weighing 70 kg, is 170 cm in height, and lives in a climate with an average temperature of 10 to 20°C. He is Caucasian and is a Western European or North American in habitat and custom” [63].

Water. Water, H₂O, makes up over 60% of human body composition. The density of water is 1.000 g/cm³ at 37°C.

Protein. For the purposes of this publication, protein is defined as almost all compounds that contain nitrogen and range in complexity from simple amino acids to nucleoproteins. For density purposes, the stoichiometrically representative protein most widely used for DXA body composition modelling is C₁₀₀H₁₅₉N₂₆O₃₂S_{0.7}, with an average molecular weight of 2257.4 and a density of 1.34 g/cm³ at 37°C [56].

Mineral. The term mineral is used to describe the inorganic molecules in the body that contain metal elements such as calcium, sodium and potassium [55]. Mineral is found in the body as either osseous or extraosseous, with the osseous component being by far the largest. The osseous component is primarily made of calcium hydroxyapatite ([Ca₃(PO₄)₂]₃Ca(OH)₂), containing over 99% of the body’s calcium and 86% of the body’s phosphorus. The density of hydroxyapatite is estimated to be 2.982 g/cm³ in its solid state [57] and this is the value used for some four component models [58]. It is readily available in powder form and can be mixed with epoxy to form anthropomorphic bone shapes or standardized blocks at different densities.

Lipid and fat. As previously stated, lipid and fat are often used interchangeably. Lipids are not water soluble but are highly soluble in organic solvents such as benzene, chloroform and diethyl ether [59, 60], and can be subdivided into categories based on their complexity. Fat is synonymous with triglyceride, containing three fatty acids that have been esterified into glycerol. Fat is easily separated from dehydrated tissue using ether, leaving behind a lipid mass that makes up connective tissues and cellular membranes. DXA cannot distinguish between chemically extracted fat and the connective tissue/cellular membranes since all lipids have similar X ray attenuation properties. This must be taken into account when using DXA in body composition models. For a reference man, approximately 90% of the body's lipid is fat [61]. The commonly accepted representative stoichiometry of fat in humans is $C_{51}H_{98}O_6$, has a molecular weight of 806 and a density of 0.900 g/cm^3 at 37°C [61].

Glycogen. Carbohydrates are principally stored as glycogen and are found in the cytoplasm of cells. The overall body content of glycogen is very small, less than 1%, but higher concentrations are found in muscle and liver tissue, approximately 1% and 2.2% of their weights, respectively. The stoichiometric representation of glycogen is $C_6H_{10}O_5$, with a density of 1.52 g/cm^3 at 37°C [56].

4.3. PRINCIPLES OF DXA

DXA was developed to solve the mass density of two unknown materials when physical measurements of the materials, such as overall thickness, are either not available or practical. Three fundamental assumptions are used to determine bone density using two energies:

- (1) Transmission of X rays through the body within two energy windows can be accurately described by a monoexponential attenuation process (Eq. (10)).
- (2) Individual image pixels of the human body can be described as a two component system, i.e. soft tissue and bone mineral, or when bone is not present, fat and lean mass. Thus, DXA is described as a three component model for body composition.
- (3) The soft tissue overlaying the bone in the image has a composition and X ray properties that can be predicted by the composition and X ray properties of the tissue near but not overlaying the bone.

The three component model used for DPA and DXA is a simplification of the molecular model as shown in Fig. 2.

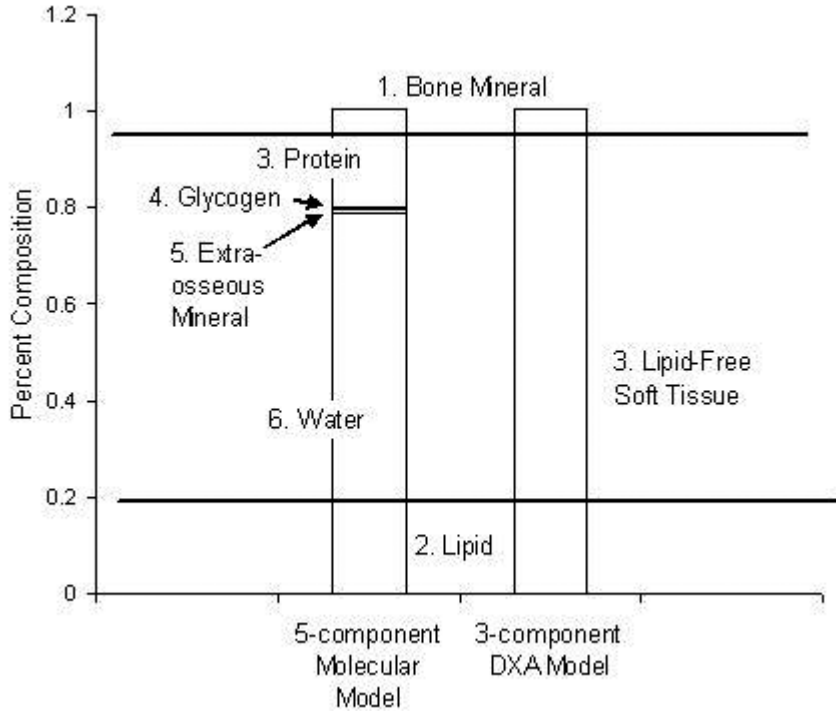


FIG. 2. The five component molecular model of body composition is compared to the three component model for DXA. Note that lipid is used instead of fat, since fat (triglycerides), membrane phospholipids and connective tissues are indistinguishable to a DXA system.

For simplicity, the equations will be derived for two monochromatic X ray beams with different energies (a high and low energy). The attenuation equation for each beam results in the following two equations:

$$I^L = I_0 e^{-\left[\left(\frac{\mu}{\rho} \right)_s^L \sigma_s + \left(\frac{\mu}{\rho} \right)_b^L \sigma_b \right]} \quad (10)$$

$$I^H = I_0 e^{-\left[\left(\frac{\mu}{\rho} \right)_s^H \sigma_s + \left(\frac{\mu}{\rho} \right)_b^H \sigma_b \right]} \quad (11)$$

where the H and L superscripts represent the high and low energy X ray beams, respectively, and σ is the areal density in units of g/cm^2 . Equations (11) and (12) are analogous to Eq. (10), where soft tissue, S, is Material 1, and bone, b, is Material 2. The equations are also written where Material 1 is fat and Material 2

is lean. Equations (11) and (12) are solved simultaneously for the bone areal density as follows:

$$\sigma_b = \frac{\left(\frac{\mu}{\rho}\right)_S^L \ln\left(\frac{I^H}{I_O^H}\right) - \ln\left(\frac{I^L}{I_O^L}\right)}{\left(\frac{\mu}{\rho}\right)_b^L - \left(\frac{\mu}{\rho}\right)_b^H \frac{\left(\frac{\mu}{\rho}\right)_S^L}{\left(\frac{\mu}{\rho}\right)_S^H}} \quad (12)$$

The ratio or R value for the soft tissue, R_S , is defined as:

$$R_S = \frac{\left(\frac{\mu}{\rho}\right)_S^L}{\left(\frac{\mu}{\rho}\right)_S^H} \quad (13)$$

and Eq. (13) can be rewritten as:

$$\sigma_b = \frac{R_S \ln\left(\frac{I^H}{I_O^H}\right) - \ln\left(\frac{I^L}{I_O^L}\right)}{\left(\frac{\mu}{\rho}\right)_b^L - \left(\frac{\mu}{\rho}\right)_b^H R_S} \quad (14)$$

In Eq. (15), the soft tissue measure is reduced to the R_S term. It should be noted that the solution for σ_S is found in the same fashion. All of the other terms in Eq. (15) are either directly measured or are defined by the known mass attenuation coefficient of bone. Using the last assumption, Eq. (15) is used to determine R_S from the tissue surrounding the bone that does not contain bone. In this region, $\sigma_b = 0$, and the intensity is exclusively attenuated by soft tissue, denoted by $I \rightarrow I_S$:

$$R_S = \frac{-\ln\left(\frac{I_S^L}{I_O^L}\right)}{-\ln\left(\frac{I_S^H}{I_O^H}\right)} \quad (15)$$

Thus, R_S is a measure of the per cent fat of the soft tissue. The numerator of Eq. (15) is graphically represented in Fig. 3. If R_S is averaged using values on either side of the bone and using a constant R over the bone, this is called the uniform distribution model [64] and is an appropriate approximation for the lumbar spine. If the per cent fat around the bone changes in a functional way, then R_S becomes a function of position explicitly defined outside the bone and interpolated over the bone. This is called the weighted linear distribution model [64] and is appropriate for areas such as the femur and long bones. In regions such as the head and upper torso, more approximations are necessary that are usually proprietary and have loose physical interpretation to solve for R_S . In short, R_S must be defined for every pixel to define the bone density. However, the calibration of the R value to soft tissue composition is not necessary unless it is desired to measure PCTFM.

4.4. THEORY OF DXA BODY COMPOSITION

In the derivation of how DXA works presented in Section 4.3, it is shown that DXA can only solve two mass components at a time. In addition, an R value can be defined in the pixels that contain no bone to find the PCTFM of those pixels. The mass of soft tissue above the bone can be solved easily after solving for the bone mass (Eq. (13)). However, the composition of the tissue that corresponds to the derived R_S still has to be determined.

For DPA, it is easy to derive the R_S values for different biological composite materials based on their mass density, atomic composition and the X ray energies used. An example is provided in Pietrobelli and Heymsfield [4]. If the soft tissue is modelled as a combination of muscle and adipose tissue, then R_S is constant for a particular PCTFM no matter how much total mass of the soft tissue is examined and can be derived from first principles (Fig. 4.) In this case, once standards of measurement have been defined, the lean and fat references, the measured R_S

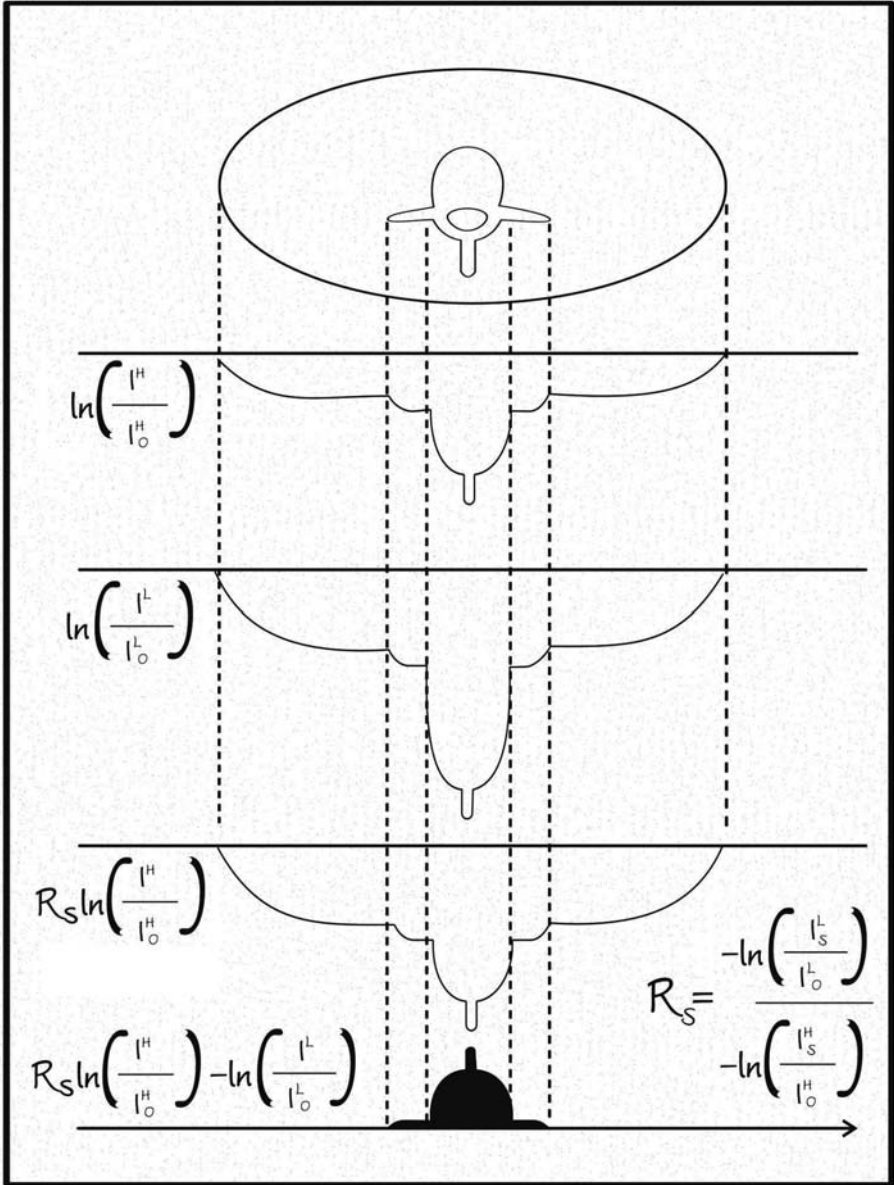


FIG. 3. Principle of DPA and DXA. The high energy absorption profile is multiplied by the soft tissue R value, R_S , which accounts for differences in high and low energy absorption of soft tissue. The soft tissue R value is measured in pixels that do not contain bone using Eq. (15) (drawing courtesy of J. Shepherd, UCSF).

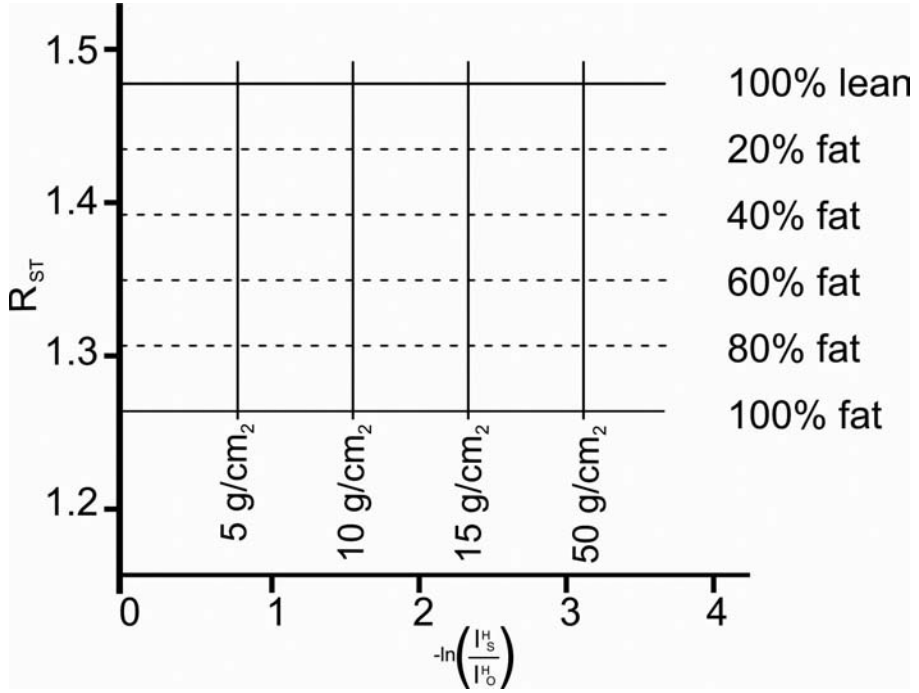


FIG. 4. Ideal relationship of R_{ST} to high energy transmission, the denominator of R_{ST} . The plot shows the high energy transmission that is approximated as a constant with respect to mass density. However, R_{ST} is constant as a function of PCTFM.

value can be converted to a PCTFM using the reference PCTFM and R value for the following equation:

$$\text{PCTFM}_S = \frac{\text{PCTFM}_{\text{Fat}} - \text{PCTFM}_{\text{Lean}}}{R_{\text{Fat}} - R_{\text{Lean}}} (R_S - R_{\text{Lean}}) + \text{PCTFM}_{\text{Lean}} \quad (16)$$

The absolute mass of an image pixel can be represented in terms of the fat and lean references as:

$$\sigma_{\text{Fat}} = \text{PCTFAT}_S \sigma_S \quad (17)$$

$$\sigma_{\text{Lean}} = (1 - \text{PCTFAT}_S) \sigma_S \quad (18)$$

Equation (17) is appropriate for DPA systems. Extensive work was done by Pietrobelli and Heymsfield [4] regarding the appropriate R values for Lunar DPA systems operating at low and high energy, 40 and 70 keV. They reported that

$R_{\text{Lean}} = 1.36$ for non-lipid soft tissue and $R_{\text{Lipid}} = 1.2$ for total lipid component. These values were well justified by reference man and phantom experiments.

However, Eq. (17) is complicated for DXA systems by beam hardening (the tendency of low energy X rays to be preferentially absorbed to high energy X rays, which shifts the average beam energy to a higher value). Thus, it is common practice to describe R_{Lean} and R_{Fat} as a function of high energy attenuation (HE), a surrogate for total mass, where PCTFT is a function of both R_S and HE where $\text{HE} = \ln(I_S^H/I_O^H)$. That is, $\text{PCTFT}_S = f(R_S, \text{HE})$. Figure 5 shows the results of scanning a calibration phantom of six different fat/lean combinations at four different thicknesses. Clearly, constant R values do not describe any one composition [65]. Figure 5 is from data acquired on a Hologic system but the same is true for any DXA system. In this case, Shepherd recalibrated the Hologic densitometer to measure breast tissue density using a model of steric acid for $\text{PCTFT}_{\text{steric acid}} = 100\%$ and the stoichiometry of fibroglandular tissue for $\text{PCTFT}_{\text{fibroglandular}} = 0\%$. Below are the forms of the equations from Ref. [65]:

$$\text{PCTFT}_S = c_1 + c_2 R_S + c_3 \text{HE} + c_4 \text{HE}^2 + c_5 R_S^2 + c_6 R_S \text{HE} \quad (19)$$

$$\text{Thickness} = d_1 + d_2 R_S + d_3 \text{HE} + d_4 \text{HE}^2 + d_5 R_S^2 + d_6 R_S \text{HE} \quad (20)$$

It should be noted that the calibration parameters, c_1-c_6 and d_1-d_6 in Eqs (20) and (21) are dependent on both the standards used for calibrating the R values as well as the average energies used for the low and high energy images. Thus, the approach outlined above can be used for DXA imaging with any two images of different average energies. However, the precision and contrast will vary as a function of the separation between the average energies.

In summary, the R_S values do not describe unique combinations of fat and non-fat soft tissue for DXA systems. DXA systems must be calibrated to lipid and non-lipid biological references as a function of tissue mass using HE.

4.5. DXA SYSTEMS

In commercially available DXA systems, the method by which low and high energy images are acquired varies according to manufacturer. For example, the exact X ray tube voltage settings are unique to each manufacturer. The need for excellent spatial registration between low and high energy images is critical, since this affects the R values. Misregistration can lead to substantial errors. For this reason, DXA is performed using electronic detectors and digital imaging

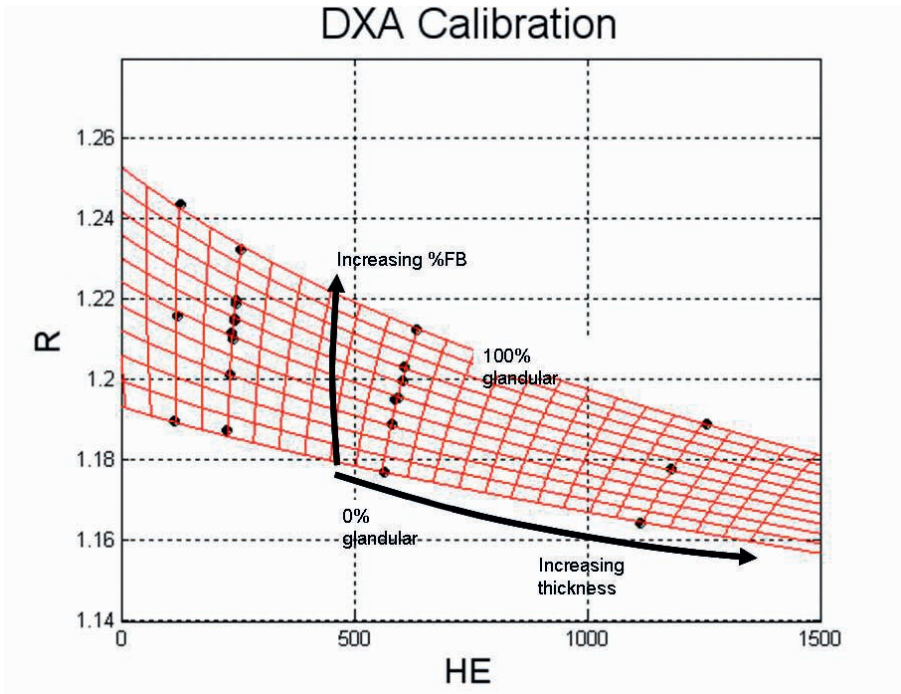


FIG. 5. DXA calibration function defined for finding breast PCTFT for pixels of varying thickness on a Hologic Delphi. This curve represented the R values as a composite of fat and fibroglandular breast lean tissue [65]. The black dots are phantom measurements at different thickness and composition. The red lines are the calibration function that was a best fit to the phantom data. For demonstration, horizontal lines show iso-composition and vertical lines show iso-volume (courtesy of J. Shepherd, UCSF).

equipment instead of film. In addition, since digital area detectors typically require several seconds, if not tens of seconds to read out, scanning linear or point detectors are the most common for whole body and large area imaging for excellent spatial registration.

DXA systems have much in common with other medical X ray imaging systems, with many of the same components. Figure 6 shows a typical X ray gantry for a DXA system including the X ray tube, filtration, pre-patient aperture, examination table or surface, pre-detector aperture and detector. Unlike plain film imaging, but similar to CT systems, the components have a fixed geometry on a gantry even when scanning. The patient lies still while the gantry scans an ROI. The scan speed and image quality are dictated by the X ray beam geometry. Pencil beam systems having only a single detector element have to 'raster' scan over an ROI, collecting one pixel at a time. Imaging time is typically 3–5 min for

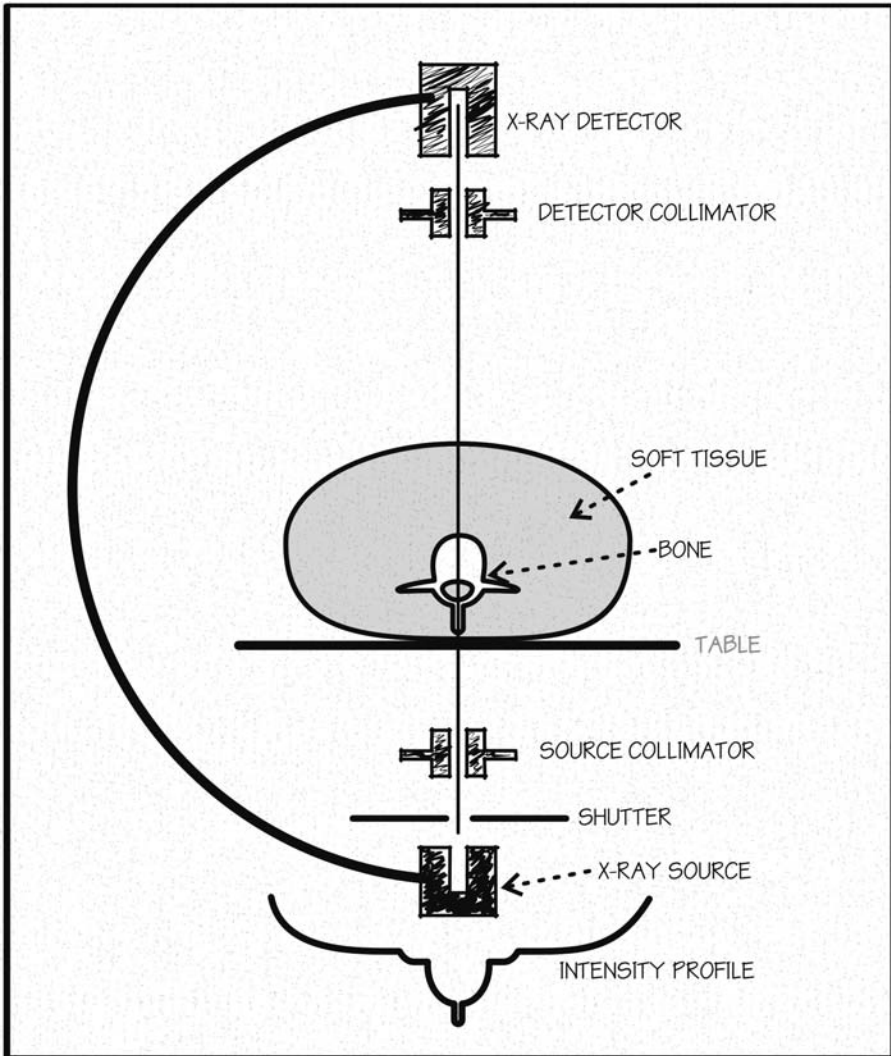


FIG. 6. Schematic diagram showing the components of a DXA system (courtesy of J. Shepherd, UCSF).

hip and spine scans, and 20 min for whole body. Fan beam systems use a linear detector array and collect ten or more pixels at a time. Thus, fan beam systems are much faster than pencil beam systems for equivalent imaging properties. Images of the spine or hip are typically acquired in less than 30 s and 3 min for whole body. Cone beam geometry uses an area detector to take ‘snap-shot’ style images. Although cone beam imaging is the fastest method to take a single energy image,

readout time between the images has limited their application in bone densitometry. If a subject takes a breath between low and high energy images, severe artefacts result and void the scan. For pencil and fan beam systems, the low and high images of the pixel (pencil beam) or row (fan beam) are collected in milliseconds before the gantry shifts to the next row. Thus, breathing is allowed during the exposure with minimal misregistration. Unlike pencil beam systems, fan and cone beam images do contain X ray scatter; however, scatter rejection is very high for fan beam compared to cone beam systems.

It is important to note that fan, pencil and cone beam systems project the three dimensional human body onto the two dimensional image in different ways [66–73]. The problem is illustrated in Fig. 7. The pencil beam image is projected perpendicular to the plane of the table, the fan beam image may be projected under a certain angle in the direction parallel to the fan width, and the cone beam image may be projected under an angle in both image directions. Thus, even if identical ROIs are outlined on the resulting images, these ROIs are projections of different physical volumes of interest. This difference between pencil, fan and cone beam ROIs is one of definition. DXA ROI definitions are arbitrary; both projections and measurements are equally valid.

An additional difference between pencil beam versus fan and cone beam systems is the so called fan beam (and cone beam) magnification. The size of the projected area of a volume of interest depends on the position of the object

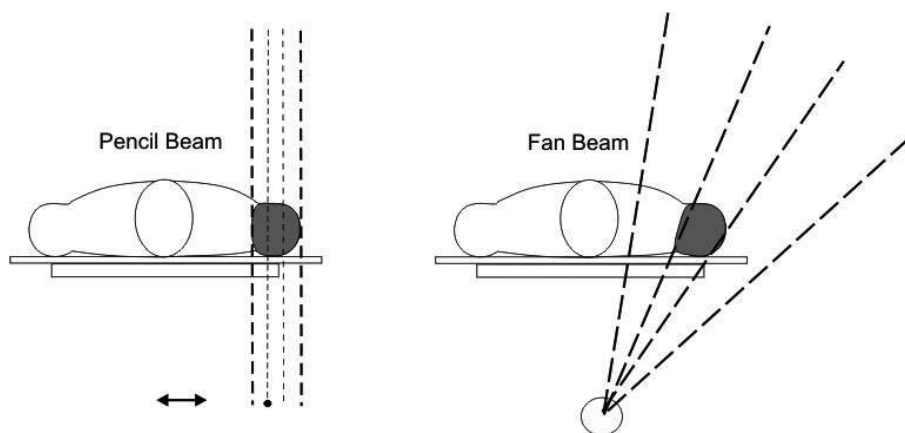


FIG. 7. Pencil and fan beam geometries project the same ROI differently. The pencil beam image is projected perpendicular to the plane of the table, whereas the fan beam projection depends on the position of the object within the beam. The projected images, therefore, encompass different physical volumes of tissue when projected back to the X ray source (courtesy of J. Shepherd, UCSF).

between the X ray tube and the detector. Thus, in fan beam systems, BMC and BA appear to decrease the further the object is from the source [74]. Since the precise location of the bone along the X ray path is generally not known, magnification errors in BMC and BA can be challenging to correct. It is important to note that measurement of aBMD is relatively immune to the effects of magnification [68] but for direct geometrical measurements, such as the femoral neck axis length, errors up to 10% have been reported [75]. In addition, magnification and its associated error only occur in the dimension along the fan length. The image dimension in the direction of the scanning motion does not have any magnification. For cone beam systems, magnification is in both dimensions.

4.6. GENERATING DUAL ENERGY IMAGES: VOLTAGE SWITCHING VERSUS K-EDGE FILTERING

In all DXA systems on the market, the X ray tubes used are standard tungsten anode tubes with focal spot sizes on the order of 0.5 to 1 mm². However, there are differences in how the dual energy images are created. The two methods in use are voltage switching systems made by Hologic and K edge filtering systems made by Norland (Norland, Cooper Surgical, Madison, WI, United States of America) and GE Lunar (GE Healthcare, Madison, WI, United States of America).

In a voltage switching system, two X ray tube voltage settings are used to create low and high energy images. The X ray tube power supply switches between a low (70 kVp) and high (140 kVp) voltage setting during alternate half cycles of the power supply. The resulting pulses are very short, 8.33 ms for 60 Hz and 10 ms for 50 Hz systems. Copper or brass is used to pre-harden the high energy beam, removing the low energy part of the spectrum and minimizing the overlap between low and high X ray spectra. The filter, voltage switching and detectors are all electronically and mechanically synchronized to sequentially collect low and high energy information for each position of the X ray gantry.

In a K edge filter system, the X ray tube is operated in a steady direct current mode and a K absorption edge filter splits a single X ray spectrum into low and high energy components. The X ray tube kVp is set such that the K edge places a notch in the X ray spectrum that simulates the dual peaked energy spectrum similar to ¹⁵³Gd. With an X ray voltage of 100 kV, one of several rare earth filters are used between the patient and the X ray tube by different manufacturers including cerium ($Z = 58$) and samarium ($Z = 62$). In these systems, since both high and low energy X rays are intermixed, the energy separation is done at the detector using pulse height measurements. In summary,

the means by which the dual energy images are created can be different. The strengths and weaknesses of the two approaches are discussed by Wahner [76].

5. DXA SCAN ACQUISITION

5.1. DXA REGIONS OF INTEREST

There are several ROIs that can be defined, with each having unique information to offer. The optimal site depends on the intent of the scan. For bone density, regions with higher contents of cancellous (high turnover) bone are more sensitive to osteoporotic and treatment changes. However, longitudinal studies suggest that most ROIs currently defined (spine, femur, radius and calcaneus) are useful for predicting general fracture risk (i.e. fractures of any bone). Of the measures available from DXA, BMD, BMC and AREA, the best assessment of risk is BMD [77]. However, the definition of osteoporosis from the World Health Organization (WHO) considers only the BMD of the femur neck. WHO criteria for diagnosing osteoporosis are given in Section 7.2.1. Only the whole body scan mode can measure fat, lean and bone mass. The most common regions and scan modes are outlined below.

5.1.1. Spine

This ROI is the most common for diagnosis of osteoporosis. The scan typically starts at L5 and ends at T12. The patient lies supine on the scanning table, with their knees flexed and shins elevated on a positioning cube to eliminate lumbar lordosis and flatten the spine against the table top. The aBMD measure of interest is typically for the total of L1–L4 in the posteroanterior projection (X ray tube is behind the patient and the detectors over their abdomen). The aBMD from this projection includes not only the vertebral bodies but the processes as well. Artefacts and error sources are common for older patients, resulting from extraneous calcifications in the walls of the aorta, deformations from degenerative disc and apophyseal joint disease with its consequent hyperostosis. These types of artefacts typically cause aBMD to be falsely elevated [78]. Other conditions that can cause falsely elevated aBMD are vertebral wedge (crush fracture), Paget's disease of bone, sclerotic metastases and haemopoietic tissue in the marrow of vertebrae. An example PA spine scan is shown in Fig. 8.

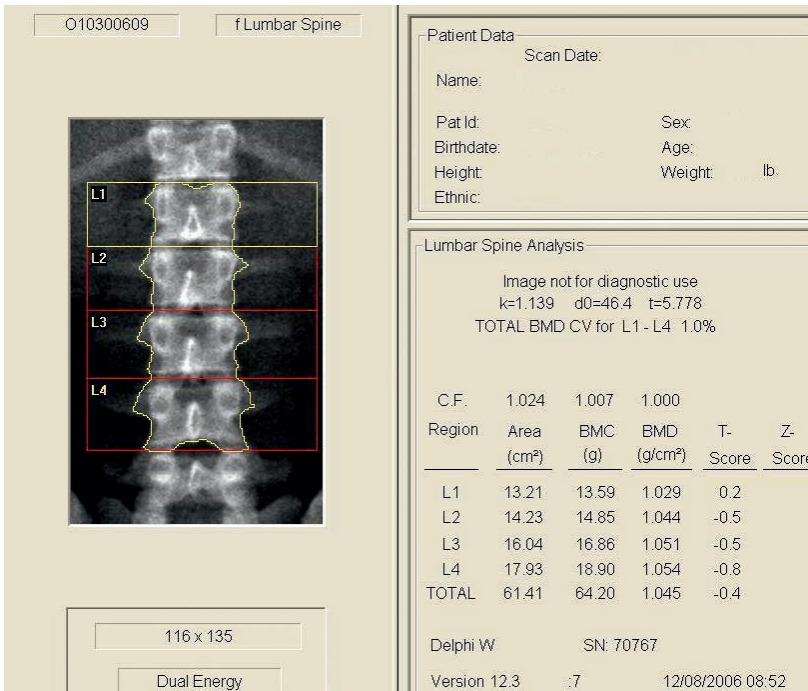


FIG. 8. Example of a DXA PA spine report. L1–L4 has been analysed and the total reported. It should be noted that the spine is centred in the scan, there is no curvature to the spine, the iliac crest is slightly visible and there is no twisting, all signs of good scan acquisition technique (courtesy of J. Shepherd, UCSF).

The development of the lateral spine projection was aimed at isolating the vertebral body from the posterior processes to increase the percentage of trabecular bone being analysed. By pairing the lateral scan with the vertebral width from the PA scan, the true volumetric density of the vertebral body can be estimated. The age related change in adults of lateral BMD is higher than with PA spine, and the correlation of volumetric BMD measured by lateral DXA and QCT is high, and stronger than that between PA–DXA and QCT [79]. However, overlap of the iliac crest and L4 and the ribs with L1 reduce the typical usable ROI to L2–L3. Furthermore, the precision of lateral BMD is typically worse than PA–DXA, such that its ability to monitor change is similar to PA spine [80, 81].

5.1.2. Proximal femur

The proximal femur is a common scan site because of the high mortality associated with fractures at this site. In the United States of America, 24% of hip

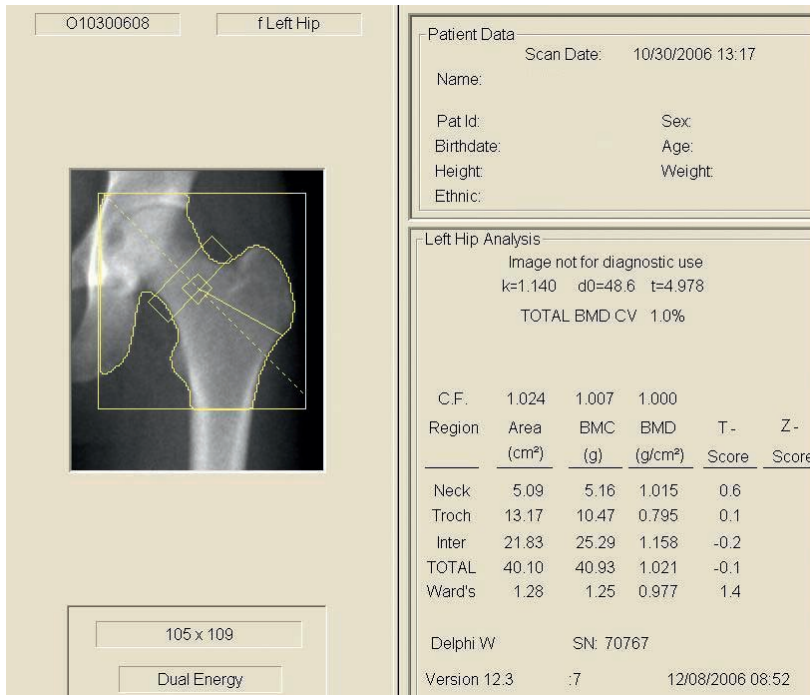


FIG. 9. Typical DXA scan report for the proximal femur. It should be noticed that the axis of the shaft is vertical in the image. This image has a fairly pronounced lesser trochanter that could signal that the femur was not fully rotated. However, the femoral neck has the appearance of being elongated and, thus, this patient most likely has a very pronounced less trochanter (courtesy of J. Shepherd, UCSF).

fracture patients aged 50 and older die in the year following their fracture. In scanning the proximal femur, the leg is slightly abducted and internally rotated using a positioning device in order to maximize the projection of the femoral neck. Each DXA manufacturer has a different and unique positioner to accomplish this. By not rotating the femur adequately, the femoral neck is foreshortened and this falsely increases the BMD. Positioning of the femoral neck is, therefore, critical to maintaining good precision and comparability to reference data. The ROIs quantified are typically the total, femoral neck, trochanter, intertrochanter and Ward's regions. A typical femur report is shown in Fig. 9. The specific definition for each ROI is different for each manufacturer. The total femur and femoral neck regions are commonly used for diagnosis, and the trochanter and Ward's triangle regions are seldom used except for research. The regions are shown in detail in Fig. 10.

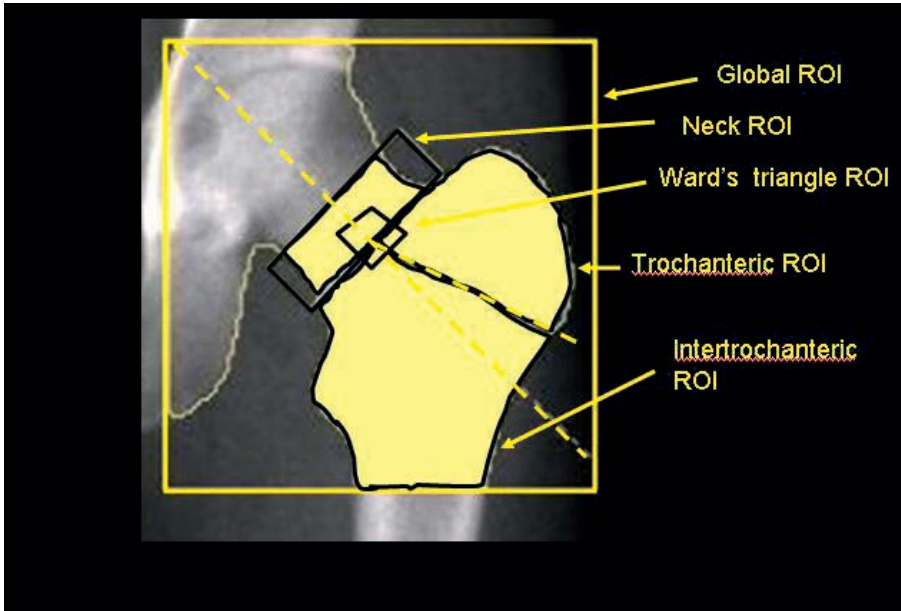


FIG. 10. Femur ROIs. The total femur ROI is the sum of the three shaded regions (femoral neck, trochanter, intertrochanter). The Ward's triangle ROI (small rectangle) overlaps the other regions and is not a unique area in the total femur (courtesy of J. Shepherd, UCSF).

5.1.3. Forearm

DXA scanning of the forearm is performed with the patient sitting on a chair next to the scanner table with the forearm resting on the table top, the hand in a fist and, on some scanners, secured on a positioning board with a restraining strap. In children, it may be necessary to scan the forearm at their side while lying on the scanner. A typical DXA scan report is shown in Fig. 11. Forearm BMD measurements are typically reported for the ultradistal, distal (mid-radius) and shaft (one-third radius) regions. The ultradistal site is useful because it contains the highest percentage of trabecular bone in the forearm. The one-third radius region is useful as a site containing entirely cortical bone.

5.1.4. Total body

Total body DXA for bone mineral is of interest because it offers a comprehensive view of total body mineral. This can be useful for calcium balance studies and paediatric studies interested in developmental bone mass. A

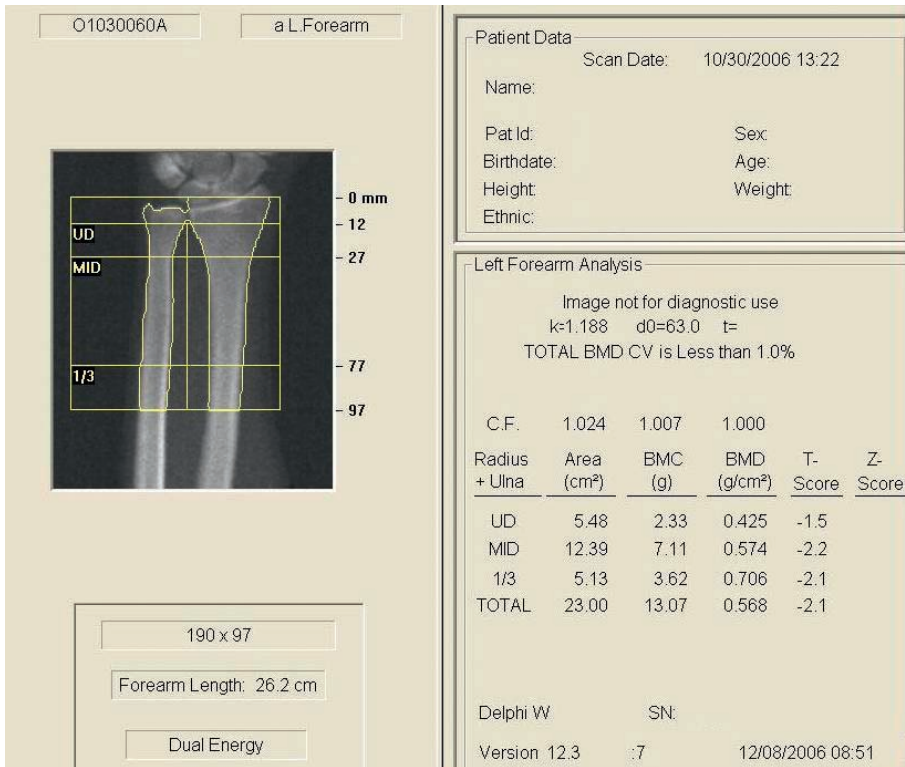


FIG. 11. Typical forearm DXA scan of the right forearm. It should be noted that the forearm is centered in the image, and that the radius and ulna are straight. If there is substantial deviation from the above, the scan should be reacquired (courtesy of J. Shepherd, UCSF).

typical whole body DXA scan is shown in Fig. 12. For precise results, it is imperative that the patient be placed on the scanning table in a supine position, with all parts of the body, including the arms, included in the scan field. Total body scans measure BMC and average BMD of the total skeleton together. Subregion values are also reported for the skull, arms, ribs, thoracic and lumbar spine, pelvis and legs [82]. In addition to BMC and BMD, total body DXA quantifies the composition of soft tissue in terms of fat and lean mass [83]. However, DXA cannot solve bone mineral, fat and soft tissue lean mass simultaneously. Thus, in areas where the X ray beam does not intersect bone, it is possible to estimate the masses of fat and lean tissue separately [4]. When bone is present in the pixel with soft tissue, however, only BMD and total (fat and lean) STM can be measured. Extrapolation of measurements of percentage of body fat in soft tissue over adjacent bone means that a whole body DXA scan can provide

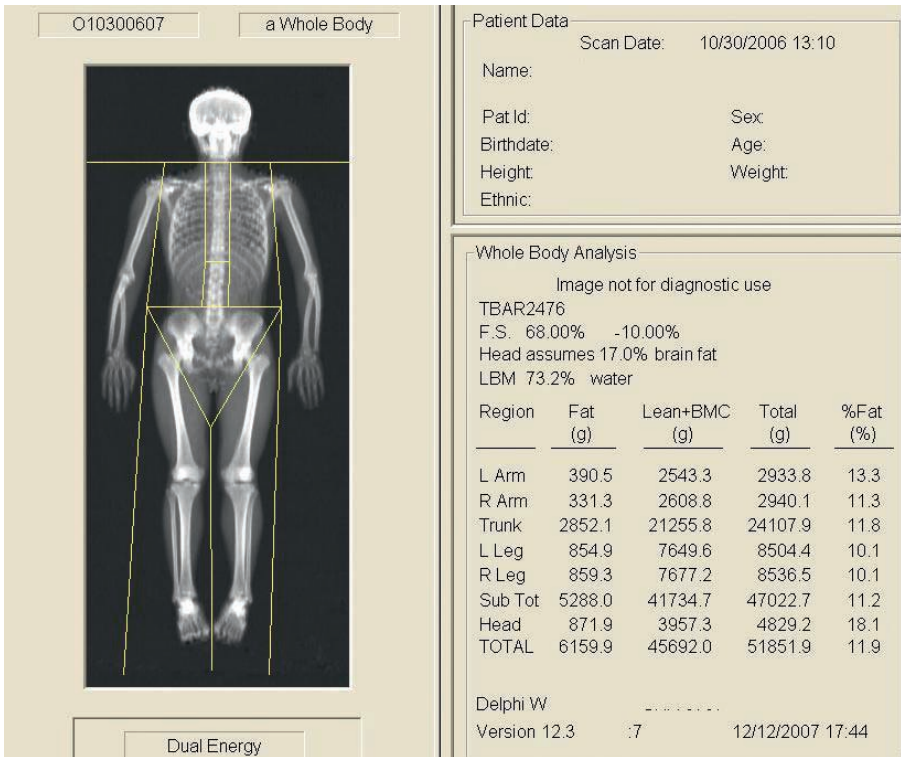


FIG. 12. Typical whole body DXA scan. It should be noted that the toes have been gently held together with a Velcro strap, the hands are flat and the body centred, straight and completely within the scan field. If part of the body is out of the scan field, some of the techniques described in the obesity analysis section must be used (courtesy of J. Shepherd, UCSF).

estimates of total body fat and lean mass as well as BMC [5]. The placement of the ROI cut lines are manufacturer specific and the reader should refer to the owner's manual of interest for placement guidelines.

5.1.5. Vertebral fracture assessment

Due to the relatively high resolution of fan beam DXA scanners, anatomical details of the examined region are depicted clearly. Using DXA to obtain lateral images of the lumbar spine allows the scanning beam — in contrast to conventional cone beam radiography — to be generally parallel to the vertebral endplates (Fig. 13). These images can be acquired as either dual or single energy for better visualization. The single energy acquisition reduces X ray noise. The

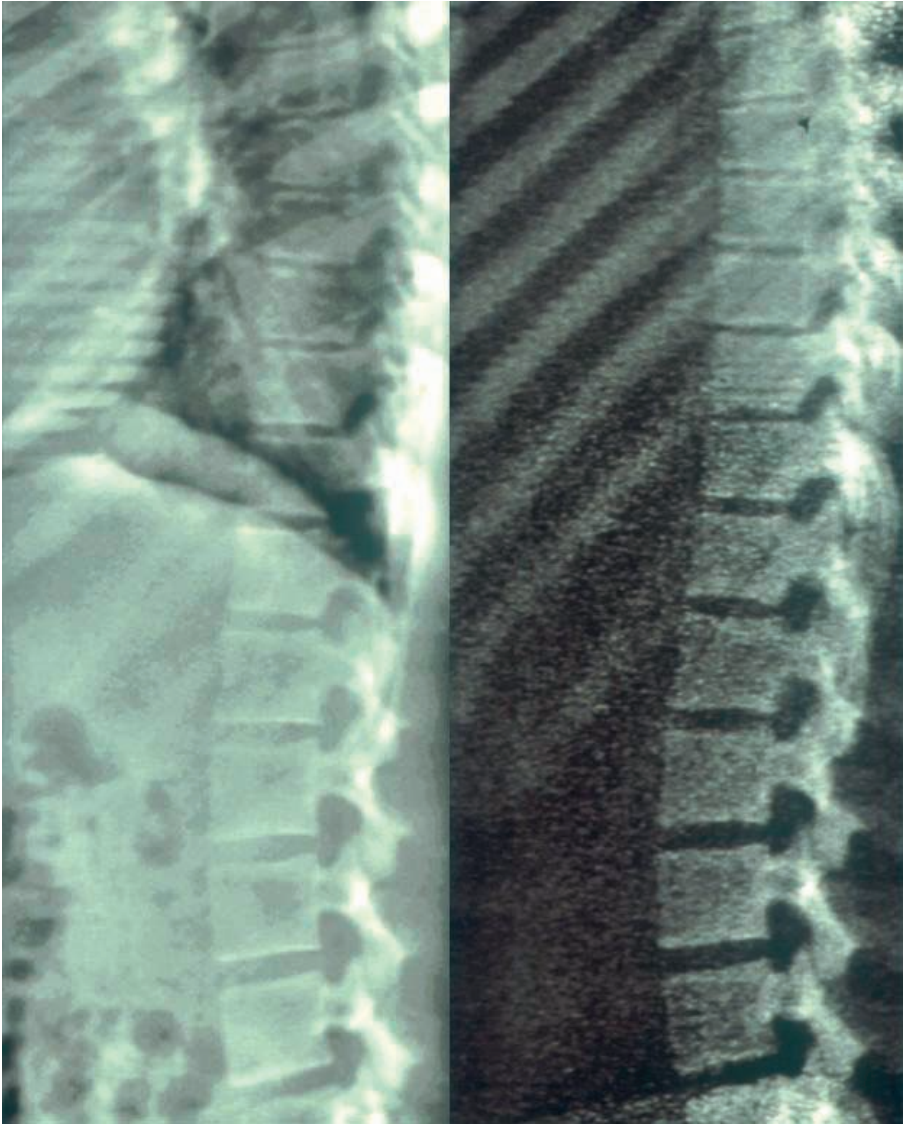


FIG. 13. Lateral vertebral assessment is used to better visualize vertebral fractures. The left image is the single energy representation. The dual energy view of the same spine is shown on the right. Fractures can be classified using scoring methods reflecting the severity of the fracture.

dual energy image reduces soft tissue artefacts. Several terms used in reference to the DXA approach, including vertebral fracture assessment, morphometric X ray absorptiometry [84], lateral vertebral analysis and instant vertebral analysis, essentially mean the same thing. In general, vertebral fracture assessment allows for better definition of vertebral dimensions than conventional X rays.

5.2. CLINICAL PROTOCOL FOR DXA ACQUISITION

The following sections describe in detail the requirements for acquiring subject scans beyond those mentioned in the operator's manual. In order to achieve the most consistent participant results, it is important to follow consistent procedures in acquiring all scans.

5.2.1. Before scanning the patient

Before patients come in for their scans, they should be informed of the following issues:

- (1) It should be ensured that patients can tolerate lying flat on their back and keeping still for at least 10 min.
- (2) The weight of subjects should be determined. All DXA systems can scan patients up to 300 lb (136 kg). If they are over 300 lb, they may need to have an alternative bone density or body composition test performed. The DXA system owner's manual should be checked for the specific limits of the system.
- (3) It should be determined whether the subjects have had any medical imaging procedure recently. If they have received contrast, such as barium or gadolinium, they should be scheduled two weeks after contrast was administered.
- (4) If patients are premenopausal, they should be asked whether there is any possibility that they might be pregnant. In some clinics, a pregnancy test may need to be administered before the examination. Patients should be informed of this possibility.
- (5) Calcium tablets should not be taken in the 24 h before the examination.
- (6) Patients should wear comfortable, loose fitting clothes, such as a sweat suit — this minimizes the need to change into a hospital gown.
- (7) Patients should avoid wearing clothing with metal components such as zippers, underwired bras or rivets.
- (8) Patients should be asked whether they have had a prior bone densitometry test. If so, the patient should bring those test results with them.

- (9) Patients should be asked to bring in the appointment information and their referring doctor's contact information if applicable.
- (10) For body composition studies, patients should be scanned in the morning after a 12 h overnight fast for consistency.

On the day of the examination, before subjects are scanned, the following should be checked:

- (1) Patients have complied with the recommendations listed above. Specifically:
 - (a) Patients should be asked again whether they have had any medical procedures in the preceding two weeks, such as CT or MRI. If they have received any contrast (barium, gadolinium, etc.), they should wait at least two weeks before their DXA scan.
 - (b) The menopausal status should be re-checked and whether a pregnancy test or question relating to possible pregnancy has been administered.
- (2) Subjects should be dressed in a hospital gown or scrubs, wearing only underpants and, if necessary, thin socks. A thin sheet may be placed over subjects for warmth.
- (3) All radio-opaque objects should be removed from the scan area (underwired bras, jewellery, belts, etc.).
- (4) When performing follow-up scans, the previous image of the baseline scan should be printed out to ensure duplicate positioning and scan parameters.

5.2.2. Scanning the patient

Positioning is, by far, the most common limiting factor to precision. Phantom scans, with no repositioning can commonly have an aBMD imprecision of 0.5%. For PA spine scans, the imprecision in vivo for the same measurement site is typically 1–1.5% because of the errors associated with projecting the patient's bones slightly differently. Patient movement during the scan causes the bone and soft tissue projection to change, slightly altering the projection. Changes in positioning between the baseline and follow-up can be difficult to detect. This error, as well as the imprecise placement of the ROI cut lines, can usually be minimized by training.

Note: When scanning subjects, it is important to keep in mind that it is much less time consuming to re-scan the subject immediately if a problem is detected, rather than having to recall the subject for a repeat of the scan on another day.

The following is a systematic method for positioning patients:

- (1) The same scan mode should always be used throughout the patient's baseline and follow-up visits (i.e. 'array' versus 'fast array', 'thick' versus 'standard', etc.).
- (2) Keeping the scan width and length set to the default settings is preferred in most situations.
- (3) For PA lumbar spine scans, it may be necessary to use a positioning block to remove the lordosis from the lower back. The spine must be straight and centred in the scan field.
- (4) For femur scans, the femur must be rotated and held in position with a positioning device. There are also dual hip scanning protocols that position both hips simultaneously. However, the positioning device may need to be adjusted between scans to scan both hips with correct abduction.
- (5) For forearm scans, the patient is scanned sitting in a chair without wheels. This may be difficult for people of short stature. For children, it may be more appropriate to have them lie prone on the table with their forearms extended above their heads or supine with the arm of interest away from their side. This may require the patient to be positioned with either end towards the foot end of the table in order to acquire the correct projection using the correct (left/right) scan mode.
- (6) Whole body is the most difficult with the most technical challenges. For whole body positioning, please refer to Fig. 14. The subject should be positioned in the centre of the table, aligned with the long axis of the scanner, with their head near the head end of the table. The subject's head should face straight up, not turned to the left or right. If required for subject comfort, only radiolucent pillows should be used. If pillows are used, however, a note should be made to use the same pillow again during follow-up measurements:
 - (a) The legs and feet should be positioned together with a Velcro strap around the ankles to help avoid movement. Feet should be kept relaxed with the toes pointed upwards (Fig. 15).
 - (b) Hands should be positioned with palms flat against the scan table. Space should be maintained between the arms and the torso when possible. If necessary, with larger or heavier subjects, the hands may be placed in a lateral position next to the hips. Hands should not be tucked under the hips to keep them in the scan field. If necessary, the subject's hands should be taped to the scan table. For patients who are too tall to fit within the scanning limits, it is acceptable for the feet to extend beyond the lower scan limit line. The knees should not be bent to keep the feet within the scan field.



FIG. 14. Example of good whole body scan positioning on a Hologic scanner (image taken from ISCD Bone Densitometry Course Lecture 9, used with permission by the ISCD).

- (7) For all scan modes, the scan should be monitored during acquisition. If the positioning is not correct or the subject moves, etc., the scan should be aborted, the subject repositioned if necessary and the scan restarted.
- (8) The patient should not be engaged in conversation because it may cause motion, but encouragement and updates on scan progress should be given.
- (9) After the examination, before the patient has left the table, it should be verified again that no movement has occurred during scanning. If the scan is not correct, the patient should be re-scanned.

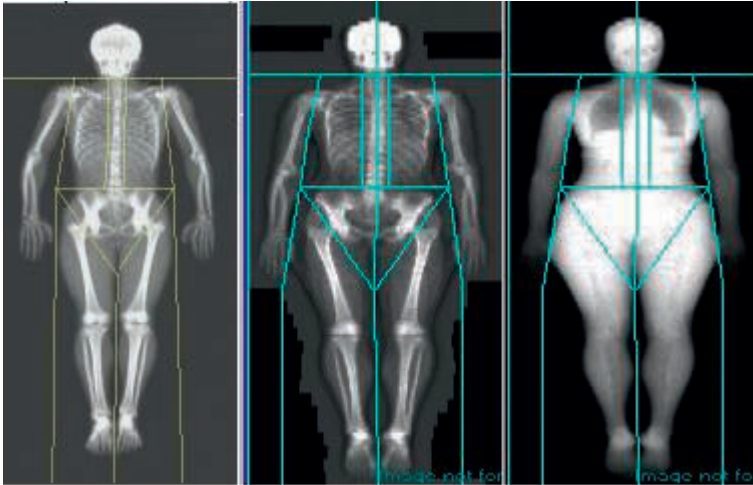


FIG. 15. Example of perfect whole body positioning. Hologic Delphi (left); GE Lunar Prodigy bone image (centre); GE Lunar Prodigy soft tissue image (right). Feet and ankles are together with the toes relaxed and pointing upwards; there is space between the arms and torso; the hands are flat on the table; the head is straight; the body and spine are straight in the centre of the table (courtesy of J. Shepherd, UCSF).

6. DXA SCAN ANALYSIS

6.1. AUTOMATIC ANALYSIS

Most DXA scanners have some type of automated placement of the ROI lines for spine and hip. For forearm and whole body, the ROI cut lines have to be placed manually. Although there has not been a movement for standardization of the ROIs, for the most part, they are the same between manufacturers. The owner's manual should be referred to for specifics. The following is a checklist for scan review to ensure that the scan was taken correctly:

- Proper positioning should be ensured. Is it the same as the baseline? Is it according to the positioning protocol outlined above?
- It should be verified that the entire body is in the scan field. Are the feet missing? Can the patient be repositioned to include the entire body? It should be noted whether some parts are excluded.
- Artefacts should be checked for including implants. Table 4 lists commonly found artefacts in whole body scans.

TABLE 4. ARTEFACTS COMMON TO WHOLE BODY SCANS
*(Imputation and hemiscan analysis is explained in the section on obesity.
 B = bone affected by artefact, ST = soft tissue affected by artefact)*

Artefact name	Notes	Arms	Legs	Trunk	Head	Hemiscan analysis?	Imputation?
Amputee	Missing bone and tissue in the ROI	B, ST	B, ST			Y	Y
Spine internal fixation	Only bone is affected			B			
Bracelet	Depends on size but will affect local ROI, usually not total	B				Y	Y
Watch	Depends on size but will affect local ROI, usually not total	B				Y	Y
Hearing aid (external)	Where battery pack is in shirt pocket			B		Y	N
Hair (thick, dense)	Rarely a problem, no codes are necessary				B		
Hand positioning	Fist or change in position can impact arm BMC but not total	B				Y	Y
House arrest anklet	Just affects leg with bracelet		B, ST			Y	Y
Hearing aid (internal ear)	Usually too small to have an impact						
Movement	Re-scan whenever possible	B, ST	B, ST	B, ST	B, ST	Y	Y
Obesity	Excessive noise can cause poor aBMD precision			B, ST		N	N
Pacemaker	Affects trunk			B, ST		Y	N
Pager	Usually affects bone and tissue of ROI			B, ST		N	N

TABLE 4. ARTEFACTS COMMON TO WHOLE BODY SCANS (cont.)
*(Imputation and hemiscan analysis is explained in the section on obesity.
 B = bone affected by artefact, ST = soft tissue affected by artefact)*

Artefact name	Notes	Arms	Legs	Trunk	Head	Hemiscan analysis?	Imputation?
Wallet	Usually affects bone and tissue of ROI			ST		N	N
Incomplete scan	Re-scan whenever possible	B, ST	B, ST	B, ST	B, ST	N	N
Penile implant				B, ST		N	N
Cast (plaster/fibreglas)	Depends on region where cast is located, both bone and tissue are affected (code 1)	B, ST	B, ST				
Pelvis reconstruction				B		N	N
Piercings	Little or no impact						
Rings	Usually has little impact on aBMD of arm						
Scoliosis	OK, since this is the true aBMD measurement for this patient						
Shoulder reconstruction	Can put metal into bone arm and trunk regions	B		B		Y	N
Breast implants				ST		N	N
Hip replacement (total or partial)			B	B		Y	Y
Knee replacement (total or partial)			B	B		Y	Y

TABLE 4. ARTEFACTS COMMON TO WHOLE BODY SCANS (cont.)
(Imputation and hemiscan analysis is explained in the section on obesity.
B = bone affected by artefact, ST = soft tissue affected by artefact)

Artefact name	Notes	Arms	Legs	Trunk	Head	Hemiscan analysis?	Imputation?
Buttons	Usually no effect					N	N
Zipper	Usually no effect					N	N

6.2. SPECIAL REGIONS AND DERIVED RESULTS

6.2.1. Skeletal muscle

The accurate measurement of skeletal muscle (SM) is important for studies of nutritional, physiological and metabolic processes. Although SM can be measured using CT or MRI, the techniques are relatively expensive and instrument access can be limited. Total body SM mass can be predicted from whole body DXA scans. LSTM from whole body DXA is comprised of the protein and water mass that make up skin, connective tissue and muscle from the appendicular, head and trunk ROIs. The appendicular lean soft tissue mass (aLSTM) is basically the muscle mass of the arms and legs. Kim et al. [85] developed a multivariate model that predicted total body SM mass from DXA aLSTM. The model population consisted of 321 men and women with a BMI <35 kg/m², 18 years old or older, that were of a diverse ethnic background of African-Americans, Asians, Caucasian and Hispanics within the United States of America. All subjects were scanned by DXA on a Lunar DPX (sw version 3.6) as well as by MRI. The DXA protocol consisted of a single whole body scan, where the arms and legs were isolated from the trunk, and analysis using the standard whole body ROIs. aLSTM (ALST in Kim et al. [85]) was defined as the sum of the LSTM in both the right and left arms and legs. The MRI scan was acquired in a GE 1.5 T 6X Horizon following a 40 slice protocol, where the slice thickness was 10 mm every 40 mm as described by Ross [86]. The MRI muscle volume was found by delineating the muscle in each slice and converting to mass using a muscle density of 1.04 g/cm³. Kim found that the best predictive model of total body SM was:

$$\text{Total body SM} = 1.13\text{aLSTM} - 0.02\text{age} + 0.61\text{sex} + 0.97(r_{\text{adj}}^2 = 0.96) \quad (21)$$

where sex = 0 for female and 1 for male, and age ≥ 18 . The standard error of the estimate (SEE) was 1.58 kg, which is comparable to SEE values for other predictive models of total body SM using anthropomorphy (2.8 kg), bioimpedance (2.7 kg), urinary 3-methyl histidine (2.3 kg) and urinary creatine (1.9 kg) [85]. However, this relationship may be different for other DXA systems and in other populations.

6.2.2. Adipose tissue

Adipose tissue is made up of lipid (85%), proteins, minerals (3%) and water (12%) [87, 88], resulting in a physical density of approximately 0.92 kg/L. It is important to note that DXA, by definition, specifically measures the mass of total lipid, not adipose tissue. However, most researchers are interested in metabolic function. Adipose can be segregated anatomically to study its metabolic function. Table 5 contains a list of terms suggested by Shen et al. [89] and their definitions to use as standards of terminology.

Visceral or organ adipose tissue is found in all three body cavities: intra-thoracic (ITAT), intra-abdominal (IAAT) and intra-pelvic (IPAT). However, most investigators report VAT as IAAT or the sum of IAAT and IPAT. The tree in Fig. 16 is a breakdown of the terminology proposed by Shen et al. for VAT components [89].

Clearly, DXA cannot measure overlapping components of adipose tissue. However, DXA has been used to determine its utility in monitoring select components of adipose tissue important for a particular disease.

6.2.3. Intra-abdominal adipose tissue and DXA

Using the terminology from above, IAAT is defined as the intra-abdominopelvic adipose fat. IAAT has been found to be more strongly associated with insulin resistance than SAT [90]. Direct measures of IAAT can be made using either volume MRI/CT scanning or single slices. Although the MRI/CT protocols vary, a common method used in the literature is to take a single CT slice. Patients are scanned supine with their arms outstretched above their heads, wearing light clothing. Slice thicknesses may vary but are approximately 4–10 mm and centred using an intervertebral space, e.g. the L3 to L4 intervertebral space. In most cases, a single contour tracing the peritoneum along the abdominal cavity is used to segment IAAT from SAT. The repeatability of this type of measure is typically better using CT than MRI (2% [91] versus 9–18% [92–95], respectively).

TABLE 5. PROPOSED CLASSIFICATION OF TOTAL BODY ADIPOSE TISSUE (from Shen et al. [89])

Adipose tissue component	Definition
Total adipose tissue	Sum of adipose tissue, usually excluding bone marrow and adipose tissue in the head, hands and feet.
SAT	The layer found between the dermis and the aponeuroses and fasciae of the muscles; includes mammary adipose tissue.
Superficial SAT	The layer found between the skin and a fascial plane in the lower trunk and gluteal-thigh area.
Deep SAT	The layer found between the muscle fascia and the fascial plane in the lower trunk and gluteal-thigh areas.
Internal adipose tissue	Total adipose tissue minus subcutaneous adipose tissue.
(1) VAT	Adipose tissue within the chest, abdomen and pelvis.
(2) Non-visceral internal adipose tissue	Internal adipose tissue minus VAT.
(a) Intramuscular adipose tissue	Adipose tissue within a muscle (between fascicles).
(b) Perimuscular adipose tissue	Adipose tissue inside the muscle fascia (deep fascia), excluding intramuscular adipose tissue.
(i) Intermuscular adipose tissue	Adipose tissue between muscles.
(ii) Paraosseal adipose tissue	Adipose tissue in the interface between muscle and bone (e.g. paravertebral).
(c) Other non-visceral adipose tissue	Orbital adipose tissue; aberrant adipose tissue associated with pathological conditions (e.g. lipoma).

Hill et al. 2007 [96] derived a measure equivalent to the IAAT area in the CT slice of L3/L4 using whole body DXA and a skinfold measure for post-menopausal women. Forty-one post-menopausal women with BMI values from 26 to 37 received the three body composition measures. Their relationship was found to be:

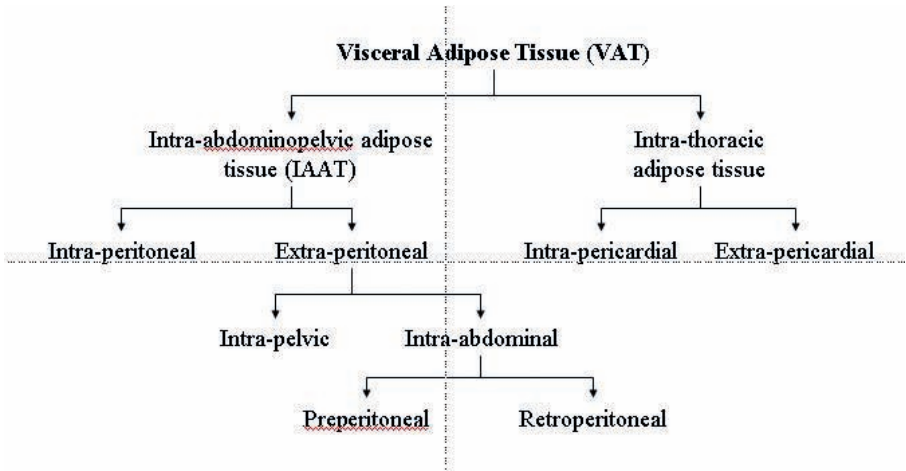


FIG. 16. Classification of VAT as defined by Shen et al. [90].

$$\begin{aligned}
 \text{IAAT area (cm}^2\text{)} &= 51.84 + 0.031 \left(\frac{\text{cm}^2}{\text{g}} \right) \text{FM}_{\text{abdominal}} \\
 &+ 1.342 \left(\frac{\text{cm}^2}{\text{mm}} \right) \text{abdominal skinfold} \quad (22)
 \end{aligned}$$

$\text{FM}_{\text{abdominal}}$ was defined as the DXA FM in grams within a 10 cm tall ROI anchored on top of the iliac crests and extending to the edges of the abdominal soft tissue (Lunar Prodigy, software version 7.52). It should be noted that this DXA ROI incorporated the L3/L4 CT slice level and was found to have a coefficient of variation (CV) for repeat measures of 2.6%. The abdominal skinfold measure was made on a vertical fold taken 5 cm to the right of the omphalion (navel) using Harpenden calipers. This multivariate model correlated with actual CT IAAT with a Pearson's correlation coefficient of $r = 0.82$ and a SEE of 22.3 cm^2 (17%). The model compared better to CT than the other IAAT estimates in the study, including waist circumference ($r = 0.74$), DXA 10 mm region alone ($r = 0.782$) and abdominal skinfold alone ($r = 0.60$).

Treuth et al. [97] compared CT measures of IAAT to DXA using women over a broad age range (17 to 77 years) and BMI (17 to 43 kg/m^2). Although not explicitly defined, Treuth et al. appeared to use a definition for IAAT as the CT slice pixel area highlighted in the intra-abdominal cavity when adipose tissue was defined as pixels with Hounsfield units between -190 and -30 . The CT slice was 5 mm thick and centred in the L4–L5 intervertebral gap. Treuth derived a

multivariate model, including sagittal diameter (cm, supine diameter at the umbilicus), age and waist circumference (cm, narrowest part of torso), and either DXA trunk or pelvic PCTFM (GE Lunar DPX-L, software version not reported). The Treuth equation is shown below:

$$\begin{aligned} \text{IAAT area (cm}^2\text{)} = & -208.2 + 0.78 \left(\frac{\text{cm}^2}{\text{g}} \right) \text{FM}_{\text{trunk}} \\ & + 4.62 \left(\frac{\text{cm}^2}{\text{cm}} \right) \text{sagittal diameter} \\ & + 0.75 \left(\frac{\text{cm}^2}{\text{y}} \right) \text{age} + 1.73 \left(\frac{\text{cm}^2}{\text{cm}} \right) \text{waist} \end{aligned} \quad (23)$$

The Treuth relationship correlated with $r^2 = 0.81$ and $\text{SEE} = 23.3 \text{ cm}^2$. Treuth tested similar special ROIs, such as Hill's as well as skinfolds; however, they did not survive in her analysis.

Svendsen [98] developed an equation that included post-menopausal women only:

$$\begin{aligned} \text{IAAT area (cm}^2\text{)} = & -503.0 + 23.4 \left(\frac{\text{cm}^2}{\text{g}} \right) \text{FM}_{\text{abdominal}} \\ & + 508.2 \left(\frac{\text{cm}^2}{\text{cm}} \right) \text{WHR} + 36.3 \left(\frac{\text{cm}^2}{\text{cm}} \right) \log \sum \text{skinfolds} \end{aligned} \quad (24)$$

where $\text{FM}_{\text{abdominal}}$ was a DXA subregion measured with a square ROI in the lumbar region, $\text{WHR} = \text{waist to hip ratio}$, and ' $\sum \text{skinfolds}$ ' = the sum of abdominal, suprailiac and subscapular skinfold thicknesses. Svendsen reported an $r^2 = 0.91$ to IAAT area by CT.

In a similar study to Hill et al., Kamel et al. [99] reported that DXA was in better agreement with CT than with anthropomorphic measures. However, there were important differences. In the Kamel et al. study, MRI was used instead of CT, seven 10 mm thick slices, four above and two below the slice on the L4/L5 intervertebral space, were used to define IAAT versus a single navel slice, and the DXA ROI was a central ROI that did not extend to the abdominal edge but to the extent of the rib cage. Using these definitions, the DXA central adipose tissue region, waist circumference and waist to hip ratio were all similar in their correlations to MRI IAAT ($r = 0.74, 0.75, 0.70$, respectively, in women and less in men). However, it is hard to compare the Kamel and Hill studies due to their unique designs.

6.2.4. Subcutaneous adipose tissue

As shown in Table 5, SAT in the lower trunk and gluteal-thigh region can be subdivided into superficial and deep SAT separated by a fascial plane (Fig. 17). Deep SAT is located primarily in the posterior half of the abdomen, while superficial SAT is more evenly distributed around the abdominal circumference [89, 100]. Differences have been reported between these two adipose tissue layers [89, 101–103]. Deep SAT has shown robust correlations to insulin resistance in both men and women, while superficial SAT showed little or no association [100]. Thus, the measure of SAT without distinction to these sub-components dilutes the relationship. Furthermore, since whole body DXA scans cannot discern the separating facial plane, and the fact that the superficial and deep SAT overlap each other in DXA images, the ability of DXA to discern either component uniquely is unlikely.



FIG. 17. Abdominal axial CT scans of an (A) obese and a (B) thin subject. SAT is divided into superficial and deep SAT by a fascial plane, as indicated by the white arrows [89]. It is unlikely that DXA could be used to discern superficial from deep SAT (used with permission from Obesity Research).

SAT in the abdomen was examined in the Hill study outlined above. The correlations of total abdominal SAT defined CT area versus DXA was found to be $r = 0.788$, while simple hip circumference [104] was $r = 0.826$. Thus, there was no benefit from measuring SAT with DXA compared with the relatively simple hip circumference measure.

6.2.5. Standardized bone mineral density

There are systematic differences in the absolute values of BMD between manufacturers. For this reason, BMD values across manufacturers cannot be directly compared and are not interchangeable. Thus, measurements of the same patient from two different systems cannot be compared to calculate a change in bone density. Attempts have been made to eliminate the average differences in calibration. Genant et al. [27] compared the three largest DXA manufacturers using 100 women scanned on each system and derived sBMD units for the spine. Lu et al. [105, 106] derived equations for the hip, and Shepherd et al. [107] for the forearm. The hip and spine equations are shown in Table 6. The use of sBMD significantly reduces the differences between devices. For example, the difference in aBMD between Hologic and GE systems of 10% is reduced to approximately 2% using sBMD [27]. However, no attempt has been made to standardize BMC, and sBMD values have not been derived for other ROIs, including the lateral spine, fingers, heel or whole body. Note that if one wants to compare values from two specific densitometers, a cross-calibration study must be performed to understand the specific differences between the systems.

TABLE 6. EQUATIONS TO DERIVE sBMD FOR TOTAL SPINE, TOTAL HIP, TROCHANTER AND FEMORAL NECK. THE PARAMETERS IN THE TABLE ARE USED WITH THIS EQUATION: $sBMD = 1000 (A + B \times BMD)$ [105]

Manufacturer	Parameter	Total spine	Femoral neck	Trochanter	Total hip
Hologic	<i>A</i>	0.018	0.019	-0.017	0.006
	<i>b</i>	1.055	1.087	1.105	1.008
Lunar	<i>a</i>	-0.022	-0.023	-0.042	-0.031
	<i>b</i>	0.968	0.939	0.949	0.979
Norland	<i>a</i>	0.100	0.006	0.057	0.026
	<i>b</i>	0.9743	0.985	0.961	1.012

6.2.6. Bone mineral apparent density

As discussed previously, aBMD measured by DXA is a two-dimensional assessment, not assessing the third or depth dimension. Thus, in the case of comparing two subjects with the same bone mass density (mass per unit volume as would be measured by QCT), the taller of the two patients has larger bones and, thus, a higher DXA aBMD [108]. This is due to the fact that DXA aBMD cannot differentiate between high density small bones and low density large bones. This results in a systematic overestimation of DXA aBMD in larger subjects and underestimation in smaller patients. For the spine, Carter et al. suggested a quantity called bone mineral apparent density (BMAD), defined as:

$$\text{BMAD} = \text{BMC} \times (\text{AREA})^{-1.5} \text{ (mg/cm}^3\text{)} \quad (25)$$

to correct for this error. This models the spine as a rectilinear volume with a bone depth equal to the average dimension of the vertebrae projected in the image. Shepherd et al. have applied the BMAD principle to whole body scanning to reduce the effects of body size and the effects of the changing mass fraction of the head in growing children [109], referred to as whole body bone mineral apparent density (WBMAD). This model used the body height without the head, and body depth was assumed to be equivalent to body skeletal width. However, the use of BMAD, WBMAD and other similar approaches has not been shown to improve accuracy nor the association between fracture risk and aBMD [110]. BMAD reduces the association between DXA aBMD and body weight by 50% [111], supporting assumptions that the relationship between weight and DXA aBMD may be partially attributable to a lack of accuracy [112].

6.3. OBESE PATIENTS

There are several challenges in the scanning and analysis of heavy patients. First, the DXA systems have weight limits and table dimensions that restrict the size of the person to be scanned (Table 7). DXA scanner table weight limits are generally 300 lb (136 kg). The owner's DXA systems manual should be checked to determine the weight limits of the particular model, as some systems can scan up to 450 lb (205 kg).

Obese patients are 'thicker' and attenuate the X ray more. Thus, some manufacturers provide special scan modes and analysis techniques for such patients. These scan modes, in general, have the same X ray tube voltage settings but with either higher mAs or slower scan time to increase the X ray flux:

TABLE 7. WEIGHT LIMITS AND TABLE DIMENSIONS OF FULL SIZE DENSITOMETERS OF VARIOUS MANUFACTURERS AND MODELS (adapted from Brownbill and Ilich [113])

Manufacturer/model	Weight limit kg (lb)	Scan dimensions (cm)
GE Lunar iDXA	205 (450)	197.5 × 66
GE Lunar Prodigy Advance	159 (350)	197.5 × 60
GE Lunar Prodigy	159 (350)	197.5 × 60
GE Lunar DPX-NT	136 (300)	195 × 57.6
Hologic Discovery Series	205 (450)	195.6 × 67 (A), 65 (W/Wi)
Hologic QDR Series	136 (300)	195.6 × 67 (A), 65 (W/Wi)
Norland XR-46, XR-36	114 (250)	193 × 64

- *GE Lunar users*: GE systems will automatically alert the user to the need for the ‘thick’ scan mode if the patient’s weight exceeds a particular level. The dose is increased from 0.4 μSv to 0.8 μSv .
- *Hologic users*: Hologic provides a ‘high power whole body’ scan mode. This mode should be used if there is a noticeable increase in X ray noise in the torso region. The dose is increased from 8.5 μSv to 28.3 μSv .

It is also sometimes difficult to fit an obese patient into the scan field. There are several methods for dealing with this:

- (1) *Bed sheet wrapping*: For those who are slightly too big for the width of the scan field, a bed sheet may be wrapped around the patient to compress the body to within the scan field. The disadvantage of this technique is that good separation between the arms and torso is not possible.
- (2) *Hemiscan protocol*: A hemiscan protocol is where the patient is positioned off the centre line of the scan table to ensure that one side, typically the right side, is completely included in the scan field (Fig. 18, right). Tataranni and Ravussin [114] found that the accuracy of DXA body composition results of half body scanning were not different from whole body scanning ($r^2 \geq 0.98$). The equations used to determine whole body composition from hemiscans are as follows:

Equations for calculating whole body results from hemiscans

$$\text{BMC}_{\text{whole body}} = \text{BMC}_{\text{half body}} \times 2$$

$$\text{AREA}_{\text{whole body}} = \text{AREA}_{\text{half body}} \times 2$$

$$\text{FM}_{\text{whole body}} = \text{FM}_{\text{half body}} \times 2$$

$$\text{LSTM}_{\text{whole body}} = \text{LSTM}_{\text{half body}} \times 2$$

It should be noted that the equations and definitions for aBMD and PCTFM do not change. For systems with stationary scanning tables, a gurney can be wheeled along next to the scanner and positioned at the same table height to make this positioning easier. To properly analyse hemiscans, the software ROIs must include a centre line to divide the body into two axial pieces (Fig. 15, centre). If this is not an option, hemiscan analysis is not possible.

- (3) *Imputation of arms and legs*: If neither of the above methods is available or do not work, one can position the patient by slightly shifting the patient off-axis, such that the entire trunk is on the table but the left arm and leg is not fully scanned. In this case, the right arm and leg values are used for the left arm and leg. It should be noted that the entire trunk region needs to be included. The only reason for using this procedure is because the software packages do not subdivide the trunk soft tissue into left and right (i.e. Hologic software versions 12.5 and below). No published validation for imputation values is available to our knowledge, but it is reasonable to assume that the accuracy is similar to the hemiscan method. The equations for imputation are more complicated than for hemiscan analysis and are given below:

Equations for calculating whole body result by imputation from shifted scans

$$\text{BMC}_{\text{total imputed}} = \text{BMC}_{\text{total shifted}} - \text{BMC}_{\text{left leg}} - \text{BMC}_{\text{left arm}} + \text{BMC}_{\text{right arm}} + \text{BMC}_{\text{right arm}}$$

$$\text{AREA}_{\text{total imputed}} = \text{AREA}_{\text{total shifted}} - \text{AREA}_{\text{left leg}} - \text{AREA}_{\text{left arm}} + \text{AREA}_{\text{right arm}} + \text{AREA}_{\text{right arm}}$$

$$\text{FM}_{\text{total imputed}} = \text{FM}_{\text{total shifted}} - \text{FM}_{\text{left leg}} - \text{FM}_{\text{left arm}} + \text{FM}_{\text{right arm}} + \text{FM}_{\text{right arm}}$$

$$\text{LSTM}_{\text{total imputed}} = \text{LSTM}_{\text{total shifted}} - \text{LSTM}_{\text{left leg}} - \text{LSTM}_{\text{left arm}} + \text{LSTM}_{\text{right arm}} + \text{LSTM}_{\text{right arm}}$$

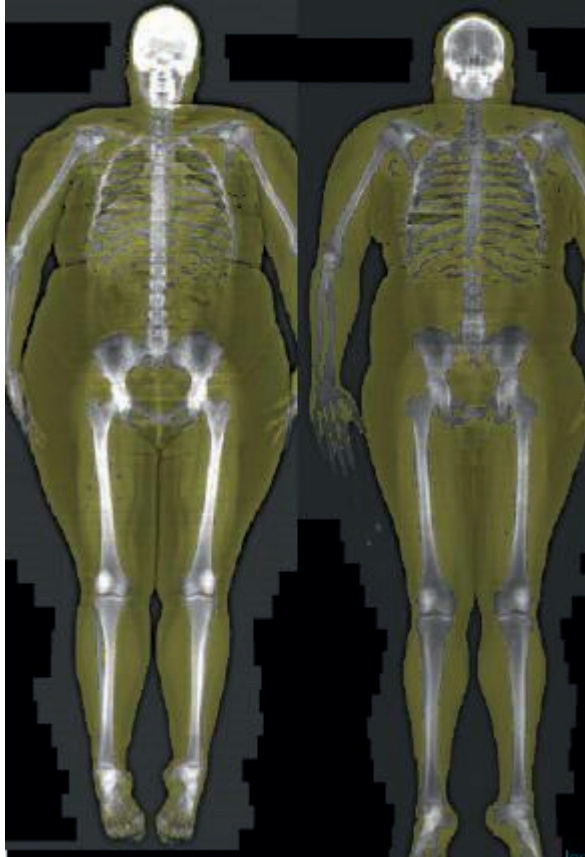


FIG. 18. Inaccurate scan since both arms are lost (left). Patient should be re-scanned for hemiscan analysis. Shifted scan appropriate for imputation of the left side (right) (images courtesy of Mary K. Oates, CA, United States of America).

It should be noted that the equations and definitions for aBMD and PCTFM, and TBM do not change.

6.4. CHILDREN

Scanning children is challenging for several reasons. First, children often cannot or will not hold still for the 3–10 min necessary to complete a whole body DXA scan. Motion artefacts are common and can be the cause of scans being rejected. Second, standard scan modes are optimized for adult bone densities and body sizes. The small bone sizes and low body masses can challenge whole body

algorithms in terms of both accuracy and precision. Lastly, the scan ROIs may not be appropriate for the very young. In this section, the protocols used for the scanning of children are outlined.

Two scan modes are mostly used for infants and children under 6 years old: whole body and spine. Whole body allows for the measure of soft tissue and total BMC. However, it is difficult to achieve high quality whole body scans due to movement. A typical whole body scan takes 3–5 min. Infant spine scans can be as short as 15 s and the infant can be held by the shoulders and legs outside the scan field. W. Koo has undertaken extensive studies of bone density in infants. The whole body protocol below was used by Koo to scan infants from several hours old to 1 year old, and from 2 to 12 kg in weight.

Infant scanning protocol based on Koo et al. [115]

- (1) A cotton blanket should be placed to cover the entire local scan area. Note that on some systems, a scanning paediatric platform may be needed to precondition the X ray beam (e.g. the Hologic QDR–1000/*W*). The instructions of the manufacturer should be followed.
- (2) Whole body or spine DXA scan protocols specific to infants should be used if available.
- (3) For infants less than 3 months old, the subject should be swaddled in a thin cotton blanket, 70 cm × 90 cm in size and weighing 120 g, or something similar without additional clothing.
- (4) For infants over 3 months old, subjects should be scanned in only a cotton diaper.
- (5) Subject should be scanned without sedative or restraint if possible.
- (6) DXA measure should be attempted when the infant has been calmed after spontaneous movement or crying.
- (7) The infant should be placed in the prone position. The arm and leg positions should be in a relaxed splayed position, such that there is no overlap of the arms and legs with any other part of the body.
- (8) The scan should be attempted up to three times until a technically satisfactory scan has been acquired. A technically satisfactory scan is one that has completely scanned the infant with less than four discontinuities or ‘breaks’ in the lateral edges of bones.
- (9) Scan analysis can be performed with either the automated scan analysis with regions similar to adults’ analysis or with special ROIs.

Koo found that non-metallic objects commonly used with very young babies, rubber pacifiers, IV catheters, plastic ID tags, umbilical cord clamp, urine bag and feeding tubes, did not significantly impact the BMC results of whole body DXA scans. Cotton blankets and diapers also did not seem to have any significant effect on BMC. However, Koo did not test for the impact on the soft tissue components and, depending on the mass of these objects, they may impact the soft tissue results. The scanning procedure must be consistent between visits and include the same accessories if at all possible.

Appendix III provides a review list of known paediatric reference data.

6.5. QUALITY CONTROL

Scanner QC procedures are used to monitor scanner performance throughout the course of a study or during general use. Longitudinal QC procedures consist of daily procedures used to monitor the performance of a single scanner over time. Cross-calibration procedures are used to monitor scanner variation between systems. An additional QC measure is the use of the DXA Bone Densitometer Report (see Appendix I). The DXA operator completes and archives this report monthly in addition to a copy of the QC scans, including the air scans on the sites' specific transfer media (CD, Superdisc, DVD, etc.). Both longitudinal QC and cross-calibration will be discussed in this section.

6.5.1. Scanning the spine phantom

The following is a step by step procedure for scanning the spine QC phantom. The procedure assumes that a biography already exists for the phantom:

- (1) It should be ensured that the phantom serial number is entered in the Pat ID field. The phantom number may be read from the label on the side of the phantom:
 - (a) *Hologic users*: The Hologic spine phantom should be scanned at least every day that a study patient is scanned, but at least three times per week.
 - (b) *GE Lunar users*: The Lunar Aluminum spine phantom should be scanned every day a patient is scanned, but at least three times per week.
- (2) These scans are analysed automatically and added to the QC database.
- (3) The QC plot should be reviewed for aBMD. If the aBMD for L1–L4 falls outside acceptable limits, the phantom should be re-scanned. If the aBMD from the second scan also falls outside the limits, the service provider for

the system should be called. If the aBMD from the second scan falls within the limits, normal scanning for the day should be continued.

- (4) The Bone Densitometer Report (see Appendix I) is completed at the end of each month by the operator and submitted and filed in the clinic's quality assurance binder. The report tracks scanner maintenance and repairs as well as operator changes, which may be useful to outside quality reviewers.

6.5.2. Air scan procedure (table top radiographic uniformity)

This test is performed only on Hologic systems with whole body scanning software. A scan of the table should be performed once per week, the same day that the tissue bar is scanned.

6.5.2.1. Hologic users with software version 12.1 or higher

This is an automatic procedure called 'table top radiographic uniformity'. No biography needs to be created.

6.5.2.2. Hologic users with software version less than 12.1

- (1) First, a patient biography needs to be created in the following manner (zeros '0' should be used in the biography, not the letter 'O'):

Name: Air scan

Patient ID:

Sex: F

Referring physician:

Patient comment: AIR SCAN

- (2) Everything should be removed from the table and a scan of the entire table performed using the whole body scan mode.
- (3) Using Windows Explorer, the C:\QDR\Utilities directory should be accessed.
- (4) The service icon should be copied onto the desktop as a shortcut (this should remain on the desktop).
- (5) The Hologic software should be entered in the usual manner.
- (6) An air scan should be acquired as described above.
- (7) The Hologic software should be exited without shutting down.
- (8) The service icon shortcut should be double clicked. This will return you to the Hologic software in service mode.
- (9) From the Menu on top of the screen, Utilities->Service utilities->Table top radiographic uniformity should be selected.
- (10) The most recent air scan should be selected and OK pressed.

- (11) An image of the air scan will appear, and a scan printout similar to the output below. The image will typically not look very pretty. It should ideally look like random ‘white noise’ (i.e. static on a TV set; Fig. 19). Streaks may be visible.

Report Date: 8/8/02

Selected scan = P:\DXA_DATA\CTASC\PA02626A.R0P

Total points per phase in row: 109

Total lines in column: 150

Lines with a standard deviation greater than 2.0

<i>Phase Line</i>	<i>mean</i>	<i>stdev</i>	<i>min</i>	<i>max</i>
<i>Global Stats:</i>				
<i>1</i>	<i>586.92</i>	<i>1.03</i>	<i>582</i>	<i>590</i>

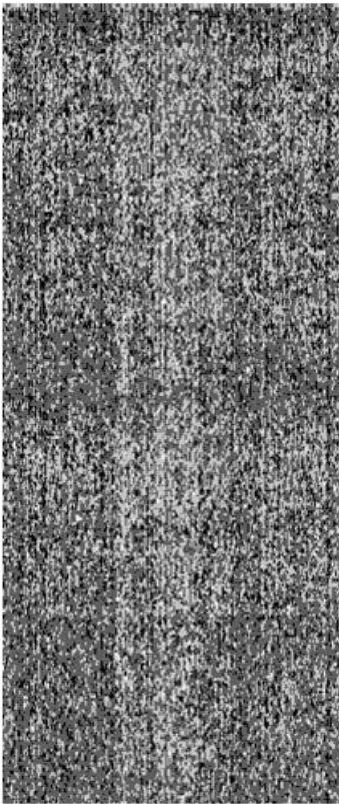


FIG. 19. Air scans acquired on a Hologic whole body scanner. These type of scans are acquired without any scan objects in the field and are a test of scan background uniformity. The left image is an example of a good uniformity with a global SD of 1.0. The right image has a non-uniformity most likely caused by aperture misalignment. The global SD was 11.9 and failed the quality test described in Section 6.5.2 (courtesy of J. Shepherd, UCSF).

- (12) If the global standard deviation (SD) is less than 2.0, the scanner is functioning properly.
- (13) If the result is above 2.0, the air scan should be repeated and the results reviewed. If the SD remains over 2.0, these results should be emailed to your service representative for immediate review. The number to look at is shown above in bold (1.03 in this example).
- (14) No further analysis should be performed on these scans.

6.5.3. Whole body quality control for DXA

There are few options for whole body DXA QC. Commercially available phantoms include the Hologic whole body phantom, the Bioimaging variable composition phantom (Bioimaging, Inc., Waltham, MA, United States of America) and the OrthoMetrics whole body phantom (OrthoMetrics, Inc., White Plains, NY, United States of America). All of these phantoms have been used for longitudinal calibration corrections and cross-calibration between similar systems. At the present time, none of the phantoms has been shown to be appropriate for cross-calibration between systems of different makes and models.

The assembled Hologic phantom is shown in Fig. 20. A DXA image of the phantom is shown in Fig. 21. The phantom weighs 40 kg assembled. Before lifting or transporting the phantom, it should be broken down into its individual components. Lifting the entire phantom assembly should not be attempted.

When scanning the whole body phantoms, the table should first be centred if necessary. The phantom should be positioned in the centre of the scanner, with

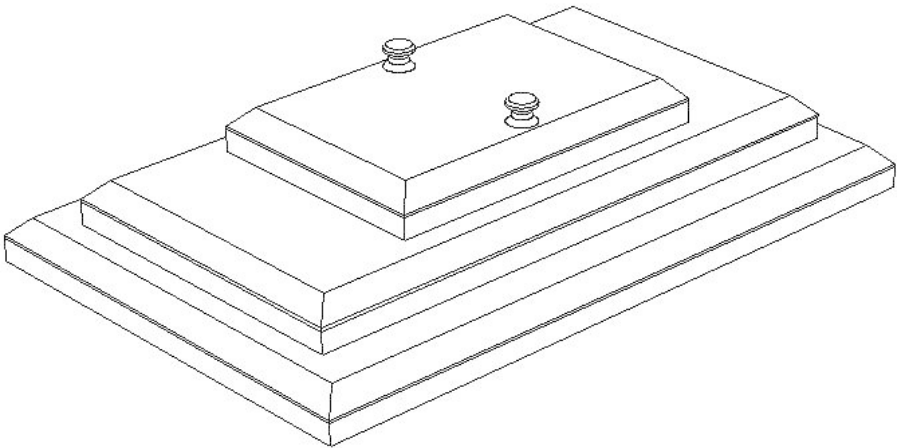


FIG. 20. Whole body phantom assembly (used with permission from Hologic, Inc.).

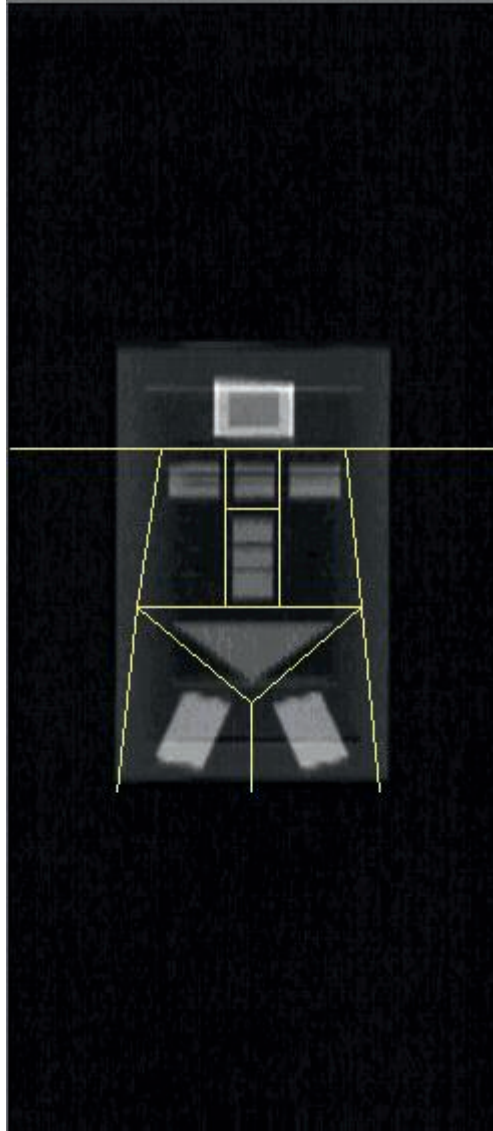


FIG. 21. DXA image of the whole body phantom (courtesy of J. Shepherd, UCSF).

the phantom end marked 'head' towards the head of the table. The laser centering lights should be aligned with the centering marks on the surface of the phantom. The phantom should be parallel with the central long axis of the table. It should be ensured that there is nothing else on the table. The phantom should be using

the standard adult whole body scan mode. The default scan length and scan width should be accepted. The whole table should be scanned.

When performing cross-calibration procedures, before proceeding to the next scan, the phantom should be repositioned by sliding the phantom down to the foot of the table and then re-centring. Using table paper or a sheet will help to protect the table surface. This should be repeated again for a total of two scans per day for five consecutive work days.

6.5.4. Special paediatric phantoms

Picaud et al. [116] reported on a novel phantom made of acrylic (for FM), polyvinyl chloride (for LSTM) and aluminium (for bone mass) whose combinations were made to mimic infants in body weight and composition during the first year of life for spine DXA scans. Using a set of phantoms, they showed that adult spine aBMD software used on children can lack sensitivity for smaller less dense bone. Using a Hologic QDR-2000 with the phantom set, they reported a three to five times lower BMC when scanning with the adult software versus the paediatric spine software.

6.5.5. Research studies

Changes in scanners, software or location of scanners can have a large impact on the integrity of study data. For this reason, such changes are typically not allowed for the duration of a study or clinical trial without prior notification and approval of the study's principal investigator.

6.5.6. Training of personnel

Ideally, all personnel who scan patients should be trained by the manufacturer on the proper use of the DXA system. All manufacturers provide several hours of hands-on training when a system is initially purchased. However, it is recognized that this training might not be available or affordable at a later date, and that this training is most often cursory. Thus, the following are guidelines, based on the training guidelines for the State of California, United States of America, to help a local clinic either seek or provide training for DXA personnel:

- (1) *DXA instructor.* The instructor should:
 - (a) Be a physician, physicist, technologist, technician, manufacturer representative or equivalent, qualified by training and experience to perform and instruct in the use of X ray bone densitometry equipment.

- (b) Have at least one year of experience performing X ray bone densitometry procedures.
 - (c) Offer some didactic teaching based on the system's owner's manual, scientific literature and personal experience; some laboratory training on patient positioning, scan analysis and QC procedures; and some clinical training on osteoporosis, bone disease and patient artefacts.
 - (d) Should create a training record to show that new DXA users were trained in the above way.
- (2) *Curriculum for technologists.* The curriculum should provide for the acquisition of such knowledge, skills and abilities with sufficient breadth to assure competence in the student's operation of X ray bone densitometry equipment:
- (a) The training (didactic, laboratory and clinical) should extend over a period of at least 3 d but not more than 1 month to ensure good retention.
 - (b) The didactic curriculum should include at least the following (18 h total):
 - (i) Radiation physics, biology and protection (3 h);
 - (ii) Bone and body composition biology, bone disease and therapy, and densitometry parameters (3 h);
 - (iii) X ray bone densitometry equipment (4 h);
 - (iv) Computers and image formation (3 h);
 - (v) Anatomy and positioning (4 h);
 - (vi) Ethics and patient handling (1 h).
 - (c) The laboratory curriculum should consist of at least 4 h of training that includes:
 - (i) Scanning and analysis of phantoms;
 - (ii) Evaluation of existing patient images.
 - (d) Supervised clinical education should consist of the acquisition, by the student, of at least 20 scans that include the following (it should be noted that these scans can all be acquired on the same five patients if allowed by local regulatory approval):
 - (i) Posterior/anterior spine (five patients);
 - (ii) Proximal femur (five patients);
 - (iii) Forearm (five patients);
 - (iv) Whole body (five patients).
- (3) *Clinical supervisor.* Each clinical site should have a supervisor responsible for the oversight of day to day clinical operations. The clinical supervisor should:
- (a) Be a physician who is either a radiologist, or an MD who has taken the above technologist's training, or who has received a radiography supervisor and operator certificate or permit from a local regulatory board charged with regulating the use of DXA systems.

- (b) Provide general supervision of the DXA technologist once the student is deemed capable of performing the assigned procedures and duties accurately and safely.
 - (c) Provide regular written evaluations (i.e. at least annually) of each technologist's ability to perform clinical procedures.
- (4) *Precision assessments.* Every DXA technologist should conduct a precision assessment on the instrument and patient population they will be scanning on a regular basis. The details are given below:
- (a) Patients should be informed of the benefits and risks before they are included in a precision assessment.
 - (b) Patients that are representative of the practice's typical population should be used.
 - (c) The scan modes in use for clinical or study needs where the change in the parameter is important for individual patients should be used. For osteoporosis assessment, this is total spine aBMD, total hip aBMD and femoral neck aBMD. For whole body composition studies, this is total mass, total PCTFM, total BMC and total LSTM.
 - (d) Each technologist should scan 30 patients twice.
 - (e) The patient should be repositioned between each scan by asking them to get off the table and then back on.
 - (f) Average aBMD, BMC, TM, PCTFM and FM should be calculated using the following equation where PCTFM is given as an example:

$$\text{average(PCTFM)}_i = \frac{1}{m} \sum_{j=1}^m \text{PCTFM}_j \quad (26)$$

where average(PCTFM) is the average PCTFM for a patient i , j = the scan number and m = the total number of scans for a particular patient (i.e. 2).

- (g) The SD and CV should be calculated for each patient using the following equation:

$$\text{PCTFM_SD}_i = \frac{1}{m-1} \sqrt{\sum_{j=1}^m (\text{PCTFM}_j - \text{average(PCTFM)})^2} \quad (27)$$

$$\text{PCTFM_CV}_i = \frac{\text{PCTFM_SD}}{\text{average(PCTFM)}} 100 \quad (28)$$

- (h) The root mean square (RMS)_CV and RMS_SD should be determined for the assessment population as a whole for each of the parameters of interest:

$$\text{PCTFM_RMS_SD} = \frac{1}{n} \sqrt{\sum_{i=1}^n (\text{PCTFM_SD}_i)^2} \quad (29)$$

$$\text{PCTFM_RMS_CV} = \frac{1}{n} \sqrt{\sum_{i=1}^n (\text{PCTFM_CV}_i)^2} \quad (30)$$

where n = number of patients in the assessment.

- (i) Minimum precision standards. A technologist should be able to accomplish a RMS_CV better (smaller) than those listed in Table 8 for the following parameters. If not, retraining should be performed until such precision can be accomplished.

6.5.7. Precision and repeatability

Imprecision can be added during the scan analysis if the ROIs are placed slightly differently between the baseline and follow-up scans. Most manufacturers supply a ‘compare’ analysis feature that allows for the overlay of

TABLE 8. MINIMUM PRECISION STANDARDS FOR INDIVIDUAL TECHNOLOGISTS

Parameter	RMS_CV
Total spine aBMD	1.9% ^a
Total hip aBMD	1.8% ^a
Total neck aBMD	2.5% ^a
Total body aBMD	1.5% ^b
Total body BMC	2.0% ^b
Total PCTFM	1.9% ^b

^a From the ISCD 2005 Position Statement [117].

^b Estimated from the experience of the author.

the ROIs from a previous analysis onto the current examination. This has been shown to improve the overall precision. Many studies have measured the repeatability of DXA measures. The repeatability, also referred to as test/retest precision, of DXA measures has been described in virtually all makes and models of densitometers, using both small patient populations and phantoms. A high precision measurement of aBMD is desired for monitoring changes over time due to treatment, disease or ageing. Precision is calculated as the ‘least significant change’ (LSC) that has to be seen for there to be 95% statistical confidence that the change in the measure is not just due to chance. The LSC for 95% confidence is defined as:

$$\text{LSC} = 2.77 \times \text{precision error} \quad (31)$$

where the precision error can be expressed as either an SD in the units of the measure or as a per cent CV (% CV). Furthermore, the LSC can be combined with the expected rate of change for a disease or treatment to define the ‘monitoring time interval’. The monitoring time interval is the time in years that one should wait between measures before taking another measure based on the expectation of the LSC being surpassed. Thus, the MTI for an aBMD measure is defined as:

$$\text{MTI} = \frac{\text{LSC (g/cm}^2\text{)}}{\text{expected rate of change} \left(\frac{\text{g/cm}^2}{\text{year}} \right)} \text{ years}$$

Typical in vivo aBMD precision values reported for humans are 1–1.5% for the lumbar spine, 1% for the distal radius, 1.5–2% for the proximal femur and 1.5–2% for total body scans [118] (Table 9).

TABLE 9. IN VIVO PRECISION AND ACCURACY ESTIMATES
(from Genant *et al.* [118])

ROI	Precision (% CV)	Accuracy (% diff. from truth)
PA spine aBMD	1–2	4–10
Lat spine aBMD	2–3	5–15
Femur aBMD	1.5–3	6
Forearm aBMD	1	5
Total body aBMD	1	3

However, the reported values are almost always what are called short term precision values from duplicate or triplicate scans taken during a single patient visit. Sometimes, precision values reported from the manufacturer were assembled in younger populations using well trained and experienced operators, and may not be applicable to an actual clinical environment. In routine clinical cases and in elderly people, imprecision increases by 50 to 100%. The imprecision of phantoms may be reduced by up to 50% compared to the values given above. Long term imprecision, described using multiple scans on individuals taken only after time has passed, is larger than short term imprecision although several studies reported only small differences [119]. Although it is most accurate to use long term precision in the LSC and MTI values, short term precision is always used due to a lack of availability of long term precision for various systems and patient populations. The following recommendations will help minimize imprecision.

Strategies to minimize precision error

- (1) All operators should be formally trained in positioning and analysis for each scan mode used.
- (2) Patients should be scanned on the same densitometer, not a similar model in the same clinic. Scans from different makes and model systems cannot be quantitatively compared.
- (3) The same operator should be used for the baseline and follow-up scans.
- (4) The patient should be positioned using the standardized procedure suggested by the manufacturer or study protocol.
- (5) The scan mode should not be changed between baseline and follow-up scans. A scanner may offer a quick, normal and high resolution option for a given skeletal site. The scan mode that was used for the baseline should always be used for the follow-up.
- (6) Identical ROIs should be used for each scan and placed consistently. The 'compare' or 'copy' function should always be used if available.
- (7) Auto-analysis algorithms should be used and checked by the operator, and only modified when necessary and at a minimum.

6.5.8. Accuracy and cross-calibration of DXA systems

DXA systems should ultimately be calibrated to biological specimens of bone mineral (hydroxyapatite), human fatty acids and lean mass (combination of protein and water) by the manufacturers. However, these are not appropriate sources for calibration in the field. Each manufacturer has a specific method to

ensure that systems in the field are at their factory calibration. These procedures should be strictly adhered to. For example, Hologic Systems requires the scanning of the anthropomorphic spine phantom every morning before using the system. GE requires the scanning of their calibration phantom in the morning as well.

6.5.8.1. Validating the factory accuracy of a DXA system

The only field reference that a site might have for the accuracy of the DXA system is the values printed on the QC phantom label. Before any other calibration method is used, the DXA system should be checked for accuracy with this labelling.

Verifying DXA system factory accuracy

- (1) The manufacturer's spine phantom should be scanned as recommended ten times without repositioning.
- (2) The first scan should be analysed as instructed by the manufacturer.
- (3) The remaining scans should be analysed using the 'COMPARE' feature.
- (4) The average aBMD, BMC and AREA should be calculated.
- (5) The average aBMD, BMC and AREA should be within 1% of the values on the phantom label. If they are more than 1% different, the manufacturer's service representative should be called to correct the calibration.

6.5.8.2. Validating the accuracy of scans other than the spine scan mode

Currently, there are no known phantoms commercially available to validate the absolute accuracy of scan modes other than the spine in the field. However, there are phantoms available that can check the relative accuracy of the system to other systems in the field.

For the femur, there is the Hologic anthropomorphic femur phantom that can be used to compare the relative accuracy of different scanning systems. For the forearm, there is the European forearm phantom. For the whole body, there are several phantoms: the Hologic whole body phantom and the Bioimaging variable composition phantom (Bioimaging, Inc., Boston, MA, United States of America). However, there is little validation data available on these phantoms. These phantoms can be used in the same way as the spine phantoms by picking one of the sites as the reference instead of the phantom label. If differences are observed, there is not a convenient way to change the calibration for non-spine scan modes when the spine is in calibration. One must apply correction factors

directly to the acquired clinical or study data. It should be noted, though, that these phantoms are only valid for cross-calibrating the same make and model densitometer.

6.5.8.3. Cross-calibration between densitometers

Cross-calibration is necessary if scans are going to be compared between two systems. The LSC (Eq. (39)) is used to compare two patient values when measured on the same DXA system. The generalized least significant change (GLSC) is used to compare two scans from a patient when measured on two different DXA systems [120]. To calculate GLSC, it is necessary to do an in vivo cross-calibration assessment as well as an in vivo precision assessment on the previous system and the current system. The GLSC in absolute BMD units was defined as:

$$\text{GLSC} = 1.96 \sqrt{\frac{n+1}{n-2} S_y^2 (1-\hat{r}^2)} \quad (32)$$

and as a per cent as:

$$\% \text{GLSC} = \frac{1.96 \sqrt{\frac{n+1}{n-2} S_y^2 (1-\hat{r}^2)}}{\hat{a} + \hat{b} \mu_x} 100 \quad (33)$$

where the subscripts x and y refer to the two systems, S_y is the sample variance of cross-calibration population, \hat{b} and \hat{a} are the linear regression coefficient for the slope and offset, r is the correlation coefficient, n is the number of subjects in the study and μ_x is the population mean BMD on system x . The GLSC is not reversible and is unique, depending on which scan is taken as the baseline. The ISCD provides a cross-calibration tool on their web site that calculates the GLSC from data entry (<http://www.iscd.org/visitors/resources/calc.cfm>). The procedure to follow for calculating the GLSC is given in the following procedure.

Procedure for in vivo cross-calibration between two DXA systems

- (1) If the precision error of the previous system is known from a previous precision assessment, 30 patients representative of the facility's patient population should be scanned once on the initial system and then twice on the new system within 60 d. It should be noted that these 30 patients receive three scans at each ROI: one on the previous system and two on the new system.
- (2) If the precision error of the previous system is not known from a previous precision assessment, 30 patients representative of the facility's patient population should be scanned twice on the previous system and then twice on the new system within 60 d. It should be noted that these 30 patients receive four scans at each ROI: two scans on the previous system and two scans on the new system.
- (3) The scan data should be entered into the GLSC tool or the parameters needed for Eqs (41) and (42) calculated.
- (4) Those anatomic sites commonly measured in clinical practice, typically spine and proximal femur, should be measured.
- (5) Facilities must comply with locally applicable regulations regarding DXA.
- (6) The GLSC should be used for comparison between the previous and the new system. Inter-system quantitative comparisons can only be made if cross-calibration is performed on each skeletal site commonly measured *before* using the GLSC.
- (7) It is possible to request the manufacturer of your system to convert your database before uploading into your new system.
- (8) It should be noted that it is not possible to directly compare the values of the new system to the previous scan printouts. Previous scan values *must* be calibrated to the new system before using the GLSC.
- (9) All future scans should be compared to scans performed on the new system (System 2) using the new system's LSC.
- (10) If a cross-calibration assessment is not performed, no quantitative comparison to the prior system can be made. Consequently, a new baseline BMD and intra-system LSC should be established.

6.5.9. Monitoring the stability of a DXA system

Drifts in the calibration of a DXA system over time can lead to misinterpretation of the change in measurements. For example, a 2% drift in calibration over the period of a year will result in all patients scanned before and

after this drift to appear to have a 2% change, even though the change is only due to a calibration drift. Phantoms can be used to monitor system calibrations such that drifts can be corrected before they affect clinical or study outcomes.

6.6. ARTEFACTS

Systematic errors in DXA arise from a number of sources.

6.6.1. Soft tissue composition and baseline measurement

Many studies have described the so called fat error in DXA bone density measures related to non-uniform soft tissue composition surrounding the bone. The fat error is a direct result of the theoretical simplifications used by DXA, where the human body is approximated as a two-component model consisting of just bone and soft tissue. QCT experiments have shown that the fractional volume of soft tissue fat in the vicinity of the lumbar spine varies up to 20% [121–123]. In both in vivo and phantom measurements, aBMD errors of up to 15% have been reported [121, 124–129] and theoretical simulations confirmed the magnitude of the bias [130]. These simulations also indicated that the aBMD bias was larger in elderly and osteoporotic subjects than in younger subjects.

Formica et al., who investigated differences in baseline composition in post-menopausal women with QCT, found that a 20% difference in BMD as measured by DXA in PA and in the lateral direction, could be attributed solely to the difference in soft tissue composition [122]. However, in DXA the ‘baseline value’ is typically sampled over a volume that is much larger than the volume covered by one CT slice, which was used in these studies. Furthermore, differences in tissue composition are not equal to differences in per cent volume of fat. The impact of this patient specific bias on diagnostic decisions has, so far, only been investigated in simulations [129].

The fat error is best minimized by consistent repositioning of the patient, such that the fat uniformity is as similar as possible between baseline and follow-up scans.

6.6.2. Patient obesity, weight change and bone size

Obese patients challenge DXA scanners in several ways (Fig. 22). The obese patient is very thick and highly attenuates the X rays, resulting in poor image quality and absorptiometry statistics. Thus, precision is worse in obese patients. In addition, there have been reports of changes in whole body BA,

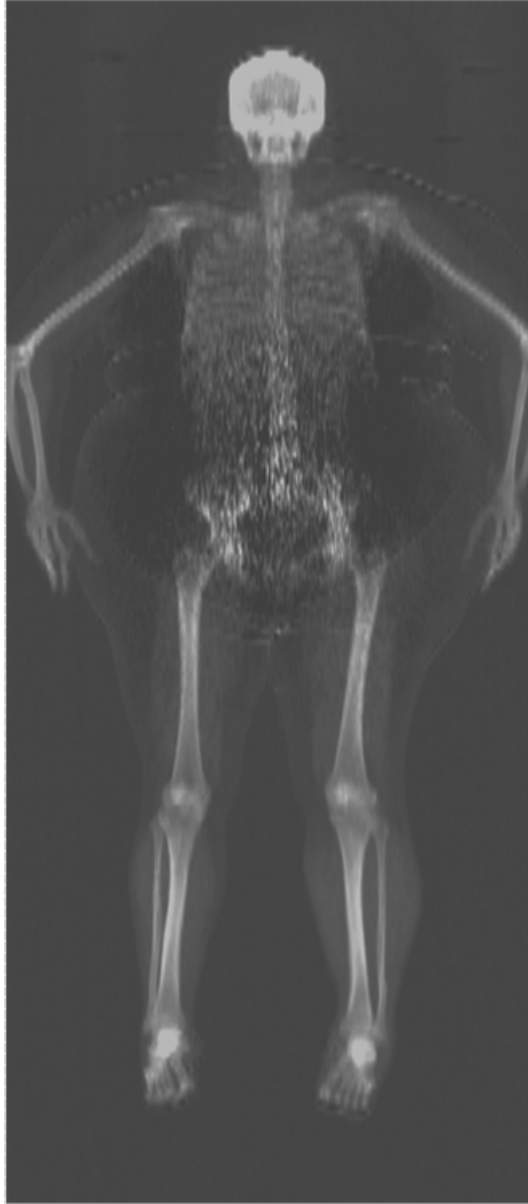


FIG. 22. Scan of an obese patient showing the noise in the abdomen that can result when the X ray flux that passes through the patient becomes very small. Most DXA scanners scan patients up to 300 lbs (136 kg) but this is primarily a table top limit. Poor scan quality can be present for much lower weights due to patient thickness (courtesy of J. Shepherd, UCSF).

aBMD and BMC after weight loss, when in fact these parameters should be independent [71, 119, 131, 132].

These findings can potentially be explained by ‘beam hardening’, which is present to a higher degree with increasing absorber thickness. In DPA, where the low and high energy images were in effect monochromatic, an influence of weight was not observed [133]. The added difficulty is that there is not a consistent error due to weight change between manufacturers and scan modes [134–136], most probably due to different beam hardening corrections being used.

6.6.3. Contrast agents from other procedures

Contrast agents for MRI, such as gadolinium, have a very high atomic number and density relative to other soft tissue. To a DXA system, it looks like bone when at full concentration and results in biased results [137]. Barium contrast for CT also has a very high atomic number and is dense at full concentration (Fig. 23). At full concentration, the contrast in the blood vessels superimposes on the bone in the projectional image, causing an increase in bone density in that region. At lower concentrations, it can make the soft tissue look leaner and account too much attenuation to the total soft tissue, reducing the DXA measure of bone density.

Any residual concentration of these contrasts in the DXA scan ROIs will cause artefacts.

Sala et al. [138] investigated the level at which diagnostic radioisotopes and radiographic contrast media interfered with whole body DXA scans. Forty patients, ten in four groups, who had previously been treated for malignant lymphomas or solid tumours, received one of the following procedures: CT (with intravenous, iodine based contrast (\pm oral contrast)), MRI (with gadolinium based contrast), GS (gallium scan), and TBS (technetium bone scan). A whole body DXA scan (Hologic QDR-4500A) was acquired before (baseline) and after the procedure on the same day and 7 d later. The difference in the DXA measures between the baseline and same day post-procedure scan are given in Table 10. After 7 d, there were no statistically significant differences between the 7 d and the baseline DXA measures.

However, well trained DXA technologists will reject scans containing contrast for questionable accuracy. Since DXA is rarely an emergency measure, one should wait about 5–7 half-lives of the contrasts in the body. Most centres treat this guideline conservatively and wait 10–14 d after any radioisotope or contrast procedure to make scheduling easier.



FIG. 23. Barium present in the DXA scan due to a barium enema (courtesy of J. Shepherd, UCSF).

TABLE 10. PER CENT CHANGE IN WHOLE BODY DXA SCAN VALUES BEFORE AND IMMEDIATELY AFTER RADIOLOGICAL PROCEDURES CONTAINING CONTRAST [138]

Procedure	TBM	BMC	FM	LBM
CT	<2%*	124.5%*	75.4%*	110%*
MRI	NS	NS	NS	NS
GS	<2%*	NS	NS	NS
TBS	NS	NS	NS	NS

* $p < 0.001$.

6.6.4. Pacemakers

Pacemakers are found in the upper left side of the torso. They contain metal and show up in a scan as dense bone. An example is shown in Fig. 24. Pacemakers increase whole body bone mass and density but do not change in mass over time. Thus, they may cause inaccuracies when comparing a patient to reference data but do not interfere with longitudinal studies. One effective way to eliminate pacemaker effects is to use the hemiscan analysis option (Section 6.3).

6.6.5. Calcium tablets

Tablets containing calcium, such as calcium supplements and stomach antacids, can cause increased aBMD and BMC results if the tablet overlays the bone, especially in spine scans. Kendler et al. performed a series of phantom and in vivo experiments where tablets that contained calcium were superimposed over the spine [139] (Fig. 25). A tablet with 500 mg of calcium, either placed on top of a phantom or taped onto a subject, increased the L1–L4 aBMD by $\leq 2.2\%$. Tablets with more calcium produced up to a 12% change in individual vertebrae for patients with low aBMD. It was concluded that a single calcium tablet is insufficient to alter the diagnostic classification of a patient when L1–L4 is used. However, if fewer vertebrae are used for the total aBMD, misclassification could occur. In addition, the precision of monitoring aBMD over time is adversely affected if a tablet was directly overlaying bone and undetected.

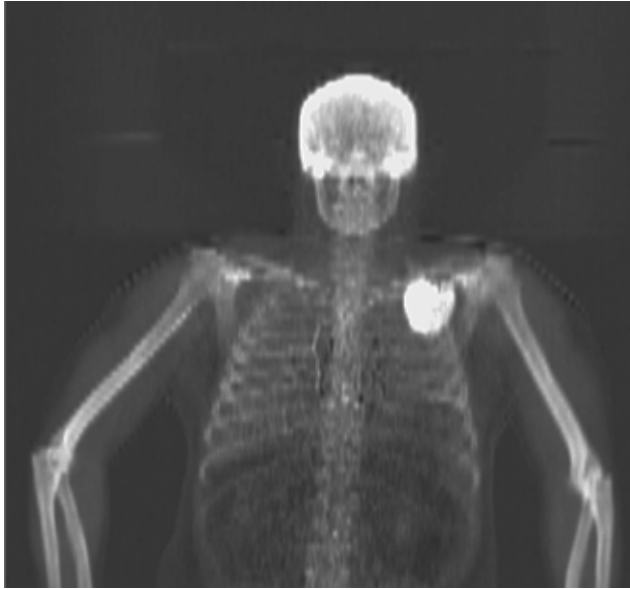


FIG. 24. Example of a pacemaker in a whole body scan (courtesy of J. Shepherd, UCSF).

6.6.6. Patient movement

Movement, in the extreme case, looks like discontinuities in the bone or soft tissue when, from visual observation, there are no physical anomalies (i.e. missing arms, misalignment of long bones, etc.) (Fig. 26). If possible, the patient should be re-scanned. As in children, after three attempts, the best scan should be used and the body parts with movement either imputed or removed using hemiscan analysis.

6.6.7. Metal in the scan field: Total hip and knee arthroplasty

Metal is a profound error source in DXA scans and presents as very dense bone. If included in a scan, it can falsely raise the aBMD and BMC to very high levels [137]. To determine what effect an artefact has on BMC and PCTFM, an ROI box should be placed around the artefact and a similar area without artefact and the difference in results noted (Figs 27 and 28). One can also determine the possible mass effect of a pillow or wig by placing an ROI in the area of question and noting the results in the area and BMC columns. Bone mapping is another useful tool to view how artefacts are analysed (bone or soft tissue).

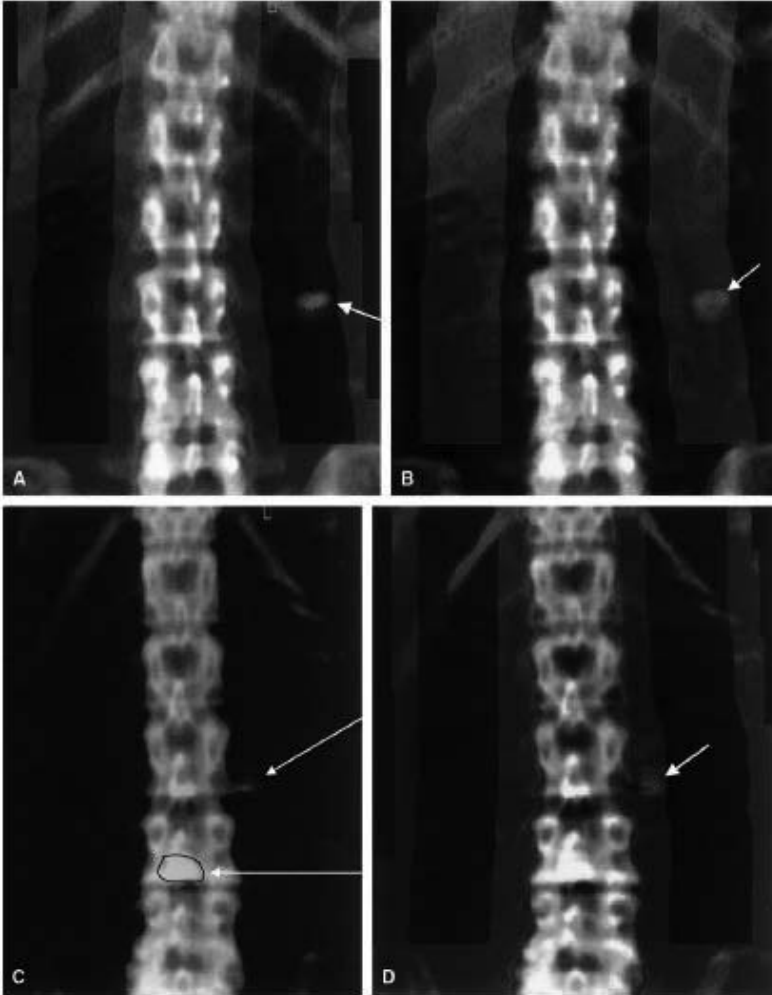


FIG. 25. GE Lunar lumbar spine DXA images and caption from Kendler et al. [139] showing calcium tablets taped to the skin of a volunteer. The image in (a) shows one 500 mg calcium tablet correctly mapped as an artefact. The image in (b) shows the same tablet mapped as soft tissue, highlighting how the algorithms are challenged by small artefacts. (c) Two 200 mg calcium tablets (arrows) totally and partly overlying bone. When totally overlying bone, the tablet (circled) is considered to be bone, although if visible to the technologist, it can be manually deleted from the analysis or the entire vertebral body can be excluded from analysis. The tablet partly overlying bone (top arrow) interferes with proper edge detection; the tablet is mapped partly as bone (green projection from edge of vertebral body, right side of image) and partly as neutral field (tablet appears as greyish-white oval shaped object at tip of top arrow). (d) Neutral field shaded green, includes part of calcium tablet as explained in (c) (used with permission from the J. Clin. Dens., Elsevier).



FIG. 26. Left arm movement appearing as a discontinuous humerus (courtesy of J. Shepherd, UCSF).



FIG. 27. Checking for the magnitude of the effect on BMC of a metal rod. By comparing the BMC of the right leg without metal to the left leg, one can determine how much the BMC is elevated on the whole body BMC (courtesy of J. Shepherd, UCSF).

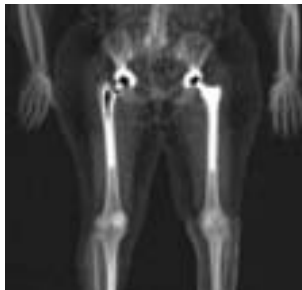


FIG. 28. Bilateral total hip arthroplasty (courtesy of J. Shepherd, UCSF).

7. REPORTING RESULTS

7.1. DEMOGRAPHIC INFORMATION NEEDED

A DXA report should identify the patient, convey the validity of the study and provide a clear interpretation of the examination, and recommendations. The rationale of what to include in a DXA report has been previously described in an ISCD publication [140]. There is a minimum of elements that should be included in a DXA report, no matter whether it is a central scan for osteoporosis or a whole body scan for body composition.

Essential elements of a DXA report

- (1) Date of examination.
- (2) Patient demographics (name, date of birth or age, sex, race or ethnicity, height, weight).
- (3) Requesting physician.
- (4) Names of those receiving a copy of report.
- (5) Indications for test.
- (6) Manufacturer and model of instrument and software version.
- (7) Measurement value(s).
- (8) Reference database (if applicable) used to determine the percentiles, fracture risk estimates, *T* and *Z* score.
- (9) Skeletal site/ROI scanned.
- (10) Quality of test: excellent, limited, not completed, poor, etc.
- (11) Limitations of the test if any.
- (12) Other clinical risk factors identified during the examination.
- (13) Estimations based on measures: fracture risk, obesity, heart disease due to calcified artery, etc.
- (14) General statements that a medical evaluation for secondary causes of low aBMD, high PCTFM, low PCTFM, etc., may be appropriate.
- (15) Recommendations for follow-up imaging.

7.2. REFERENCE DATA AND ASSOCIATED VALUES

Reference data are used to compare the individual to a population. The average values acquired from a DXA scan, such as aBMD, BMC, PCTFM, etc., differ between groups by age, sex and ethnicity. Therefore, there have been many studies to describe a variety of ethnicities for both sexes. For example, Fig. 29 shows total hip aBMD versus age for Hispanic, black and non-Hispanic Caucasians for both males and females living in the United States of America [141]. Care must be used to compare individuals to the reference curves that best match their age, sex and ethnicity if looking for normality. For example, if the aBMD of a black male is compared to the Caucasian male reference curve, the black male would appear to have unusually high aBMD for his age, when in fact the aBMD may be normal when compared to other black men. Much of these differences can be attributed to bone size.

Reference data have two practical purposes for DXA systems: determining fracture risk (T scores) and determining how an individual compares to their peers (Z scores). When determining fracture risk with values such as the T score, it may be appropriate to compare everyone, men and women of different ethnicities, to the same reference curve after adjustments

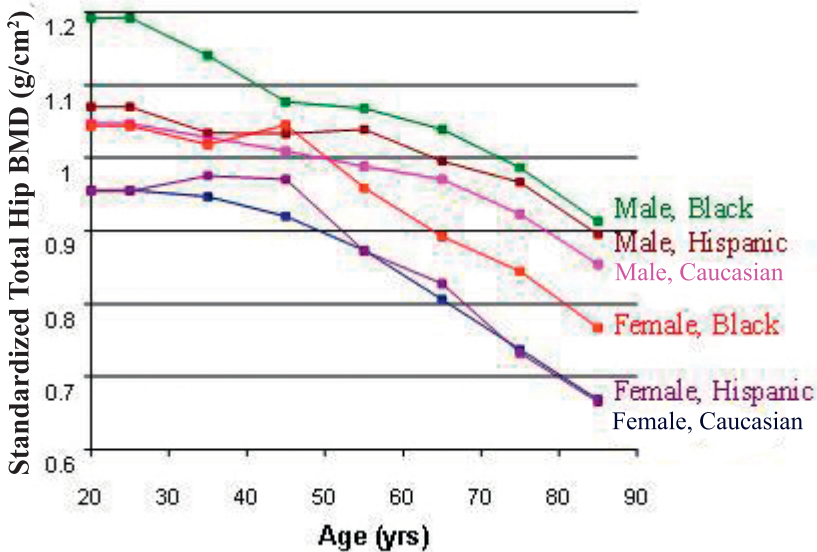


FIG. 29. Hip reference data from the NHANES III Study [141]. aBMD is shown in standardized sBMD units (plot courtesy of J. Shepherd, UCSF).

for bone size, since bone strength is a material property. Since more is known regarding how aBMD relates to fracture risk in Caucasian women than in men or other ethnicities, it is recommended that Caucasian women be used to calculate T scores and how the T score relates to fracture risk (see Section 7.2.2). WHO recommends calculating all adult T scores from the Caucasian women's reference values from the NHANES III study. It is important to note that reference data are acquired using a manufacturer specific positioning protocol, analysis procedures and software version. If the clinical patient is positioned differently than described by the manufacturer's manual, analysed with different ROIs or software version, significant bias can occur. For example, substantial differences have been reported for the total femur aBMD at different angles of rotation [142].

7.2.1. Use of reference data for generating T and Z scores

The T score is the primary diagnostic value used for osteoporosis as in the elderly, post-menopausal women and men over 50 years, the T score is inversely related to fracture risk. A T score is the difference between the patient's aBMD and a young reference aBMD in units of the population SD. Since the report of the WHO study group published in 1994 [143], the ISCD has been one of several organizations developing guidelines for scan interpretation based on the use of T scores and Z scores [7]. The T score was first introduced in the late 1980s and is defined as:

$$T \text{ score} = \frac{\text{aBMD}_{\text{patient}} - \text{aBMD}_{\text{Young Adult Mean}}}{\text{SD}_{\text{Young Adult Mean}}} \quad (34)$$

SD is the standard deviation of the population of young adults. aBMD can also be expressed as a Z score, the difference between the patient's aBMD and an age and typically ethnicity matched reference aBMD and SDs:

$$Z \text{ score} = \frac{\text{aBMD}_{\text{patient}} - \text{aBMD}_{\text{age-, ethnicity-matched adult mean}}}{\text{SD}_{\text{age-, ethnicity-matched adult mean}}} \quad (35)$$

The *T* score is used to diagnose osteoporosis in older adults while the *Z* score is used to diagnose low bone mass in young adults and children. A frequent presumption is that the *T* and *Z* scores should be very similar or identical for younger individuals. However, current guidelines are to derive the *T* score from one particular reference population. The original WHO criteria are stated in Table 11.

TABLE 11. WHO CRITERIA FOR DIAGNOSING OSTEOPOROSIS FROM *T*-SCORES [143]. IT SHOULD BE NOTED THAT THIS CRITERION IS EXCLUSIVELY APPLICABLE FOR POST-MENOPAUSAL WOMEN AND MEN OVER 50, AND NOT FOR YOUNGER ADULTS OR CHILDREN

Status	Criteria
Normal	aBMD is within 1 SD of a 'young normal' adult (<i>T</i> score at -1.0 and above)
Low bone mass (osteopenia)	aBMD is between 1 and 2.5 SD below that of a 'young normal' adult (<i>T</i> score between -1 and -2.5)
Osteoporosis	aBMD is 2.5 SD or more below that of a 'young normal' adult (<i>T</i> score at or below -2.5)
Severe (established) osteoporosis	<i>T</i> score at or below -2.5 and one or more fractures

TABLE 12. *T* SCORE REFERENCE VALUES FOR FEMORAL NECK aBMD (GM/cm²) NHANES III, PHASE 1, 1988-1991 [144]. IT SHOULD BE NOTED THAT THESE aBMD VALUES ARE IN HOLOGIC CALIBRATION UNITS

Sex (race/ethnicity)	Age range	<i>N</i>	aBMD mean (g/cm ²)	SD (g/cm ²)
Female (non-Hispanic/Caucasian)	20-29	194	0.849	0.109
Male (non-Hispanic/Caucasian)	20-29	207	0.930	0.138

In addition, WHO recommends that the T scores to diagnose osteoporosis in men and women, and to define prevalence of disease, should be derived exclusively from the femoral neck aBMD values for Caucasian females, 20–29 years old, found in the NHANES III database [144]. These values are implemented on all the major bone densitometer brands after conversion to their respective calibrations. The values given in Ref. [144] are for Hologic systems and are shown in Table 12.

There is still debate as to whether men should be compared to the female reference data or to a male reference data set. For example, the ISCD states in their position document that osteoporosis can be diagnosed using a T score less than or equal to -2.5 from either the spine, total hip, femoral neck or one-third radius, and that men should be compared to men and women to women. However, the WHO criteria are not directly applicable to DXA bone density measures not acquired at the spine, hip or one-third radius. The WHO criteria should not be applied to other bone density measures, including QCT of the spine or hip, peripheral densitometry systems using ultrasound, DXA or other technologies that scan the fingers, metacarpals or heels.

7.2.2. Fracture risk models

The current WHO guidelines for diagnosing and treating osteoporosis are based on a comprehensive fracture risk model called WHO FRAX. The WHO FRAX algorithm estimates the likelihood for a person to break a hip or other major bone due to low bone mass or osteoporosis over a period of ten years. The National Osteoporosis Foundation (NOF) has prepared a clinician's guide to osteoporosis that discusses the details of the FRAX model and the use of fracture risk versus BMD alone (see http://www.nof.org/professionals/NOF_Clinicians%20_Guide.pdf). In summary, the major recommendations to the clinician regarding the diagnosis of osteoporosis are outlined in the text box. However, clinicians should refer to the entire NOF report for details.

The WHO FRAX model is very easy to use. It is available on the Sheffield University web site (<http://www.shef.ac.uk/FRAX/>). It is important to note that the WHO FRAX algorithm only pertains to individuals that have not been treated for osteoporosis. An example screen capture is shown in Fig. 30. There is currently no fracture risk model for women once they have been treated with chemoprevention agents. The advantage of using the WHO FRAX model is that it takes into account major risk factors and has been validated in study

populations in Europe, North America, Asia and Australia. However, there is still a need to calculate T scores for BMD. The WHO FRAX model insists that T scores be calculated with female, Caucasian NHANES III reference data regardless of ethnicity and gender. To include regional variations in risk factors, one must use the version of the tool that best describes the ethnicity of the patient. The NOF in the United States of America has incorporated the FRAX model into treatment guidelines [145]. The recommendations are given at the end of this section. However, guidelines for initiating treatment can vary from country to country. In the next section, the acquisition of local reference data for calculating Z scores is covered with some examples from the literature.

Calculation Tool

Please answer the questions below to calculate the ten year probability of fracture with BMD.



Weight Conversion:
pound:

Height Conversion:
inch:

Country : **US(Caucasian)**
Name / ID : Ms. Jane Doe
About the risk factors i

Questionnaire:

1. Age (between 40-90 years) or Date of birth
Age: Y: M: D:

2. Sex Male Female

3. Weight (kg)

4. Height (cm)

5. Previous fracture No Yes

6. Parent fractured hip No Yes

7. Current smoking No Yes

8. Glucocorticoids No Yes

9. Rheumatoid arthritis No Yes

10. Secondary osteoporosis No Yes

11. Alcohol 3 more units per day No Yes

12. Femoral neck BMD
T-score

BMI: 19.8
The ten year probability of fracture (%)

with BMD	
Major osteoporotic	30
Hip fracture	2.7

FIG. 30. Screen clipping of the WHO FRAX fracture risk model from <http://www.shef.ac.uk/FRAX/>. The example shown is for a female Caucasian living in the United States of America. Other countries and ethnicities are also available.

**NOF recommendations to the clinician for
initiating osteoporosis treatment [145]**

For post-menopausal women and men aged 50 and older:

- (1) Patients should be counselled on the risk of osteoporosis and related fractures.
- (2) Secondary causes should be checked.
- (3) Advice on adequate amounts of calcium (at least 1200 mg/d, including supplements if necessary) and vitamin D (800 to 1000 IU per day of vitamin D3 for individuals at risk of insufficiency) should be given.
- (4) Regular weight bearing and muscle strengthening exercises should be recommended to reduce the risk of falls and fractures.
- (5) Patients should be advised to avoid tobacco smoking and excessive alcohol intake.
- (6) For women aged 65 and older and men aged 70 and older, BMD testing should be recommended.
- (7) For post-menopausal women and men aged 50–70, BMD testing should be recommended where there is concern based on their risk factor profile.
- (8) BMD testing should be recommended to those who have suffered a fracture to determine the degree of disease severity.
- (9) Treatment should be initiated in those with hip or vertebral (clinical or morphometric) fractures.
- (10) Therapy should be initiated in those with BMD *T* scores <-2.5 at the femoral neck, total hip or spine by DXA, after appropriate evaluation.
- (11) Treatment should be initiated in post-menopausal women and in men aged 50 and older with low bone mass (*T* score -1 to -2.5 , osteopenia) at the femoral neck, total hip or spine and ten year hip fracture probability $\geq 3\%$ or a ten year all major osteoporosis related fracture probability of $\geq 20\%$ based on the United States of America adapted WHO absolute fracture risk model.
- (12) Current FDA approved pharmacologic options for osteoporosis prevention and/or treatment are bisphosphonates (alendronate, ibandronate, risedronate and zoledronate), calcitonin, oestrogens and/or hormone therapy, raloxifene and parathyroid hormone (PTH 1–34).
- (13) BMD testing performed in DXA centres using accepted quality assurance measures is appropriate for monitoring bone loss (recommendation: every 2 years). For patients on pharmacotherapy, it is typically performed two years after initiating therapy and at two year intervals thereafter.

7.2.3. Use of *Z* scores in children

Low bone density in children is not a normal occurrence and is usually associated with a secondary condition, such as corticosteroid use, autoimmune diseases, etc. It does not make sense to apply *T* scores to those who have not achieved peak bone mass; thus, *Z* scores are used. The ISCD states that children with a *Z* score of -2 or below measured at the spine or whole body should be considered to have 'low bone mass' [146]. It is not considered appropriate to use the term osteoporosis except in the elderly. The reference data tables from the NICHD Bone Mineral Density in Children Study (BMDCS) [147] in Appendix III can be used to calculate both *Z* scores and percentiles when using Hologic systems. The BMDCS divided their population of 1500 healthy boys and girls by ethnicity and sex. The ethnicity is grouped in the tables by black and non-black. The non-black contains Caucasian, Asian and Hispanic children. In many parts of the world, these US reference data may not represent the local population and the collection of local reference data may be necessary to truly understand what aBMD values are normal for a region. Reference values for children in the United Kingdom [148] and the Netherlands [149] have also been published. There is still considerable discussion around the most appropriate ways of reporting bone mass in children, and how best to correct for differences in body size and pubertal status. The ISCD has recently published several position papers on these topics which might be of interest to the reader [146].

7.2.4. Reference ranges for PCTFM

Unfortunately, there is no consensus on how body fat is linked with morbidity or mortality. Most studies to date have used BMI as a surrogate measure of body fatness. Thus, no accepted published body fat ranges exist at the time of writing. There are general guidelines using BMI for being underweight ($<18.5 \text{ kg/m}^2$), overweight ($\geq 25 \text{ kg/m}^2$) and obesity ($\geq 30 \text{ kg/m}^2$). However, Gallagher et al. [150] found that the relationship between BMI and per cent fat measured by DXA is not a simple one. The best estimates (lowest SEE and highest correlation coefficients) are for functions that include age, sex and ethnicity with BMI to predict per cent body fat. However, there is some evidence that per cent body fat may be an improved phenotypic characteristic than BMI or simple weight loss. Allison et al. [151] found that although weight loss among individuals not severely obese was associated with increased mortality rate, fat loss was associated with decreased mortality rate.

Gallagher has derived a relationship between DXA PCTFM and BMI that includes statistically significant associations of sex, age and ethnicity [150]. The DXA PCTFM model had a similar correlation coefficient and SEE to BMI as the

four component PCTFM (r values of 0.90 versus 0.89 and SEE of 4.31% versus 3.97%, respectively). The differences between the PCTFM measures from DXA and the four component model were small but significant with a relationship of:

$$\text{PCTFAT}_{\text{DXA}} = -1.7 + 1.06\text{PCTFAT}_{4\text{C}} \quad (36)$$

where $r = 0.95$ and $\text{SEE} = 3.2\%$, and both the slope and intercept were statistically significant with $p < 0.001$. In the clinical range between 10 and 50% though, this results in less than a 1.5% bias. Thus, current BMI guidelines can be converted into PCTFM guidelines. However, this generates unique PCTFM threshold values of underweight, normal and obesity by sex, race and age.

7.2.5. How to collect local reference data

As the standardization of the diagnosis of osteoporosis is with a single reference database as outlined by WHO criteria, local reference values are primarily valuable for body composition analysis and in younger (paediatric) populations for determining Z scores. Local reference values can be defined as either 'healthy', 'representative' or 'normal'. Unfortunately, there are no standard definitions for these terms. For example, the BMDCS study is a healthy cohort that excluded all children with bone disease, children taking any medications that may affect bone density, children with multiple fractures, etc. [147]. The NHANES III study is a representative cohort of women recruited randomly by postal code throughout the United States of America, regardless of health status [144].

This guide for obtaining normative ranges was modelled after an investigator's guide used by one of the manufacturers. The number of subjects and the age distributions are based on statistical justifications not mentioned here. If the investigator deviates substantially from this protocol, statistical power and relevance may be lost, especially if collecting fewer numbers.

The following describes the procedures for adult reference data collections. The investigator will need to recruit a minimum of 300 participants for each group desired, separated by sex and ethnicity. For example, adequately describing two distinct ethnic groups for both sexes requires 1200 participants (i.e. 50 subjects for each decade, sex and ethnicity between 20 and 80 years old) (Table 13). The investigator will also need to capture all biological information. A QC phantom scan needs to be performed at least on the days that the subject is scanned but preferably three times a week to daily. The measurements and ROIs the investigator acquires are dependent on their needs. If the need is exclusively

TABLE 13. RECRUITMENT GOALS FOR ADULT REFERENCE DATA STUDY FOR EACH SEX AND ETHNIC GROUP

Decade of age	Total number of subjects
20–29	50
30–39	50
40–49	50
50–59	50
60–69	50
70–79	50
Total	300

for bone density assessment in adults, spine, hip and forearm DXA are appropriate. For body composition studies, whole body needs to be included. Each site is measured once for each subject and the results are recorded on the CRF. The CRFs can then be sent to a statistician for analysis.

Demographics, medical history and drug therapies should be noted on a completed patient information questionnaire as shown in Appendix II.

There is some debate as to the statistical method used to evaluate reference data. The simplest analysis is to calculate a population mean and SD for each ten year age group. *Z* scores can then be generated by comparing a patient's measure to the decade reference values. Others have suggested that a quinquennial analysis of the means [152] offers better resolution for separating pre- and post-menopausal women than other fitting approaches. Regression models can be used to achieve more age resolution and stability in the *Z* score values through each decade. Several approaches can be used; non-linear and piecewise linear models have been used in the past. For a non-linear model, the measure is plotted against age. The highest order regression (i.e. age, age², age³) yielding a significant improvement over the next lower order regression model should be considered as the basis for the final reference data equation. *Z* scores are then calculated using this equation to generate the measure mean and SD for the patient's age. The SEE is used for the average SD across the entire age range. However, this assumes that the distributions around the mean values are normal.

The most sophisticated approach is to take skew into account in the distributions around the mean values. Cole has developed a model and software that calculates percentile curves without assumptions of how normal the

distribution is. This method, called LMS, is a fitting procedure that employs three cubic splines to generate centile estimates for age or size related growth [153]. T. Cole offers a free program to perform this type of analysis (<http://homepage.mac.com/tjcole/FileSharing1.html>). The L curve, a Box–Cox power transformation of the measured variable, characterizes skewness; the M curve is the median for the measure (e.g. aBMD); and the S curve represents the CV of the measure. Z scores and centiles can be generated from the L, M and S values. To obtain a Z score for an individual subject, the following equation is used:

$$Z = [(measurement/M)L - 1]/(L \times S) \quad (37)$$

where the measurement represents the result from a DXA scan (aBMD, BMC, PCTFM, etc.), and L, M and S are age specific values. Similarly, the centiles for age are obtained using the equation:

$$centile = M(1 + L \times S \times Z)^{1/L} \quad (38)$$

where L, M and S are for the required age and sex, and Z is the standard normal deviate for the corresponding centile (e.g. for the 50th centile, Z = 0). Examples of this type of reference data curve are the CDC growth charts [154], and the children's aBMD and BMC reference data curves by Kalkwarf [147]. In Appendix III, Table 14 contains a review of known paediatric reference data. Reference data from Kalkwarf are also given in Table 15 for US Spine BMD, in Table 16 for US whole body BMD, in Table 17 for US Spine BMC and in Table 18 for US whole body BMC.

Appendix I

DXA DENSITOMETER QC REPORT

(Please copy this and fill out on a monthly basis. Place completed forms in the site QC binder)

Site name and location: _____

Scanner serial number: _____ Spine phantom number: _____

(1) Is a new/different scanner being used for any patients since the date of the last report?

Yes No If so, what is the make of the new scanner? _____

(a) Was the scanner change approved in advance by all study investigators associated with this system?

Yes No By whom? _____

(2) Have there been any software changes?

Yes No If yes, indicate the following:

Old SW version: _____ New SW version: _____ Date installed: _____

(a) Was the software change approved in advance by all study investigators associated with this system?

Yes No By whom? _____

(3) Were there any operator changes?

Yes No If yes, please identify them:

Operator	Added / Departed	Date of Change	Date of Manufacturer's Training
_____	_____	_____	_____
_____	_____	_____	_____
_____	_____	_____	_____
_____	_____	_____	_____

(4) Were there any maintenance/recalibration/repair problems?

Yes No If yes, indicate:

Service performed	Date of Service
_____	_____
_____	_____
_____	_____
_____	_____

Please attach a copy of the service report if available.

(5) Additional comments (use reverse side if necessary)

Main operator: _____ Date: _____ Telephone no.: _____

Appendix II

DXA PATIENT QUESTIONNAIRE

(This questionnaire is based on the sample provided by the International Society for Clinical Densitometry at <http://www.iscd.org>).

Please complete this questionnaire while waiting for your bone mineral density test. A technologist may review this document with you. A staff member will measure your weight and height.

Name (print): _____

Date: _____

Date of birth: _____

Is there a chance that you are pregnant? Yes No

Have you had a barium X ray in the last 2 weeks? Yes No

Have you had a nuclear medicine scan or injection of an X ray dye in the last week?
Yes No

Have you had hyperparathyroidism or a high calcium level in your blood?
Yes No

Have you ever had surgery of the spine or hips? Yes No

If you answered YES to any of the above, speak to our receptionist right away.

(1) Sex: Male Female

(2) Check one:
__White __Black __Asian __Hispanic __Other _____

Country of birth: _____

(3) Have you ever had a bone density test? Yes No

If YES, when and where? _____

(4) Have you had a recent weight change? Yes No

If YES, tell us about it: _____

(5) Your tallest height (late teens or young adult): _____

(6) Have you ever broken a bone? Yes No

Bone broken	Simple fall?	If not a simple fall, please describe the circumstances	Age when this occurred

- (7) Has a parent or sibling had a broken hip from a simple fall or bump?
Yes No
- (8) Has a parent or sibling had any other type of broken bone from a simple fall or bump?
Yes No
- (9) How many times have you fallen in the last year? _____
- (10) Have you ever had surgery of the spine, hips, legs or arms?
Yes No

If YES, describe what type of surgery you had and which side was affected:

- (11) Are you currently receiving or have you previously received prednisone pills (cortisone)? Yes, currently ____ Yes, previously ____ No _____
 If YES, for how long? _____ What is your dose? ____ mg or _____ pills each day

- (12) Please list your prescription medications:

- (13) Are you currently receiving or have you previously received any of the following medications?

	No	Yes	For how long?
Medication for seizures or epilepsy			
Chemotherapy for cancer			
Medication for prostate cancer			
Medication to prevent organ transplant rejection			

(14) Have you been diagnosed with any of the following conditions?

Condition	When	Comments
Chronic kidney disease		
Chronic liver disease		
Hyperthyroidism		
Hyperprolactinemia		
Premenopausal amenorrhea (excluding pregnancy)		
Oophorectomy in women under 50 years		
Hypogonadism		
Rheumatoid arthritis		
Ankylosing spondylitis		
Paget's disease		
Cancer		
Established osteoporosis		

(15) Have you been treated with any of the following medications?

Medication	Ever?	Currently?	If currently, how long?
Hormone replacement therapy (oestrogen)			
Steroids over 50 mg/day			
Anti-seizure medication			
Tamoxifen			
Raloxifene (Evista)			
Testosterone			
Etidronate (Didronel/Didrocal)			
Alendronate (Fosamax)			
Risedronate (Actonel)			
Intravenous pamidronate (Aredia)			
Clodronate (Bonefos, Ostac)			
Calcitonin (Miacalcin nasal spray)			
PTH (Forteo)			
Zoledronic acid (Zometa)			
Sodium fluoride (Fluotic)			

- | | | |
|---|-----|----|
| (16) Do you take any calcium supplements? | Yes | No |
| (17) Do you take any vitamin D supplements (including multivitamins and halibut liver oil)? | Yes | No |
| (18) Do you smoke? | Yes | No |

For women only:

- | | | |
|---|-----|----|
| (19) Are you still having menstrual periods? | Yes | No |
| (20) Before the menopause, did you ever miss your periods for 6 months or more, besides during pregnancy? | Yes | No |
| (21) Have you had your menopause?
If yes, at what age? _____ | Yes | No |
| (22) Have you had a hysterectomy?
If yes, at what age? _____ | Yes | No |
| (23) Have you had both of your ovaries removed?
If yes, at what age? _____ | Yes | No |

Appendix III

NORMATIVE DXA DATA FOR PAEDIATRIC SUBJECTS

TABLE 14. SUMMARY OF NORMATIVE DATA IN PAEDIATRIC SUBJECTS FROM GORDON et al. [155]
(*the sex of all subjects is male and female unless otherwise noted*)

Year of publication	[Ref.]	DXA system	Number	Age	Ethnicity/nationality	Sites
1991	[156]	Hologic 1000	207	9–18	Caucasian (Swiss)	Femoral neck, spine (L2–L4)
1999	[157]	Hologic 1000 pencil beam	423 ^a	9–25	Asian, black, Hispanic, Caucasian	Femoral neck, total hip, total body, spine (L2–L4)
1997	[158]	Hologic 1000 pencil beam	343	5–19	Caucasian (Denmark)	Total BMD, BMC, BA
2002	[159]	Hologic 1000/2000	256	3–18	Caucasian, black, other	Spine, proximal and distal femur
2001	[160]	Hologic 2000	982	5–18	Caucasian, black, Hispanic	Total body (corrected for size)
1996	[161]	Hologic 2000 (array)	234 ^a	8–17	Caucasian (Canada)	Femoral neck, total body, spine (L1–L4)
1993	[162]	Hologic 2000 FB	234	8–16	Caucasian (Canada)	Lumbar and total BMC and BMD
2005	[163]	Hologic 4500	>1000	3–20	Unknown (United States of America)	Spine, total hip, whole body
2002	[164]	Hologic 4500	231	5–22	Mostly Caucasian	Total body BMC (tibial pQCT)
2007	[165]	Hologic 4500 A + Discovery	179	3–18	Canadian	Whole body, spine, proximal femur

TABLE 14. SUMMARY OF NORMATIVE DATA IN PAEDIATRIC SUBJECTS FROM GORDON et al. [155] (cont.)
(the sex of all subjects is male and female unless otherwise noted)

Year of publication	[Ref.]	DXA system	Number	Age	Ethnicity/nationality	Sites
2004	[166]	Hologic 4500A	363	10–17	Arab/Lebanese	Spine, total body, femoral neck, distal third of radius
2004	[166]	Hologic 4500A	363	10–17	Arab/Lebanese	Spine, total body, femoral neck, distal third of radius (volumetric)
2007	[167]	Hologic 4500A + Discovery A	179	3–18	Canadian	Whole body BMC + body composition
2006	[168]	Hologic QDR 4500	345	2–18	Turkish	Spine, femur BMD, BMDvol
2007	[147]	Hologic QDR 4500	1554	7–17	Caucasian, black, Hispanic	Spine, hip, total body, forearm
2004	[169]	Hologic QDR 4500 W	422 ^b	12–18	Caucasian, black (United States of America)	Spine L2–L4, femoral neck BMD
2007	[148]	Hologic QDR Discovery	442	6–17	British	Spine, hip, total body
2001	[170]	Lunar DPX	255	6–14	Caucasian (Brazil)	Spine BMC and BMD
1996	[171]	Lunar DPX	209	5–27	Caucasian (Australia)	Spine (L1–L4), femoral neck, mid to shaft femur
2003	[172]	Lunar DPX	459	3–30	Caucasian	Total body (corrected for lean body mass)
2005	[173]	Lunar DPX to L	562	5–18	Polish	Spine, total body

TABLE 14. SUMMARY OF NORMATIVE DATA IN PAEDIATRIC SUBJECTS FROM GORDON et al. [155] (cont.)
(the sex of all subjects is male and female unless otherwise noted)

Year of publication	[Ref.]	DXA system	Number	Age	Ethnicity/nationality	Sites
2004	[174]	Lunar DPX L pencil beam	646	5–18	Unknown (United Kingdom)	Spine, total body (corrected for lean body mass)
1994	[175]	Lunar DPX to L	471	3 months to 21 years	Caucasian (Spain)	Spine (L2–L4)
2005	[176]	Lunar DPX to L/GE or Prodigy	1508	5–18	Caucasian, black, Asian	Spine, total body BMD and BMAD
2004	[177]	Lunar DPX, DPX to L	1218	6–18	Caucasian, black, Asian, Hispanic	Total body BMC, BMD
2002	[149]	Lunar DPXL/PED	444	4–20	Caucasian (Netherlands)	Total body, spine (L1–L4) body composition, BMAD, Tanner stages
1997	[178]	Lunar DPXL/PED	500	4–20	Dutch Caucasian, black, Asian	Spine, total body, BM, BMDvol
1995	[179]	Norland XR to 26	778	2–20	Caucasian (Argentina)	Whole body, spine, femoral neck, radius, trochanter

TABLE 14. SUMMARY OF NORMATIVE DATA IN PAEDIATRIC SUBJECTS FROM GORDON et al. [155] (cont.)
(the sex of all subjects is male and female unless otherwise noted)

Year of publication	[Ref.]	DXA system	Number	Age	Ethnicity/nationality	Sites
1998	[180]	Norland XR to 26, Norland 278	179	12–13	Chinese	Spine L2–L4 BMD, distal radius (BMC)
2004	[168]	Norland XR to 35	102	3–15	Turkish	Spine, femoral neck BMD

^a The number of scans included in these databases exceeds the number of subjects because individuals were scanned repeatedly in these longitudinal studies.

^b All subjects female.

TABLE 15. LUMBAR SPINE aBMD: LMS VALUES AND SELECTED MODELLED PERCENTILES BY SEX, RACE AND AGE
 (from Kalkwarf et al. [147], used with permission from the Endocrine Society)

Male, Non-Black											Female, Non-Black																				
Age (n ¹)	LMS Parameters Modeled Percentile						LMS Parameters Modeled Percentile						Age (n)	LMS Parameters Modeled Percentile																	
	L	S	3rd	10th	M 50 ^b	90th	97th	L	S	3rd	10th	M 50 ^b		90th	97th	L	S	3rd	10th	M 50 ^b	90th	97th									
7 (135)	.474	.111	.423	.455	.527	.605	.643	7 (147)	-.616	.116	.431	.458	.528	.618	.668	8 (158)	-.477	.112	.442	.476	.552	.634	.675	8 (177)	-.524	.117	.449	.479	.553	.646	.698
8 (158)	.477	.112	.442	.476	.552	.634	.675	8 (177)	-.524	.117	.449	.479	.553	.646	.698	9 (132)	.484	.113	.459	.494	.574	.661	.703	9 (152)	-.438	.118	.467	.499	.578	.676	.730
9 (132)	.484	.113	.459	.494	.574	.661	.703	9 (152)	-.438	.118	.467	.499	.578	.676	.730	10 (157)	.519	.114	.474	.511	.595	.685	.729	10 (174)	-.314	.124	.487	.523	.610	.718	.777
10 (157)	.519	.114	.474	.511	.595	.685	.729	10 (174)	-.314	.124	.487	.523	.610	.718	.777	11 (174)	.616	.116	.489	.529	.618	.712	.758	11 (178)	-.048	.140	.508	.552	.660	.791	.861
11 (174)	.616	.116	.489	.529	.618	.712	.758	11 (178)	-.048	.140	.508	.552	.660	.791	.861	12 (158)	.872	.118	.510	.555	.653	.753	.800	12 (175)	.443	.152	.546	.605	.742	.894	.971
12 (158)	.872	.118	.510	.555	.653	.753	.800	12 (175)	.443	.152	.546	.605	.742	.894	.971	13 (131)	1.25	.121	.540	.595	.707	.815	.865	13 (159)	.870	.137	.622	.688	.833	.981	1.051
13 (131)	1.25	.121	.540	.595	.707	.815	.865	13 (159)	.870	.137	.622	.688	.833	.981	1.051	14 (157)	1.28	.125	.593	.655	.784	.907	.962	14 (157)	.781	.119	.712	.774	.910	1.052	1.119
14 (157)	1.28	.125	.593	.655	.784	.907	.962	14 (157)	.781	.119	.712	.774	.910	1.052	1.119	15 (150)	.692	.126	.674	.736	.873	1.018	1.087	15 (164)	-.582	.110	.769	.828	.958	1.097	1.164
15 (150)	.692	.126	.674	.736	.873	1.018	1.087	15 (164)	-.582	.110	.769	.828	.958	1.097	1.164	16 (144)	.213	.125	.746	.807	.950	1.112	1.194	16 (105)	.471	.105	.799	.855	.982	1.118	1.185
16 (144)	.213	.125	.746	.807	.950	1.112	1.194	16 (105)	.471	.105	.799	.855	.982	1.118	1.185	17 (70)	-.211	.123	.800	.859	1.003	1.179	1.273	17 (70)	-.211	.123	.800	.859	1.003	1.179	1.273

Male, Black											Female, Black																				
Age (n)	LMS Parameters Modeled Percentile						LMS Parameters Modeled Percentile						Age (n)	LMS Parameters Modeled Percentile																	
	L	S	3rd	10th	M 50 ^b	90th	97th	L	S	3rd	10th	M 50 ^b		90th	97th	L	S	3rd	10th	M 50 ^b	90th	97th									
7 (35)	2.79	.103	.415	.466	.549	.615	.642	7 (37)	.814	.118	.446	.485	.570	.657	.698	8 (44)	2.37	.110	.439	.491	.583	.658	.690	8 (50)	.759	.118	.463	.502	.590	.681	.724
8 (44)	2.37	.110	.439	.491	.583	.658	.690	8 (50)	.759	.118	.463	.502	.590	.681	.724	9 (47)	2.05	.114	.458	.511	.608	.691	.727	9 (45)	.685	.118	.486	.527	.618	.714	.760
9 (47)	2.05	.114	.458	.511	.608	.691	.727	9 (45)	.685	.118	.486	.527	.618	.714	.760	10 (45)	1.79	.118	.473	.526	.628	.717	.757	10 (55)	.576	.118	.524	.567	.664	.768	.818
10 (45)	1.79	.118	.473	.526	.628	.717	.757	10 (55)	.576	.118	.524	.567	.664	.768	.818	11 (49)	1.47	.122	.492	.545	.651	.750	.794	11 (48)	.433	.118	.584	.630	.737	.854	.912
11 (49)	1.47	.122	.492	.545	.651	.750	.794	11 (48)	.433	.118	.584	.630	.737	.854	.912	12 (46)	.995	.128	.526	.579	.692	.806	.859	12 (61)	.269	.118	.659	.710	.829	.962	1.029
12 (46)	.995	.128	.526	.579	.692	.806	.859	12 (61)	.269	.118	.659	.710	.829	.962	1.029	13 (52)	.490	.134	.580	.634	.758	.894	.961	13 (58)	.113	.119	.727	.781	.911	1.059	1.135
13 (52)	.490	.134	.580	.634	.758	.894	.961	13 (58)	.113	.119	.727	.781	.911	1.059	1.135	14 (57)	.158	.135	.649	.706	.841	.998	1.079	14 (63)	-.021	.119	.777	.834	.971	1.131	1.214
14 (57)	.158	.135	.649	.706	.841	.998	1.079	14 (63)	-.021	.119	.777	.834	.971	1.131	1.214	15 (44)	-.021	.132	.722	.781	.924	1.095	1.185	15 (49)	-.127	.119	.811	.870	1.011	1.179	1.268
15 (44)	-.021	.132	.722	.781	.924	1.095	1.185	15 (49)	-.127	.119	.811	.870	1.011	1.179	1.268	16 (44)	-.137	.127	.775	.835	.981	1.157	1.252	16 (26)	-.212	.119	.836	.895	1.040	1.214	1.307
16 (44)	-.137	.127	.775	.835	.981	1.157	1.252	16 (26)	-.212	.119	.836	.895	1.040	1.214	1.307	17 (21)	-.231	.124	.806	.866	1.012	1.19	1.287	17 (21)	-.231	.124	.806	.866	1.012	1.19	1.287

* Percentile values should be interpolated for children who are between birthdays.
 + Number of observations in that age category

TABLE 16. WHOLE BODY aBMD: LMS VALUES AND SELECTED MODELLED PERCENTILES BY SEX, RACE AND AGE
 (from Kalkwarf et al. [147], used with permission from the Endocrine Society)

Female, Non-Black															
Male, Non-Black						Female, Non-Black									
Age (n ^a)	LMS Parameters Modeled Percentile					Age (n)	LMS Parameters Modeled Percentile								
	L	S	3rd	10th	M 50 ^b		90th	97th	L	S	3rd	10th	M 50 ^b	90th	97th
7 (134)	-433	.070	.636	.662	.723	.793	.828	7 (146)	-1.118	.072	.612	.636	.695	.766	.805
8 (154)	-471	.068	.673	.699	.762	.833	.870	8 (173)	-.952	.072	.644	.670	.732	.806	.846
9 (128)	-.506	.066	.706	.733	.797	.869	.906	9 (150)	-.792	.072	.674	.702	.767	.844	.884
10 (156)	-.538	.065	.735	.762	.827	.900	.938	10 (173)	-.618	.072	.706	.736	.805	.885	.927
11 (172)	-.568	.064	.761	.789	.855	.929	.968	11 (176)	-.414	.074	.740	.772	.847	.933	.977
12 (156)	-.602	.064	.789	.818	.886	.964	1.004	12 (171)	-.154	.077	.780	.816	.900	.994	1.042
13 (130)	-.645	.066	.822	.853	.926	1.010	1.053	13 (157)	.148	.078	.830	.871	.963	1.064	1.113
14 (156)	-.696	.070	.861	.896	.977	1.072	1.122	14 (156)	.433	.076	.882	.925	1.021	1.123	1.173
15 (151)	-.755	.075	.907	.946	1.038	1.146	1.205	15 (161)	.638	.072	.919	.963	1.059	1.159	1.207
16 (140)	-.815	.079	.954	.996	1.098	1.221	1.287	16 (105)	.754	.070	.939	.983	1.079	1.177	1.224
17 (70)	-.872	.082	.996	1.041	1.151	1.285	1.358								
Male, Black															
Age (n)	LMS Parameters Modeled Percentile					Age (n)	LMS Parameters Modeled Percentile								
	L	S	3rd	10th	M 50 ^b		90th	97th	L	S	3rd	10th	M 50 ^b	90th	97th
7 (35)	3.756	.064	.664	.706	.778	.835	.859	7 (37)	2.402	.062	.657	.690	.753	.810	.834
8 (43)	3.241	.065	.701	.744	.820	.883	.910	8 (49)	2.012	.063	.687	.720	.787	.849	.876
9 (46)	2.780	.066	.736	.779	.857	.925	.954	9 (45)	1.635	.065	.713	.747	.817	.884	.914
10 (45)	2.364	.066	.767	.809	.890	.961	.992	10 (53)	1.164	.067	.746	.781	.855	.928	.962
11 (49)	1.979	.067	.794	.835	.918	.994	1.027	11 (47)	.525	.070	.796	.832	.912	.996	1.036
12 (46)	1.573	.069	.819	.861	.947	1.029	1.066	12 (58)	-.174	.073	.851	.889	.975	1.072	1.121
13 (51)	1.079	.075	.846	.891	.987	1.082	1.126	13 (53)	-.786	.076	.895	.933	1.025	1.133	1.192
14 (55)	.623	.087	.878	.929	1.043	1.161	1.218	14 (58)	-.293	.078	.932	.970	1.066	1.186	1.254
15 (45)	.375	.094	.921	.978	1.107	1.246	1.314	15 (47)	-.1677	.080	.960	.999	1.098	1.228	1.304
16 (43)	.242	.091	.975	1.032	1.162	1.304	1.374	16 (22)	-.1918	.081	.977	1.016	1.117	1.253	1.336
17 (19)	.117	.082	1.027	1.080	1.201	1.334	1.400								

* Percentile values should be interpolated for children who are between birthdays.

+ Number of observations in that age category

TABLE 17. LUMBAR SPINE BMC: LMS VALUES AND SELECTED MODELLED PERCENTILES BY SEX, RACE AND AGE (from Kalkwarf et al. [147], used with permission from the Endocrine Society)

Female, Non-Black															
Age (n [†])	LMS Parameters Modeled Percentile						Age (n)	LMS Parameters Modeled Percentile							
	L	S	3 rd	10 th	M 50 th	90 th		97 th	L	S	3 rd	10 th	M 50 th	90 th	97 th
7 (135)	.259	.146	14.1	15.4	18.7	22.4	24.3	7 (147)	-.584	.146	13.7	14.8	17.6	21.5	23.8
8 (158)	.261	.146	15.6	17.1	20.7	24.9	27.0	8 (177)	-.553	.153	14.9	16.2	19.5	23.9	26.6
9 (132)	.263	.147	17.1	18.7	22.7	27.3	29.7	9 (152)	-.515	.159	16.2	17.6	21.4	26.5	29.6
10 (157)	.265	.148	18.5	20.3	24.7	29.7	32.3	10 (174)	-.450	.168	17.7	19.4	23.8	29.8	33.5
11 (174)	.266	.150	19.9	21.9	26.7	32.2	35.0	11 (178)	-.295	.182	20.0	22.1	27.7	35.2	39.7
12 (158)	.269	.158	21.8	24.1	29.7	36.2	39.5	12 (175)	.010	.195	23.5	26.5	34.0	43.6	49.0
13 (131)	.281	.178	24.6	27.6	34.9	43.5	48.0	13 (159)	.326	.196	28.2	32.2	41.8	53.2	59.2
14 (157)	.318	.198	28.6	32.6	42.5	54.3	60.5	14 (157)	.471	.184	33.0	37.5	48.1	60.2	66.4
15 (150)	.374	.194	35.2	40.1	52.1	66.0	73.2	15 (164)	.510	.172	36.5	41.2	52.0	64.0	70.1
16 (144)	.415	.179	42.0	47.5	60.4	75.2	82.8	16 (105)	.522	.162	38.8	43.4	54.1	66.0	71.9
17 (70)	.417	.173	46.6	52.4	66.1	82.0	89.8								

Female, Black															
Age (n)	LMS Parameters Modeled Percentile						Age (n)	LMS Parameters Modeled Percentile							
	L	S	3 rd	10 th	M 50 th	90 th		97 th	L	S	3 rd	10 th	M 50 th	90 th	97 th
7 (35)	1.039	.143	14.1	15.8	19.3	22.9	24.5	7 (37)	-.947	.142	14.6	15.7	18.5	22.6	25.2
8 (44)	.871	.148	15.7	17.6	21.6	25.8	27.7	8 (50)	-.785	.149	15.5	16.7	20.0	24.5	27.4
9 (47)	.673	.152	17.3	19.3	23.8	28.5	30.9	9 (45)	-.556	.159	16.7	18.2	22.0	27.3	30.5
10 (45)	.445	.157	18.8	20.9	25.8	31.2	34	10 (55)	-.243	.174	18.7	20.6	25.6	32.2	36.0
11 (49)	.139	.163	20.6	22.8	28.2	34.7	38.1	11 (48)	.017	.188	22.2	24.9	31.7	40.3	45.0
12 (46)	-.279	.174	23.3	25.7	31.9	40.2	45.0	12 (61)	.102	.187	27.5	30.8	39.3	49.8	55.5
13 (52)	-.503	.190	27.1	30.0	37.7	48.9	55.9	13 (58)	.203	.179	32.4	36.3	45.9	57.5	63.6
14 (57)	-.245	.203	31.8	35.6	45.8	59.9	68.4	14 (63)	.152	.175	36.3	40.4	50.8	63.3	70.0
15 (44)	.063	.206	36.7	41.6	54.3	70.6	79.6	15 (49)	.032	.170	39.2	43.4	54.0	67.1	74.3
16 (44)	.137	.198	41.1	46.5	60.3	77.4	86.8	16 (26)	-.072	.165	41.4	45.6	56.2	69.6	77.0
17 (21)	.065	.189	44.5	49.9	63.8	81.6	90.7								

* Percentile values should be interpolated for children who are between birthdays.
† Number of observations in that age category

TABLE 18. WHOLE BODY BMC: LMS VALUES AND SELECTED MODELLED PERCENTILES BY SEX, RACE AND AGE (from Kalkwarf et al. [147], used with permission from the Endocrine Society)

Female, Non-Black															
Age (n [*])	LMS Parameters Modeled Percentile						Age (n)	LMS Parameters Modeled Percentile							
	L	S	3rd	10 th	M 50 th	90 th		97 th	L	S	3rd	10 th	M 50 th	90 th	97 th
7 (134)	-.404	.111	682.8	726.3	833.6	964.6	1035.8	7 (146)	-.806	.112	658.6	698.3	799.5	930.6	1006.1
8 (154)	-.377	.110	760.0	808.7	928.3	1027.6	1152.4	8 (173)	-.813	.111	729.3	773.1	884.7	1029.4	1112.7
9 (128)	-.353	.110	835.8	889.4	1020.6	1179.4	1265.2	9 (150)	-.822	.112	798.4	846.5	969.0	1128.3	1220.2
10 (156)	-.33	.110	908.0	966.3	1108.9	1280.9	1373.6	10 (173)	-.803	.117	872.7	927.8	1069.3	1255.2	1363.3
11 (172)	-.302	.111	985.7	1050.0	1207.1	1396.2	1497.8	11 (176)	-.642	.136	954.4	1025.4	1210.2	1456.6	1601.6
12 (156)	-.259	.116	1085.2	1159.6	1341.5	1560.9	1678.9	12 (171)	-.141	.158	1056.3	1157.2	1412.1	1733.1	1911.2
13 (130)	-.192	.127	1214.3	1306.8	1534.4	1810.8	1960.2	13 (157)	.514	.157	1192.1	1327.5	1640.9	1986.4	2158.9
14 (156)	-.121	.141	1382.9	1501.4	1795.0	2154.6	2349.9	14 (156)	.884	.141	1352.9	1503.0	1829.7	2163.3	2321.4
15 (151)	-.104	.146	1592.4	1734.1	2086.1	2518.7	2754.2	15 (161)	1.042	.127	1483.7	1633.9	1953.1	2270.0	2417.6
16 (140)	-.158	.143	1796.3	1951.6	2339.1	2818.5	3081.2	16 (105)	1.140	.118	1569.7	1716.6	2025.0	2326.9	2466.2
17 (70)	-.256	.139	1964.7	2126.3	2532.3	3040.5	3322.0								

Female, Black															
Age (n)	LMS Parameters Modeled Percentile						Age (n)	LMS Parameters Modeled Percentile							
	L	S	3rd	10 th	M 50 th	90 th		97 th	L	S	3 rd	10 th	M 50 th	90 th	97 th
7 (35)	2.266	.092	732.3	794.9	911.2	1011.2	1055.9	7 (37)	-.860	.099	743.2	783.2	883.7	1011.2	1083.2
8 (43)	1.980	.099	803.6	876.2	1014.5	1136.4	1189.2	8 (49)	-.793	.105	798.3	844.1	959.5	1106.8	1190.3
9 (46)	1.690	.107	874.4	957.0	1119.0	1266.2	1331.1	9 (45)	-.671	.111	856.3	909.0	1041.8	1210.4	1305.6
10 (45)	1.383	.116	948.4	1041.6	1230.9	1409.7	1490.3	10 (53)	-.303	.119	940.5	1006.1	1167.7	1364.8	1472.0
11 (49)	1.039	.128	1034.3	1139.5	1363.2	1585.6	1689.1	11 (47)	.394	.126	1076.7	1168.3	1379.6	1612.5	1729.1
12 (46)	.654	.141	1142.9	1262.2	1530.8	1816.9	1956.3	12 (58)	-.646	.127	1252.9	1367.9	1625.4	1898.3	2030.9
13 (51)	.272	.156	1283.4	1418.3	1741.1	2114.4	2307.5	13 (53)	.449	.127	1412.3	1535.6	1818.5	2128.0	2282.0
14 (55)	-.019	.164	1456.6	1606.7	1983.0	2449.4	2704.4	14 (53)	-.106	.129	1538.2	1664.8	1967.1	2317.6	2499.9
15 (45)	-.150	.164	1649.2	1812.4	2228.1	2757.1	3053.2	15 (47)	-.131	.132	1621.5	1751.3	2070.3	2456.6	2664.7
16 (43)	-.157	.154	1848.4	2019.7	2451.5	2993.9	3294.3	16 (22)	-.266	.135	1672.7	1805.4	2137.0	2549.8	2777.4
17 (19)	-.120	.139	1846.2	2219.3	2647.5	3170.2	3453.7								

* Percentile values should be interpolated for children who are between birthdays.

+ Number of observations in that age category

REFERENCES

- [1] KELLY, T.L., SLOVIK, D.M., NEER, R.M., Calibration and standardization of bone mineral densitometers, *J. Bone Miner. Res.* **4** 5 (1989) 663–669.
- [2] LASKEY, M., PHIL, D., Dual-energy X ray absorptiometry and body composition, *Nutrition* **12** 1 (1996) 45–51.
- [3] KELLY, T.L., BERGER, N., RICHARDSON, T.L., DXA body composition: Theory and practice, *Appl. Rad. Isot.* **49** 5–6 (1998) 511–513.
- [4] PIETROBELLI, A., et al., Dual-energy X ray absorptiometry body composition model: Review of physical concepts, *Am. J. Physiol.* **271** 6 Pt 1 (1996) E941–951.
- [5] BLAKE, G.M., FOGELMAN, I., Technical principles of dual energy X ray absorptiometry, *Sem. Nucl. Med.* **27** 3 (1997) 210–228.
- [6] ROSS, P.D., et al., Body size accounts for most differences in bone density between Asian and Caucasian women. The EPIC (early postmenopausal interventional cohort) study group, *Calcif. Tissue Int.* **59** 5 (1996) 339–343.
- [7] BAIM, S., et al., Official positions of the International Society for Clinical Densitometry and executive summary of the 2007 ISCD position development conference, *J. Clin. Densitom.* **11** 1 (2008) 75–91.
- [8] KOOT, V.C., et al., Evaluation of the Singh index for measuring osteoporosis, *J. Bone Joint Surg. Br.* **78** 5 (1996) 831–834.
- [9] KAWASHIMA, T., UHTHOFF, H.K., Pattern of bone loss of the proximal femur: A radiologic, densitometric, and histomorphometric study, *J. Orthop. Res.* **9** 5 (1991) 634–640.
- [10] SHEPHERD, J.A., et al., Metacarpal index and bone mineral density in healthy African-American women, *Osteoporosis Int.* **16** 12 (2005) 1621–1626.
- [11] COSMAN, F., et al., Radiographic absorptiometry: A simple method for determination of bone mass, *Osteoporosis Int.* **2** 1 (1991) 34–38.
- [12] YATES, A.J., et al., Radiographic absorptiometry in the diagnosis of osteoporosis, *Am. J. Med.* **98** 2A (1995) 41S–47S.
- [13] SCHMITT, J.C., KRANER, H., A Bone Density Scanner Using Gamma Ray Attenuation with a Ge(hp) Detector, BNL, Upton (1972).
- [14] KRANER, H., PATERSON, J.F., SMITH, J.C., Combined cortical thickness and bone density determination by photon absorptiometry, *Physics Med. Biol.* **23** (1978) 1101–1114.
- [15] WAHNER, H.W., DUNN, W.L., RIGGS, B.L., Noninvasive bone mineral measurements, *Semin. Nucl. Med.* **13** 3 (1983) 282–289.
- [16] GENANT, H.K., BOYD, D., Quantitative bone mineral analysis using dual energy computed tomography, *Invest. Radiol.* **12** 6 (1977) 545–551.
- [17] RICHARDSON, M.L., et al., Assessment of metabolic bone diseases by quantitative computed tomography, *Clin. Orthop.* **195** (1985) 224–238.
- [18] STEIN, J.A., LAZEWATSKY, J.L., HOCHBERG, A.M., Dual energy X ray bone densitometer incorporating an internal reference system, *Radiology* **165**(P) (1987) 313.
- [19] KELLY, T., et al., Quantitative digital radiography versus dual photon absorptiometry of the lumbar spine, *J. Clin. Endocr. Metabol.* **67** (1988) 839–844.

- [20] WAHNER, H.W., et al., Comparison of dual-energy X ray absorptiometry and dual photon absorptiometry for bone mineral measurements of the lumbar spine, *Mayo Clin. Proc.* **63** 11 (1988) 1075–1084.
- [21] SHENG, H.P., HUGGINS, R.A., A review of body composition studies with emphasis on total body water and fat, *Am. J. Clin. Nutr.* **32** 3 (1979) 630–647.
- [22] GILSANZ, V., Bone density in children: A review of the available techniques and indications, *Eur. J. Radiol.* **26** 2 (1998) 177–182.
- [23] SCHONAU, E., The development of the skeletal system in children and the influence of muscular strength, *Horm. Res.* **49** 1 (1998) 27–31.
- [24] NELSON, D.A., KOO, W.W., Interpretation of absorptiometric bone mass measurements in the growing skeleton: Issues and limitations, *Calcif. Tissue Int.* **65** 1 (1999) 1–3.
- [25] VAN RIJN, R.R., et al., Bone densitometry in children: A critical appraisal, *Eur. Radiol.* **13** 4 (2003) 700–710.
- [26] LEHMANN, L.A., et al., Generalized image combinations in dual KVP digital radiography, *Med. Phys.* **8** 5 (1981) 659–667.
- [27] GENANT, H.K., et al., Universal standardization for dual X ray absorptiometry: Patient and phantom cross-calibration results, *J. Bone Miner. Res.* **9** 10 (1994) 1503–1514.
- [28] ITO, M., et al., Relationship of osteophytes to bone mineral density and spinal fracture in men, *Radiology* **189** 2 (1993) 497–502.
- [29] YU, W., et al., Influence of degenerative joint disease on spinal bone mineral measurements in postmenopausal women, *Calcif. Tissue Int.* **57** 3 (1995) 169–174.
- [30] VON DER RECKE, P., et al., The impact of degenerative conditions in the spine on bone mineral density and fracture risk prediction, *Osteoporosis Int.* **6** 1 (1996) 43–49.
- [31] RAND, T., et al., Impact of spinal degenerative changes on the evaluation of bone mineral density with dual energy X ray absorptiometry (DXA), *Calcif. Tissue Int.* **60** 5 (1997) 430–433.
- [32] FROHN, J., et al., Effect of aortic sclerosis on bone mineral measurements by dual-photon absorptiometry, *J. Nucl. Med.* **32** 2 (1991) 259–262.
- [33] DRINKA, P.J., et al., The effect of overlying calcification on lumbar bone densitometry, *Calcif. Tissue Int.* **50** 6 (1992) 507–510.
- [34] FOOD AND AGRICULTURE ORGANIZATION OF THE UNITED NATIONS, INTERNATIONAL ATOMIC ENERGY AGENCY, INTERNATIONAL LABOUR ORGANISATION, OECD NUCLEAR ENERGY AGENCY, PAN AMERICAN HEALTH ORGANIZATION, WORLD HEALTH ORGANIZATION, International Basic Safety Standards for Protection against Ionizing Radiation and for the Safety of Radiation Sources, Safety Series No. 115, IAEA, Vienna (1996).
- [35] INTERNATIONAL ATOMIC ENERGY AGENCY, Radiological Protection for Medical Exposure to Ionizing Radiation, IAEA Safety Standards Series No. RS-G-1.5, IAEA, Vienna (2002).
- [36] INTERNATIONAL ATOMIC ENERGY AGENCY, Applying Radiation Safety Standards in Diagnostic Radiology and Interventional Procedures Using X Rays, Safety Reports Series No. 39, IAEA, Vienna (2006).
- [37] NATIONAL COUNCIL ON RADIATION PROTECTION, Biological Effects and Exposure Limits for “Hot Particles”, NCRP Rep. No. 130, National Council on Radiation Protection & Measurement, Bethesda, MD (1999).

- [38] BLAKE, G.M., NAEEM, M., BOUTROS, M., Comparison of effective dose to children and adults from dual X ray absorptiometry examinations, *Bone* **38** 6 (2006) 935–942.
- [39] THOMAS, S.R., et al., Effective dose of dual-energy X ray absorptiometry scans in children as a function of age, *J. Clin. Densitom.* **8** 4 (2005) 415–422.
- [40] STEEL, S.A., BAKER, A.J., SAUNDERSON, J.R., An assessment of the radiation dose to patients and staff from a lunar expert-xl fan beam densitometer, *Physiol. Meas.* **19** 1 (1998) 17–26.
- [41] NJEH, C.F., et al., Radiation dose and in vitro precision in paediatric bone mineral density measurement using dual X ray absorptiometry, *Br. J. Radiol.* **70** 835 (1997) 719–727.
- [42] BEZAKOVA, E., COLLINS, P.J., BEDDOE, A.H., Absorbed dose measurements in dual energy X ray absorptiometry (DXA), *Br. J. Radiol.* **70** (1997) 172–179.
- [43] NJEH, C.F., et al., Radiological assessment of a new bone densitometer-the lunar expert, *Br. J. Radiol.* **69** 820 (1996) 335–340.
- [44] UNITED NATIONS SCIENTIFIC COMMITTEE ON THE EFFECTS OF ATOMIC RADIATION, UNSCEAR focuses on Chernobyl accident in general assembly report, Press Release GA/9718, UNSCEAR, Vienna (2000).
- [45] INTERNATIONAL COMMISSION ON RADIATION PROTECTION, Recommendations of the International Commission on Radiation Protection, ICRP Publ. 60, Pergamon Press, Oxford (1990).
- [46] LARKIN, A., et al., QA/acceptance testing of DEXA X ray systems used in bone mineral densitometry, *Radiat. Prot. Dosimetry* (2008).
- [47] LLOYD, T., et al., Radiation dose from DXA scanning to reproductive tissues of females, *J. Clin. Densitom.* **1** 4 (1998) 379–383.
- [48] DAMILAKIS, J., et al., Embryo/fetus radiation dose and risk from dual X ray absorptiometry examinations, *Osteoporosis Int.* **13** 9 (2002) 716–722.
- [49] BOUDOUSQ, V., et al., Total dose incurred by patients and staff from BMD measurement using a new 2d digital bone densitometer, *Osteoporosis Int.* **14** 3 (2003) 263–269.
- [50] BLAKE, G.M., et al., New generation DXA scanners increase radiation dose to patients and staff, *JBMR* **11** S1 (1996) P267.
- [51] SHEAHAN, N.F., et al., Commissioning and quality assurance protocol for dual energy X ray absorptiometry (DEXA) systems, *Radiat. Prot. Dosimetry* **117** 1–3 (2005) 288–290.
- [52] HOBBIE, R.K., *Intermediate Physics for Medicine and Biology*, 3rd edn, Springer Verlag, New York (1997).
- [53] WEBB, S., *The Physics of Medical Imaging*, Taylor & Francis, London (1996).
- [54] CRC Handbook of Chemistry and Physics, LIDE, D.R. (Ed.), 89th edn, CRC Press/Taylor & Francis, Boca Raton, FL (2009).
- [55] WANG, J., et al., Body-fat measurement in patients with acquired immunodeficiency syndrome: Which method should be used? *Am. J. Clin. Nutr.* **56** 6 (1992) 963–967.
- [56] HEYMSFIELD, S.B., WAKI, M., Body composition in humans: Advances in the development of multicompartiment chemical models, *Nutr. Rev.* **49** 4 (1991) 97–108.
- [57] MENDEZ, J., et al., Density of fat and bone mineral of mammalian body, *Metabolism* **9** (1960) 472–477.

- [58] WITHERS, R.T., et al., Comparisons of two-, three-, and four-compartment models of body composition analysis in men and women, *J. Appl. Physiol.* **85** 1 (1998) 238–245.
- [59] GURR, M., HARWOOD, J., *Lipid Biochemistry*, 4th edn, Giegy Pharmaceuticals, Ardsley, NY (1962).
- [60] DIEM, K., *Constituents of Living Matter*, 6th edn, Giegy Pharmaceuticals, Ardsley, NY (1962).
- [61] SNYDER, W., et al., *Report of the Task Group on Reference Man*, Pergamon Press, Oxford (1984).
- [62] ALLEN, T.H., KRZYWICKI, H.J., ROBERTS, J.E., Density, fat, water and solids in freshly isolated tissues, *J. Appl. Physiol.* **14** (1959) 1005–1008.
- [63] RICHMOND, C.R., ICRP publication on reference man, *Br. J. Radiol.* **58** 690 (1985) 576–577.
- [64] NORD, R., PAYNE, H., *Body composition by dual-energy X ray absorptiometry: A review of the technology*, *Asia Pacific J. Clin. Nutr.* **4** (1995) 167–171.
- [65] SHEPHERD, J.A., et al., Novel use of single X ray absorptiometry for measuring breast density, *Technol. Cancer Res. Treat.* **4** 2 (2005) 173–182.
- [66] LIBOUBAN, H., et al., Comparison of pencil-, fan-, and cone-beam dual X ray absorptiometers for evaluation of bone mineral content in excised rat bone, *J. Clin. Densitom.* **5** 4 (2002) 355–361.
- [67] BLAKE, G.M., PARKER, J.C., BUXTON, F.M.A., FOGELMAN, I., Dual X ray absorptiometry: A comparison between fan beam and pencil beam scans, *Br. J. Radiol.* **66** 790 (1993) 902–906.
- [68] EIKEN, P., et al., Switching from DXA pencil-beam to fan-beam. I: Studies in vitro at four centers, *Bone* **15** 6 (1994) 667–670.
- [69] ELLIS, K.J., SHYPAILO, R.J., Bone mineral and body composition measurements: Cross-calibration of pencil-beam and fan-beam dual-energy X ray absorptiometers, *J. Bone Miner. Res.* **13** 10 (1998) 1613–1618.
- [70] RUETSCHKE, A.G., et al., Differences between dual X ray absorptiometry using pencil beam and fan beam modes and their determinants in vivo and in vitro, *J. Clin. Densitom.* **3** 2 (2000) 157–166.
- [71] TOTHILL, P., HANNAN, W.J., WILKINSON, S., Comparisons between a pencil beam and two fan beam dual energy X ray absorptiometers used for measuring total body bone and soft tissue, *Br. J. Radiol.* **74** 878 (2001) 166–176.
- [72] YAGI, D., Evaluation of the usefulness of whole body bone mineral measurement using dual energy X ray absorptiometry for the diagnosis of osteoporosis in Japanese women, *Nippon Igaku Hoshasen Gakkai Zasshi* **56** 1 (1996) 37–41.
- [73] HENZELL, S., et al., Comparison of pencil-beam and fan-beam DXA systems, *J. Clin. Densitom.* **6** 3 (2003) 205–210.
- [74] GRIFFITHS, M.R., NOAKES, K.A., POCOCK, N.A., Correcting the magnification error of fan beam densitometers, *J. Bone Miner. Res.* **12** 1 (1997) 119–123.
- [75] POCOCK, N., et al., Magnification error of femoral geometry using fan beam densitometers, *Calcif. Tissue Int.* **60** (1997) 8–10.
- [76] WAHNER, H.W., FOGELMAN, I., *The Evaluation of Osteoporosis: Dual Energy X Ray Absorptiometry in Clinical Practice*, Martin Dunitz, London (1994).

- [77] MILLER, P.D., et al., Clinical utility of bone mass measurements in adults: Consensus of an international panel, The Society for Clinical Densitometry, *Semin. Arthritis Rheum.* **25** 6 (1996) 361–372.
- [78] FRANCK, H., MUNZ, M., SCHERRER, M., Evaluation of dual-energy X ray absorptiometry bone mineral measurement-comparison of a single-beam and fan-beam design: The effect of osteophytic calcification on spine bone mineral density, *Calcif. Tissue Int.* **56** 3 (1995) 192–195.
- [79] YU, W., et al., Spinal bone mineral assessment in postmenopausal women: A comparison between dual X ray absorptiometry and quantitative computed tomography, *Osteoporosis Int.* **5** 6 (1995) 433–439.
- [80] JERGAS, M., et al., Which vertebrae should be assessed using lateral dual-energy X ray absorptiometry of the lumbar spine, *Osteoporosis Int.* **5** 3 (1995) 196–204.
- [81] RUPICH, R.C., et al., Lateral dual-energy radiography: Artifact error from rib and pelvic bone, *J. Bone Miner. Res.* **7** 1 (1992) 97–101.
- [82] HERD, R.J., et al., Total body studies in normal British women using dual energy X ray absorptiometry, *Br. J. Radiol.* **66** 784 (1993) 303–308.
- [83] LASKEY, M.A., Dual-energy X ray absorptiometry and body composition, *Nutrition* **12** 1 (1996) 45–51.
- [84] STEIGER, P., et al., Morphometric X ray absorptiometry of the spine: Correlation in vivo with morphometric radiography, *Osteoporosis Int.* **4** 5 (1994) 238–244.
- [85] KIM, J., et al., Total-body skeletal muscle mass: Estimation by a new dual-energy X ray absorptiometry method, *Am. J. Clin. Nutr.* **76** 2 (2002) 378–383.
- [86] ROSS, R., Magnetic resonance imaging provides new insights into the characterization of adipose and lean tissue distribution, *Can. J. Physiol. Pharmacol.* **74** 6 (1996) 778–785.
- [87] THOMAS, L.W., The chemical composition of adipose tissue of man and mice, *Q. J. Exp. Physiol. Cogn. Med. Sci.* **47** (1962) 179–188.
- [88] ABATE, N., et al., Estimation of adipose tissue mass by magnetic resonance imaging: Validation against dissection in human cadavers, *J. Lipid Res.* **35** 8 (1994) 1490–1496.
- [89] SHEN, W., et al., Adipose tissue quantification by imaging methods: A proposed classification, *Obes. Res.* **11** 1 (2003) 5–16.
- [90] WONG, S., JANSSEN, I., ROSS, R., Abdominal adipose tissue distribution and metabolic risk, *Sports Med.* **33** 10 (2003) 709–726.
- [91] VAGUE, J., The degree of masculine differentiation of obesities: A factor determining predisposition to diabetes, atherosclerosis, gout, and uric calculous disease, *Nutrition* **15** 1 (1999) 89–90.
- [92] ELBERS, J.M., et al., Reproducibility of fat area measurements in young, non-obese subjects by computerized analysis of magnetic resonance images, *Int. J. Obes. Relat. Metabol. Disord.* **21** 12 (1997) 1121–1129.
- [93] SEIDELL, J.C., BAKKER, C.J., VAN DER KOOY, K., Imaging techniques for measuring adipose-tissue distribution — a comparison between computed tomography and 1.5-t magnetic resonance, *Am. J. Clin. Nutr.* **51** 6 (1990) 953–957.
- [94] STATEN, M.A., TOTTY, W.G., KOHRT, W.M., Measurement of fat distribution by magnetic resonance imaging, *Invest. Radiol.* **24** 5 (1989) 345–349.
- [95] GERARD, E.L., et al., Overall body fat and regional fat distribution in young women: Quantification with MR imaging, *AJR Am. J. Roentgenol.* **157** 1 (1991) 99–104.

- [96] HILL, A.M., et al., Estimating abdominal adipose tissue with DXA and anthropometry, *Obesity (Silver Spring)* **15** 2 (2007) 504–510.
- [97] TREUTH, M.S., HUNTER, G.R., KEKES-SZABO, T., Estimating intraabdominal adipose tissue in women by dual-energy X ray absorptiometry, *Am. J. Clin. Nutr.* **62** 3 (1995) 527–532.
- [98] SVENDSEN, O.L., et al., Accuracy of measurements of body composition by dual-energy X ray absorptiometry in vivo, *Am. J. Clin. Nutr.* **57** 5 (1993) 605–608.
- [99] KAMEL, E.G., MCNEILL, G., VAN WIJK, M.C., Usefulness of anthropometry and DXA in predicting intra-abdominal fat in obese men and women, *Obes. Res.* **8** 1 (2000) 36–42.
- [100] BLUNT, B., et al., Hologic whole body phantom: Using in vitro data to correct in vivo whole body data, *J. Bone Miner. Res.* **15** Suppl. 1 (2000) S398.
- [101] LOVEJOY, J.C., SMITH, S.R., ROOD, J.C., Comparison of regional fat distribution and health risk factors in middle-aged Caucasian and African American women: The healthy transitions study, *Obes. Res.* **9** 1 (2001) 10–16.
- [102] SMITH, S.R., et al., Contributions of total body fat, abdominal subcutaneous adipose tissue compartments, and visceral adipose tissue to the metabolic complications of obesity, *Metabolism* **50** 4 (2001) 425–435.
- [103] KELLEY, D., et al., Subdivisions of subcutaneous abdominal adipose tissue and insulin resistance, *Am. J. Physiol. Endocrinol. Metabol.* **278** 5 (2000) E941.
- [104] NORTON, K., OLDS, T., *Anthropometrica*, UNSW Press, Sydney, Australia (1996).
- [105] HUI, S.L., et al., Universal standardization of bone density measurements: A method with optimal properties for calibration among several instruments, *J. Bone Miner. Res.* **12** 9 (1997) 1463–1470.
- [106] LU, Y., et al., Standardization of bone mineral density at femoral neck, trochanter and Ward's triangle, *Osteoporosis Int.* **12** 6 (2001) 438–444.
- [107] SHEPHERD, J.A., et al., Universal standardization of forearm bone densitometry, *J. Bone Miner. Res.* **17** 4 (2002) 734–745.
- [108] CARTER, D.R., BOUXSEIN, M.L., MARCUS, R., New approaches for interpreting projected bone densitometry data, *J. Bone Miner. Res.* **7** 2 (1992) 137–145.
- [109] BRISMAR, T., et al., Whole-body bone mineral apparent density (WBMD) — introduction of a new variable for evaluation of paediatric skeletal status, *Osteoporosis Int.* **11** Suppl. 3 (2000) S18.
- [110] JERGAS, M., et al., Estimates of volumetric bone density from projectional measurements improve the discriminatory capability of dual X ray absorptiometry, *J. Bone Miner. Res.* **10** 7 (1995) 1101–1110.
- [111] MAZESS, R.B., et al., Normalization of spine densitometry, *J. Bone Miner. Res.* **9** 4 (1994) 541–548.
- [112] FOGELHOLM, G.M., et al., Bone mineral density during reduction, maintenance and regain of body weight in premenopausal, obese women, *Osteoporosis Int.* **12** 3 (2001) 199–206.
- [113] BROWNBILL, R.A., ILICH, J.Z., Measuring body composition in overweight individuals by dual energy X ray absorptiometry, *BMC Med. Imaging* **5** 1 (2005) 1.
- [114] TATARANNI, P.A., RAVUSSIN, E., Use of dual-energy X ray absorptiometry in obese individuals, *Am. J. Clin. Nutr.* **62** 4 (1995) 730–734.

- [115] KOO, W.W., HOCKMAN, E.M., HAMMAMI, M., Dual energy X ray absorptiometry measurements in small subjects: Conditions affecting clinical measurements, *J. Am. Coll. Nutr.* **23** 3 (2004) 212–219.
- [116] PICAUD, J.C., et al., First all-solid pediatric phantom for dual X ray absorptiometry measurements in infants, *J. Clin. Densitom.* **6** 1 (2003) 17–23.
- [117] SHEPHERD, J.A., et al., Cross-calibration and minimum precision standards for dual-energy X ray absorptiometry: The 2005 ISCD official positions, *J. Clin. Densitom.* **9** 1 (2006) 31–36.
- [118] GENANT, H.K., et al., Noninvasive assessment of bone mineral and structure: State of the art, *J. Bone Miner. Res.* **11** 6 (1996) 707–730.
- [119] PATEL, R., et al., Long-term precision of DXA scanning assessed over seven years in forty postmenopausal women, *Osteoporosis Int.* **11** 1 (2000) 68–75.
- [120] SHEPHERD, J.A., LU, Y., A generalized least significant change for individuals measured on different DXA systems, *J. Clin. Densitom.* **10** 3 (2007) 249–258 (comments *J. Clin. Densitom.* **12** 3 407–410).
- [121] FARRELL, T.J., WEBBER, C.E., The error due to fat inhomogeneity in lumbar spine bone mineral measurements, *Clin. Phys. Physiol. Meas.* **10** 1 (1989) 57–64.
- [122] FORMICA, J.V., REGELSON, W., Review of the biology of quercetin and related bioflavonoids, *Food Chem. Toxicol.* **33** 12 (1995) 1061–1080.
- [123] SVENDSEN, O.L., et al., Are soft tissue composition of bone and non-bone pixels in spinal bone mineral measurements by DXA similar? Impact of weight loss, *Clin. Physiol. Funct. Imaging* **22** 1 (2002) 72–77.
- [124] TOTHILL, P., PYE, D.W., Errors due to non-uniform distribution of fat in dual X ray absorptiometry of the lumbar spine, *Br. J. Radiol.* **65** 777 (1992) 807–813.
- [125] TOTHILL, P., AVENELL, A., REID, D.M., Precision and accuracy of measurements of whole-body bone mineral: Comparisons between Hologic, Lunar, and Norland dual-energy X ray absorptiometers, *Br. J. Radiol.* **67** (1994) 1210–1217.
- [126] HANGARTNER, T.N., JOHNSTON, C.C., Influence of fat on bone measurements with dual-energy absorptiometry, *Bone Miner.* **9** 1 (1990) 71–81.
- [127] SVENDSEN, O.L., et al., Impact of soft tissue on in vivo accuracy of bone mineral measurements in the spine, hip, and forearm: A human cadaver study, *J. Bone Miner. Res.* **10** 6 (1995) 868–873.
- [128] KUIPER, J.W., et al., Accuracy and the influence of marrow fat on quantitative CT and dual-energy X ray absorptiometry measurements of the femoral neck in vitro, *Osteoporosis Int.* **6** 1 (1996) 25–30.
- [129] BOLOTIN, H.H., Inaccuracies inherent in dual-energy X ray absorptiometry in vivo bone mineral densitometry may flaw osteopenic/osteoporotic interpretations and mislead assessment of antiresorptive therapy effectiveness, *Bone* **28** 5 (2001) 548–555.
- [130] BOLOTIN, H.H., Analytic and quantitative exposition of patient-specific systematic inaccuracies inherent in planar DXA-derived in vivo BMD measurements, *Med. Phys.* **25** 2 (1998) 139–151.
- [131] TOTHILL, P., et al., Anomalies in the measurement of changes in total-body bone mineral by dual-energy X ray absorptiometry during weight change, *J. Bone Miner. Res.* **12** 11 (1997) 1908–1921.

- [132] REVILLA, M., et al., Influence of weight and gonadal status on total and regional bone mineral content and on weight-bearing and non-weight-bearing bones, measured by dual-energy X ray absorptiometry, *Maturitas* **28** 1 (1997) 69–74.
- [133] MARTIN, P., et al., Influence of patient's weight on dual-photon absorptiometry and dual-energy X ray absorptiometry measurements of bone mineral density, *Osteoporosis Int.* **3** 4 (1993) 198–203.
- [134] SPECTOR, E., LEBLANC, A., SHACKELFORD, L., Hologic QDR 2000 whole-body scans: A comparison of three combinations of scan modes and analysis software, *Osteoporosis Int.* **5** 6 (1995) 440–445.
- [135] PATEL, R., et al., The effect of weight change on DXA scans in a 2-year trial of etidronate therapy, *Calcif. Tissue Int.* **61** 5 (1997) 393–399.
- [136] TOTHILL, P., Dual-energy X ray absorptiometry measurements of total-body bone mineral during weight change, *J. Clin. Densitom.* **8** 1 (2005) 31–38.
- [137] ANDRICH, M.P., CAWLEY, M., CHEN, C.C., Artifacts caused by nonionic contrast media and a portacath on a dual-energy X ray absorptiometry whole-body composition study, *Clin. Nucl. Med.* **21** 5 (1996) 407–408.
- [138] SALA, A., et al., Effect of diagnostic radioisotopes and radiographic contrast media on measurements of lumbar spine bone mineral density and body composition by dual-energy X ray absorptiometry, *J. Clin. Densitom.* **9** 1 (2006) 91–96.
- [139] KENDLER, D.L., et al., Effect of calcium tablets on interpretation of lumbar spine DXA scans, *J. Clin. Densitom.* **9** 1 (2006) 97–104.
- [140] BINKLEY, N., et al., Official positions of the International Society for Clinical Densitometry and executive summary of the 2005 position development conference, *J. Clin. Densitom.* **9** 1 (2006) 4–14.
- [141] LOOKER, A.C., et al., Updated data on proximal femur bone mineral levels of US adults, *Osteoporosis Int.* **8** 5 (1998) 468–489.
- [142] SVENDSEN, O.L., et al., Measurements of bone mineral density of the proximal femur by two commercially available dual energy X ray absorptiometric systems, *Eur. J. Nucl. Med.* **19** 1 (1992) 41–46.
- [143] WORLD HEALTH ORGANIZATION, Assessment of Fracture Risk and its Application to Screening for Postmenopausal Osteoporosis, Rep. of a WHO Study Group, WHO, Tech. Rep. Ser. **843** (1994) 1–129.
- [144] LOOKER, A.C., et al., Proximal femur bone mineral levels of US adults, *Osteoporosis Int.* **5** 5 (1995) 389–409.
- [145] Physician's guide to prevention and treatment of osteoporosis, National Osteoporosis Foundation, Washington, D.C. (2008).
- [146] BAIM, S., et al., Official positions of the International Society for Clinical Densitometry and executive summary of the 2007 ISCD pediatric position development conference, *J. Clin. Densitom.* **11** 1 (2008) 6–21.
- [147] KALKWARF, H.J., et al., The bone mineral density in childhood study: Bone mineral content and density according to age, sex, and race, *J. Clin. Endocrinol. Metabol.* **92** 6 (2007) 2087–2099.
- [148] WARD, K.A., et al., UK reference data for the Hologic Qdr discovery dual-energy X ray absorptiometry scanner in healthy children and young adults aged 6–17 years, *Arch. Dis. Child* **92** 1 (2007) 53–59.

- [149] VAN DER SLUIS, I.M., et al., Reference data for bone density and body composition measured with dual energy X ray absorptiometry in Caucasian children and young adults, *Arch. Dis. Child* **87** 4 (2002) 341–347.
- [150] GALLAGHER, D., et al., Healthy percentage body fat ranges: An approach for developing guidelines based on body mass index, *Am. J. Clin. Nutr.* **72** 3 (2000) 694–701.
- [151] ALLISON, D.B., et al., Weight loss increases and fat loss decreases all cause mortality rate: Results from two independent cohort studies, *Int. J. Obes. Relat. Metabol. Disord.* **23** 6 (1999) 603–611.
- [152] TRUSCOTT, J.G., et al., Variation in lumbar spine and femoral neck bone mineral measured by dual energy X ray absorption: A study of 329 normal women, *Br. J. Radiol.* **66** 786 (1993) 514–521.
- [153] COLE, T.J., GREEN, P.J., Smoothing reference centile curves: The IMS method and penalized likelihood, *Stat. Med.* **11** 10 (1992) 1305–1319.
- [154] OGDEN, C.L., et al., Centers for disease control and prevention 2000 growth charts for the United States: Improvements to the 1977 national center for health statistics version, *Pediatrics* **109** 1 (2002) 45–60.
- [155] GORDON, C.M., et al., Special report on the 2007 pediatric position development conference of the International Society for Clinical Densitometry, *South Med. J.* (2008).
- [156] BONJOUR, J.P., et al., Critical years and stages of puberty for spinal and femoral bone mass accumulation during adolescence, *J. Clin. Endocrinol. Metabol.* **73** 3 (1991) 555–563.
- [157] BACHRACH, L.K., et al., Bone mineral acquisition in healthy Asian, Hispanic, Black, and Caucasian youth: A longitudinal study, *J. Clin. Endocrinol. Metabol.* **84** 12 (1999) 4702–4712.
- [158] MOLGAARD, C., et al., Whole body bone mineral content in healthy children and adolescents, *Arch. Dis. Child* **76** 1 (1997) 9–15.
- [159] HENDERSON, R.C., et al., Pediatric reference data for dual X ray absorptiometric measures of normal bone density in the distal femur, *AJR, Am. J. Roentgenol.* **178** 2 (2002) 439–443.
- [160] ELLIS, K.J., et al., Z score prediction model for assessment of bone mineral content in pediatric diseases, *J. Bone Miner. Res.* **16** 9 (2001) 1658–1664.
- [161] FAULKNER, R.A., et al., Bone densitometry in Canadian children 8–17 years of age, *Calcif. Tissue Int.* **59** 5 (1996) 344–351.
- [162] FAULKNER, R.A., et al., Regional and total body bone mineral content, bone mineral density, and total body tissue composition in children 8–16 years of age, *Calcif. Tissue Int.* **53** 1 (1993) 7–12.
- [163] KELLY, T., SPECKER, B., BINKLEY, N., Pediatric BMD reference database for US Caucasian children, *Bone* **36** Suppl. 1 (2005) S30.
- [164] BINKLEY, T.L., SPECKER, B.L., WITTIG, T.A., Centile curves for bone densitometry measurements in healthy males and females ages 5–22 yr, *J. Clin. Densitom.* **5** 4 (2002) 343–353.
- [165] WEBBER, C.E., et al., Age-predicted values for lumbar spine, proximal femur, and whole-body bone mineral density: Results from a population of normal children aged 3 to 18 years, *Can. Assoc. Radiol. J.* **58** 1 (2007) 37–45.

- [166] ARABI, A., et al., Sex differences in the effect of body-composition variables on bone mass in healthy children and adolescents, *Am. J. Clin. Nutr.* **80** 5 (2004) 1428–1435.
- [167] SALA, A., et al., Whole-body bone mineral content, lean body mass, and fat mass measured by dual-energy X ray absorptiometry in a population of normal Canadian children and adolescents, *Can. Assoc. Radiol. J.* **58** 1 (2007) 46–52.
- [168] HASANOGLU, A., TURNER, L., EZGU, F., Vertebra and femur bone mineral density values in Turkish children, *Turk. J. Pediatr.* **46** (2004) 298–302.
- [169] CROMER, B.A., et al., Reference values for bone mineral density in 12- to 18-year-old girls categorized by weight, race, and age, *Pediatr. Radiol.* **34** 10 (2004) 787–792.
- [170] FONSECA, A.S., et al., Bone mineral density of the lumbar spine of Brazilian children and adolescents aged 6 to 14 years, *Braz. J. Med. Biol. Res.* **34** 3 (2001) 347–352.
- [171] LU, P.W., et al., Volumetric bone mineral density in normal subjects, aged 5–27 years, *J. Clin. Endocrinol. Metabol.* **81** 4 (1996) 1586–1590.
- [172] HOGLER, W., et al., Importance of lean mass in the interpretation of total body densitometry in children and adolescents, *J. Pediatr.* **143** 1 (2003) 81–88.
- [173] PLUDOWSKI, P., et al., Reference values for the indicators of skeletal and muscular status of healthy Polish children, *J. Clin. Densitom.* **8** 2 (2005) 164–177.
- [174] CRABTREE, N., et al., UK paediatric DXA reference data (GE lunar prodigy): Effects of ethnicity, gender, and pubertal status, *Bone* **36** (2005) S42.
- [175] DEL RIO, L., et al., Bone mineral density of the lumbar spine in Caucasian Mediterranean Spanish children and adolescents: Changes related to age, sex, and puberty, *Pediatr. Res.* **35** 3 (1994) 362–366.
- [176] CRABTREE, N.J., et al., The relationship between lean body mass and bone mineral content in paediatric health and disease, *Bone* **35** 4 (2004) 965–972.
- [177] HORLICK, M., et al., Prediction models for evaluation of total-body bone mass with dual-energy X ray absorptiometry among children and adolescents, *Pediatrics* **114** 3 (2004) 337–345.
- [178] BOOT, A.M., et al., Bone mineral density in children and adolescents: Relation to puberty, calcium intake, and physical activity, *J. Clin. Endocrinol. Metabol.* **82** 1 (1997) 57–62.
- [179] ZANCHETTA, J.R., PLOTKIN, H., ALVAREZ FILGUEIRA, M.L., Bone mass in children: Normative values for the 2–20-year-old population, *Bone* **16** 4 Suppl. (1995) 393S–399S.
- [180] CHENG, J.C., et al., Determinants of axial and peripheral bone mass in Chinese adolescents, *Arch. Dis. Child* **78** 6 (1998) 524–530.

CONTRIBUTORS TO DRAFTING AND REVIEW

Al-Amiri, H.A.	Kuwait Institute for Scientific Research, Kuwait
Davidsson, L.	International Atomic Energy Agency
Ellis, K.	Baylor College of Medicine, United States of America
Heymsfield, S.	Merck & Co, Inc., United States of America
Hills, A.	Queensland University of Technology, Australia
Le Heron, J.C.	International Atomic Energy Agency
Lohman, T.	Tucson, Arizona, United States of America
McLean, D.	International Atomic Energy Agency
Pettifore, J.M.	University of the Witwatersrand, South Africa
Shepherd, J.	University of California at San Francisco, United States of America
Sherman, M.	University of California at San Francisco, United States of America
Wilson, K.	Hologic, Inc., United States of America

Consultants Meeting

Vienna, Austria: 14–16 May 2007

Technical Meetings

Vienna, Austria: 15–17 September 2008, 28–30 October 2009



IAEA

International Atomic Energy Agency

No. 22

Where to order IAEA publications

In the following countries IAEA publications may be purchased from the sources listed below, or from major local booksellers. Payment may be made in local currency or with UNESCO coupons.

AUSTRALIA

DA Information Services, 648 Whitehorse Road, MITCHAM 3132
Telephone: +61 3 9210 7777 • Fax: +61 3 9210 7788
Email: service@dadirect.com.au • Web site: <http://www.dadirect.com.au>

BELGIUM

Jean de Lannoy, avenue du Roi 202, B-1190 Brussels
Telephone: +32 2 538 43 08 • Fax: +32 2 538 08 41
Email: jean.de.lannoy@infoboard.be • Web site: <http://www.jean-de-lannoy.be>

CANADA

Bernan Associates, 4501 Forbes Blvd, Suite 200, Lanham, MD 20706-4346, USA
Telephone: 1-800-865-3457 • Fax: 1-800-865-3450
Email: customer-care@bernan.com • Web site: <http://www.bernan.com>

Renouf Publishing Company Ltd., 1-5369 Canotek Rd., Ottawa, Ontario, K1J 9J3
Telephone: +613 745 2665 • Fax: +613 745 7660
Email: order.dept@renoufbooks.com • Web site: <http://www.renoufbooks.com>

CHINA

IAEA Publications in Chinese: China Nuclear Energy Industry Corporation, Translation Section, P.O. Box 2103, Beijing

CZECH REPUBLIC

Suweco CZ, S.R.O., Klecakova 347, 180 21 Praha 9
Telephone: +420 26603 5364 • Fax: +420 28482 1646
Email: nakup@suweco.cz • Web site: <http://www.suweco.cz>

FINLAND

Akateeminen Kirjakauppa, PO BOX 128 (Keskuskatu 1), FIN-00101 Helsinki
Telephone: +358 9 121 41 • Fax: +358 9 121 4450
Email: akatilau@akateeminen.com • Web site: <http://www.akateeminen.com>

FRANCE

Form-Edit, 5, rue Janssen, P.O. Box 25, F-75921 Paris Cedex 19
Telephone: +33 1 42 01 49 49 • Fax: +33 1 42 01 90 90
Email: formedit@formedit.fr • Web site: <http://www.formedit.fr>

Lavoisier SAS, 145 rue de Provigny, 94236 Cachan Cedex
Telephone: + 33 1 47 40 67 02 • Fax +33 1 47 40 67 02
Email: romuald.verrier@lavoisier.fr • Web site: <http://www.lavoisier.fr>

GERMANY

UNO-Verlag, Vertriebs- und Verlags GmbH, Am Hofgarten 10, D-53113 Bonn
Telephone: + 49 228 94 90 20 • Fax: +49 228 94 90 20 or +49 228 94 90 222
Email: bestellung@uno-verlag.de • Web site: <http://www.uno-verlag.de>

HUNGARY

Librotrade Ltd., Book Import, P.O. Box 126, H-1656 Budapest
Telephone: +36 1 257 7777 • Fax: +36 1 257 7472 • Email: books@librotrade.hu

INDIA

Allied Publishers Group, 1st Floor, Dubash House, 15, J. N. Heredia Marg, Ballard Estate, Mumbai 400 001,
Telephone: +91 22 22617926/27 • Fax: +91 22 22617928
Email: alliedpl@vsnl.com • Web site: <http://www.alliedpublishers.com>

Bookwell, 2/72, Nirankari Colony, Delhi 110009
Telephone: +91 11 23268786, +91 11 23257264 • Fax: +91 11 23281315
Email: bookwell@vsnl.net

ITALY

Libreria Scientifica Dott. Lucio di Biasio "AEIOU", Via Coronelli 6, I-20146 Milan
Telephone: +39 02 48 95 45 52 or 48 95 45 62 • Fax: +39 02 48 95 45 48
Email: info@libreriaaeiou.eu • Website: www.libreriaaeiou.eu

JAPAN

Maruzen Company, Ltd., 13-6 Nihonbashi, 3 chome, Chuo-ku, Tokyo 103-0027
Telephone: +81 3 3275 8582 • Fax: +81 3 3275 9072
Email: journal@maruzen.co.jp • Web site: <http://www.maruzen.co.jp>

REPUBLIC OF KOREA

KINS Inc., Information Business Dept. Samho Bldg. 2nd Floor, 275-1 Yang Jae-dong SeoCho-G, Seoul 137-130
Telephone: +02 589 1740 • Fax: +02 589 1746 • Web site: <http://www.kins.re.kr>

NETHERLANDS

De Lindeboom Internationale Publicaties B.V., M.A. de Ruyterstraat 20A, NL-7482 BZ Haaksbergen
Telephone: +31 (0) 53 5740004 • Fax: +31 (0) 53 5729296
Email: books@delindeboom.com • Web site: <http://www.delindeboom.com>

Martinus Nijhoff International, Koraalrood 50, P.O. Box 1853, 2700 CZ Zoetermeer
Telephone: +31 793 684 400 • Fax: +31 793 615 698
Email: info@nijhoff.nl • Web site: <http://www.nijhoff.nl>

Swets and Zeitlinger b.v., P.O. Box 830, 2160 SZ Lisse
Telephone: +31 252 435 111 • Fax: +31 252 415 888
Email: infoho@swets.nl • Web site: <http://www.swets.nl>

NEW ZEALAND

DA Information Services, 648 Whitehorse Road, MITCHAM 3132, Australia
Telephone: +61 3 9210 7777 • Fax: +61 3 9210 7788
Email: service@dadirect.com.au • Web site: <http://www.dadirect.com.au>

SLOVENIA

Cankarjeva Zalozba d.d., Kopitarjeva 2, SI-1512 Ljubljana
Telephone: +386 1 432 31 44 • Fax: +386 1 230 14 35
Email: import.books@cankarjeva-z.si • Web site: <http://www.cankarjeva-z.si/uvoz>

SPAIN

Diaz de Santos, S.A., c/ Juan Bravo, 3A, E-28006 Madrid
Telephone: +34 91 781 94 80 • Fax: +34 91 575 55 63
Email: compras@diazdesantos.es, carmela@diazdesantos.es, barcelona@diazdesantos.es, julio@diazdesantos.es
Web site: <http://www.diazdesantos.es>

UNITED KINGDOM

The Stationery Office Ltd, International Sales Agency, PO Box 29, Norwich, NR3 1 GN
Telephone (orders): +44 870 600 5552 • (enquiries): +44 207 873 8372 • Fax: +44 207 873 8203
Email (orders): book.orders@tso.co.uk • (enquiries): book.enquiries@tso.co.uk • Web site: <http://www.tso.co.uk>

On-line orders

DELTA Int. Book Wholesalers Ltd., 39 Alexandra Road, Addlestone, Surrey, KT15 2PQ
Email: info@profbooks.com • Web site: <http://www.profbooks.com>

Books on the Environment

Earthprint Ltd., P.O. Box 119, Stevenage SG1 4TP
Telephone: +44 1438748111 • Fax: +44 1438748844
Email: orders@earthprint.com • Web site: <http://www.earthprint.com>

UNITED NATIONS

Dept. I004, Room DC2-0853, First Avenue at 46th Street, New York, N.Y. 10017, USA
(UN) Telephone: +800 253-9646 or +212 963-8302 • Fax: +212 963-3489
Email: publications@un.org • Web site: <http://www.un.org>

UNITED STATES OF AMERICA

Bernan Associates, 4501 Forbes Blvd., Suite 200, Lanham, MD 20706-4346
Telephone: 1-800-865-3457 • Fax: 1-800-865-3450
Email: customercare@bernan.com • Web site: <http://www.bernan.com>

Renouf Publishing Company Ltd., 812 Proctor Ave., Ogdensburg, NY, 13669
Telephone: +888 551 7470 (toll-free) • Fax: +888 568 8546 (toll-free)
Email: order.dept@renoufbooks.com • Web site: <http://www.renoufbooks.com>

Orders and requests for information may also be addressed directly to:

Marketing and Sales Unit, International Atomic Energy Agency

Vienna International Centre, PO Box 100, 1400 Vienna, Austria
Telephone: +43 1 2600 22529 (or 22530) • Fax: +43 1 2600 29302
Email: sales.publications@iaea.org • Web site: <http://www.iaea.org/books>



IAEA

International Atomic Energy Agency

RELATED PUBLICATIONS

**INTRODUCTION TO BODY COMPOSITION ASSESSMENT
USING THE DEUTERIUM DILUTION TECHNIQUE
WITH ANALYSIS OF URINE SAMPLES
BY ISOTOPE RATIO MASS SPECTROMETRY**

IAEA Human Health Series No. 13

STI/PUB/1451 (75 pp.; 2010)

ISBN 978-92-0-103310-9

Price: €35.00

**INTRODUCTION TO BODY COMPOSITION ASSESSMENT
USING THE DEUTERIUM DILUTION TECHNIQUE WITH
ANALYSIS OF SALIVA SAMPLES BY FOURIER
TRANSFORM INFRARED SPECTROMETRY**

IAEA Human Health Series No. 12

STI/PUB/1450 (92 pp.; 2010)

ISBN 978-92-0-103210-2

Price: €37.00

**STABLE ISOTOPE TECHNIQUE TO ASSESS INTAKE
OF HUMAN MILK IN BREASTFED INFANTS**

IAEA Human Health Series No. 7

STI/PUB/1429 (67 pp.; 2010)

ISBN 978-92-0-114009-8

Price: €32.00

**ASSESSMENT OF BODY COMPOSITION AND TOTAL
ENERGY EXPENDITURE IN HUMANS BY STABLE
ISOTOPE TECHNIQUES**

IAEA Human Health Series No. 3

STI/PUB/1370 (133 pp.; 2009)

ISBN 978-92-0-111708-3

Price: €38.00

The IAEA has contributed to the development and transfer of technical expertise in the use of dual energy X ray absorptiometry (DXA) in Member States by supporting national and regional nutrition projects through its technical cooperation programme and coordinated research projects addressing priority areas in nutrition. This publication provides information on the theoretical background and practical application of state of the art methodology for bone mineral density measurements and body composition assessment using DXA. It was developed by an international group of experts and is intended for nutritionists, radiation technologists, researchers and health professionals.

IAEA HUMAN HEALTH SERIES

INTERNATIONAL ATOMIC ENERGY AGENCY
VIENNA
ISBN 978-92-0-110610-0
ISSN 2075-3772